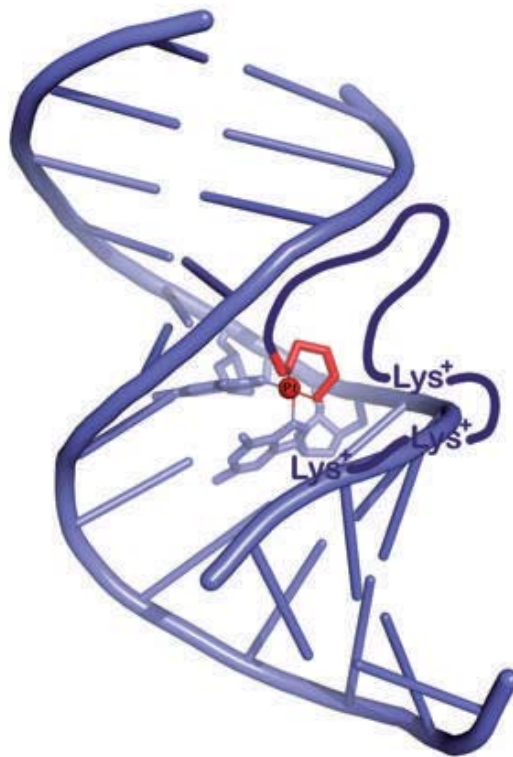


Mariana Simona Damian

DNA Bending Molecules for Improvement of Cisplatin Binding



Cuvillier Verlag Göttingen
Internationaler wissenschaftlicher Fachverlag

DNA Bending Molecules for Improvement of Cisplatin Binding

DISSERTATION

zur Erlangung

des mathematisch-naturwissenschaftlichen Doktorgrades

“Doctor rerum naturalium”

der Georg-August-Universität Göttingen

vorgelegt von

Mariana Simona Damian (geb. Balan)

aus Iași, Romania

Göttingen 2010

Bibliografische Information der Deutschen Nationalbibliothek

Die Deutsche Nationalbibliothek verzeichnet diese Publikation in der Deutschen Nationalbibliografie; detaillierte bibliografische Daten sind im Internet über <http://dnb.d-nb.de> abrufbar.

1. Aufl. - Göttingen : Cuvillier, 2010

Zugl.: Göttingen, Univ., Diss., 2010

978-3-86955-580-5

This work was supported by the *Deutsche Forschungsgemeinschaft* (**IRTG 1422**)

Prof. Dr. Ulf Diederichsen (Referent)

Institut für Organische und Biomolekulare Chemie

Georg-August-Universität Göttingen

Prof. Dr. Franc Meyer (Korreferent)

Institut für Anorganische und Biomolekulare Chemie

Georg-August-Universität Göttingen

© CUVILLIER VERLAG, Göttingen 2010

Nonnenstieg 8, 37075 Göttingen

Telefon: 0551-54724-0

Telefax: 0551-54724-21

www.cuvillier.de

Alle Rechte vorbehalten. Ohne ausdrückliche Genehmigung des Verlages ist es nicht gestattet, das Buch oder Teile daraus auf fotomechanischem Weg (Fotokopie, Mikrokopie) zu vervielfältigen.

1. Auflage, 2010

Gedruckt auf säurefreiem Papier

978-3-86955-580-5

The work described in this doctoral thesis has been carried out under the guidance and supervision of Prof. Dr. Ulf Diederichsen at the Institut für Organische und Biomolekulare Chemie of the Georg-August-Universität Göttingen between November 2006 and May 2010.

I thank Prof. Dr. Ulf Diederichsen for the interesting research topic and for his encouraging guidance, constant advice, the freedom of research, confidence and generous support throughout this work.

**DNA Bending Molecules for
Improvement of Cisplatin
Binding**

To my family,

Table of Contents

1. Introduction and Outline	- 1 -
2. DNA – Model System for Drug Interaction	- 7 -
2.1 DNA Properties.....	- 7 -
2.2 Major and Minor Groove Site Binding.....	- 8 -
2.3 DNA-Metal Interaction.....	- 10 -
2.4 DNA Intercalation.....	- 12 -
3. DNA Binding Pt(II) Molecules and Analogs	- 15 -
3.1 Cisplatin.....	- 15 -
3.1.1 What is Cisplatin?.....	- 15 -
3.1.2 Mode of Action.....	- 15 -
3.1.3 DNA – Final Target for Active Cisplatin Binding	- 17 -
3.1.4 Structural Changes Induced by Pt-DNA Adduct Formation	- 18 -
3.1.5 Consequences of Distorted DNA: Protein Binding of the Pt-DNA Adducts	- 19 -
3.1.6 Cisplatin Resistance.....	- 21 -
3.2 New Improved Platinum Drugs	- 23 -
3.2.1 General Classical Considerations	- 23 -
3.2.2 Classical Platinum Compounds	- 23 -
3.2.3 Non-Classical Platinum Compounds: New Approaches for Platinum Drug Design.....	- 24 -
3.2.4 The Approach of This Study.....	- 26 -

4. Synthesis and DNA Binding Studies of Cisplatin Analogs Modified with Nonspecifically DNA Targeting Peptides	- 29 -
4.1 Synthesis of Platinum Complex/Nonspecific Peptide Chimera	- 29 -
4.1.1 Synthesis of Platinum Chelating Building Blocks	- 29 -
4.1.2 Synthesis of Peptide Oligomers and of the Platinum Complex/Peptide Chimera	- 32 -
4.2 DNA Binding Studies of the Cisplatin Analogs.....	- 34 -
4.2.1 Plasmid Binding Studies.....	- 35 -
4.2.2 Oligonucleotide Binding Studies.....	- 37 -
4.2.3 Fluorescence Intercalation Studies	- 40 -
4.2.4 Thermal Melting Studies	- 43 -
4.2.5 Conclusions	- 45 -
5. Synthesis and DNA Binding Studies of Cisplatin Analogs Modified with Specifically DNA Targeting Peptides Derived from IHF	- 47 -
5.1 IHF – Integration Host Factor	- 47 -
5.1.1 General Structure.....	- 47 -
5.1.2 Interaction with DNA – Binding and Bending.....	- 48 -
5.1.3 IHF Mimicking Molecules	- 50 -
5.1.4 Platinum Modified IHF Mimicking Molecules	- 52 -
5.2 Synthesis of Unnatural Amino Acids	- 54 -
5.3 Synthesis of Platinated-IHF Mimicking Peptides	- 61 -
5.3.1 The Cyclopeptide Synthesis	- 61 -
5.3.2 The Linker-Lysine Dendrimer Synthesis	- 62 -
5.3.3 Assembly of the IHF Mimic and Platination.....	- 64 -
5.3.4 Complete Synthesis of the IHF Mimic on the Resin	- 66 -

5.4 Preliminary DNA Binding Experiments	- 69 -
6. Summary	- 75 -
7. Zusammenfassung	- 79 -
8. Experimental Part	- 83 -
8.1 General	- 83 -
8.1.1 Solvents	- 83 -
8.1.2 Reagents	- 83 -
8.1.3 Reactions	- 83 -
8.1.4 Lyophilization	- 84 -
8.1.5 Chromatography	- 84 -
8.2 Characterization	- 85 -
8.2.1 Mass Spectrometry	- 85 -
8.2.2. Nuclear Magnetic Resonance Spectroscopy (NMR)	- 85 -
8.2.3 Optical Rotations	- 86 -
8.3 Solid Phase Peptide Synthesis (SPPS)	- 86 -
8.3.1 Loading of the Resin	- 86 -
8.3.2 Automated SPPS	- 86 -
8.3.3 Manual SPPS	- 87 -
8.3.4 Kaiser Test	- 88 -
8.3.5 Manual MW-SPPS	- 88 -
8.3.6 Cleavage	- 88 -
8.3.7 Post-Cleavage Work-Up	- 89 -
8.4 Binding Studies	- 89 -
8.4.1 Fluorescence Spectroscopy	- 89 -

8.4.2 UV-Thermal Melting Analysis	- 89 -
8.4.3 5' - ³² P-end DNA Labeling.....	- 90 -
8.4.4 Radio-labeled DNA Gelshift Studies	- 90 -
8.4.5 Platinum Induced Agarose Gel Mobility Shift Assays.....	- 91 -
8.4.6 Agarose Gel Mobility Shift Assays-IHF Preliminary Studies	- 91 -
8.4.7 Polymerase Chain Reaction (PCR).....	- 91 -
8.5 Synthesis of Platinum Complex/Nonspecific Peptide Chimera	- 93 -
8.5.1 Synthesis of Platinum Chelating Building Blocks	- 93 -
8.5.2 Synthesis of Peptide Oligomers and of the Platinum Complex/ Peptide Chimera	- 103 -
8.6 Synthesis of Unnatural Amino Acids	- 108 -
8.7 Synthesis of Platinated-IHF Mimicking Peptides	- 128 -
9. Abbreviations	- 139 -
10. References	- 145 -

1. Introduction and Outline

DNA (deoxyribonucleic acid) is the major target for many metal based antitumor drugs. The interactions between metal complexes and DNA are determined by the structural and kinetic properties of the metal complex, but also by its affinity towards the biopolymer caused by the structural and electrostatic characteristics of both, ligand and DNA.^[1-5] Regarding kinetics, some metal coordinating compounds with relatively slow metal-ligand exchange rates, comparable to rates of cell division processes, are very active in killing cancer cells. The classical example is that of cisplatin, but also of other platinum based drugs. Improving the understanding of the antitumor action mechanism, as well as the development of new platinum based drugs with higher target specificity has always been considered a challenge for research.

Cisplatin (*cis*-diamminedichloroplatinum(II), cDDP, Platinol, Platinol-AQ) is one of the most successful metal-based anticancer drugs discovered almost 50 years ago.^[6-8] Its main intracellular target is nuclear DNA. The antitumour activity derives from its capacity to form especially intrastrand crosslinks between two adjacent guanine or adenine-guanine bases.^[9-13] The resulting DNA-GG/AG adducts induce disruption of the base pairing within the double helical structure with the bending of the helix with consequences on replication and transcription machinery (Figure 1.1).^[14-18] Bent structures are recognized by proteins, such belonging to the high mobility group (HMG proteins), which shield the DNA from repair processes, and thus, leading to induction of apoptosis.^[13,19-21]

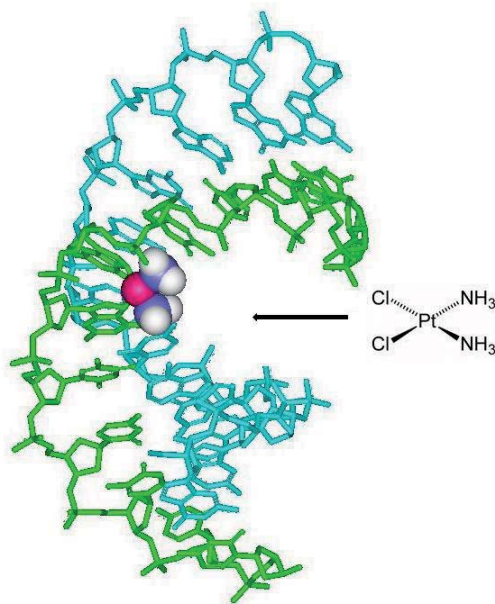


Figure 1.1 Cisplatin-GG-intrastrand DNA adduct.^[11]

Modification and optimization of the anticancer drug cisplatin is still of interest with respect to enhanced selective cell targeting and DNA binding efficiency. Although novel platinum based anticancer drugs have been developed, their structural variation is rather limited.^[22] Typically, a cationic metal complex or metabolite is used to enable electrostatic interaction with the polyanionic DNA backbone.^[23-25] Association of such complexes to the DNA backbone facilitates covalent binding,^[26-30] and thus, can be expected to improve the therapeutic efficacy. The lower *pH*- and the lower chloride concentration inside the cells (especially the cancer cells), compared to the blood stream, allow hydrolysis of cisplatin complexes in the cellular environment. This leads to formation of positively charged species with an increased affinity towards its cellular target.^[31,32] Hence, the mechanistically importance of the charged metal complex is indicated.

Attractive approaches include modification of the platinum coordination sphere, as well as the design of hybrid molecules of the cisplatin binding moiety. In such approaches, peptide motifs seem to be promising candidates. Peptides with cell penetrating, directing or recognizing properties can be implemented.^[33-37]

In this study, positively charged peptides were investigated with the potential of inducing DNA structural distortions, such as bending, caused by charge neutralization of the dsDNA helix.^[38,39] Placement of fixed charges near the negatively charged DNA surface should induce bending through asymmetric reduction or enhancement of the inter-phosphate repulsive forces (responsible for the DNA stiffness). The resulting bent DNA is more likely to facilitate binding of cisplatin derivatives. The approach presented in this work for the design of cisplatin analogs with potentially improved reactivity and selectivity is based on platinum/peptide chimera.

Two different approaches were followed to combine DNA kinking with facilitated and specific covalent platinum binding: i) the use of *nonspecific* DNA binding peptides;^[40] ii) the use of *specific* DNA binding peptides derived from proteins or natural products.^[41]

The first approach makes use of platinum-peptide conjugates in which the cisplatin analogue is covalently linked to peptides that vary with respect to the number of positively charged amino acids. We anticipate that the presence of charged peptides should facilitate in particular DNA pre-association by adhesion at the DNA phosphodiester backbone, followed by bending of the DNA target (Figure 1.2). Bending of DNA is thought to be essential in the nucleobase platination mechanism since DNA is bent in the resulting covalently platinated product.^[20]

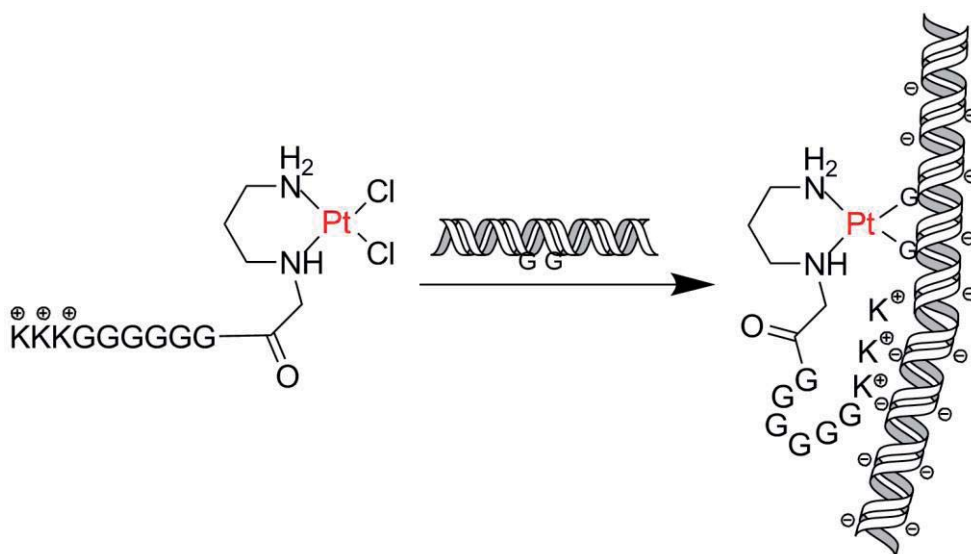


Figure 1.2 Representative example of cisplatin analog based on *nonspecific* DNA binding platinum/peptide conjugate.

In the second approach, the Integration Host Factor (IHF) cocrystal structure with double stranded DNA^[42-44] (Figure 1.3, left) serves as a lead concept for designing peptides that not only bind to DNA, but also induce bending.^[41] This approach uses the DNA bending mimic of IHF in combination with a covalently bound platinum binding site as cisplatin analogue. It is assumed for this construct to provide a double effect by influence on both, DNA binding ability and specificity.

IHF is a small heterodimeric protein that functions as an architectural factor in many cellular processes of prokaryotes. It consists of an α - and β -subunit, that specifically bind to the minor groove of DNA and bend the double strand by about 180°.^[43,44] The stacking interactions between the DNA bases are interrupted by intercalation of proline residues situated at the tip of the two flexible β -ribbon arms. The bend is stabilized by interactions with the positively charged α -helical body of the protein due to its contents of basic amino acids, such as arginine or lysine.^[45]

The chosen IHF mimicking peptide (Figure 1.3, right) includes a small lysine dendrimer which is linked to a cyclopeptide core, responsible for specific DNA recognition in the minor groove, followed by bending of the double strand.^[41] Because of the high net positive charges, the lysine dendrimer imitates the body of

the protein and stabilizes bending by electrostatic interactions. More precisely, the second strategy involves incorporation of newly synthesized artificial amino acids with a suitable donor atom pattern for platinum coordination, in the linker region of the IHF mimicking peptide, followed by platination.

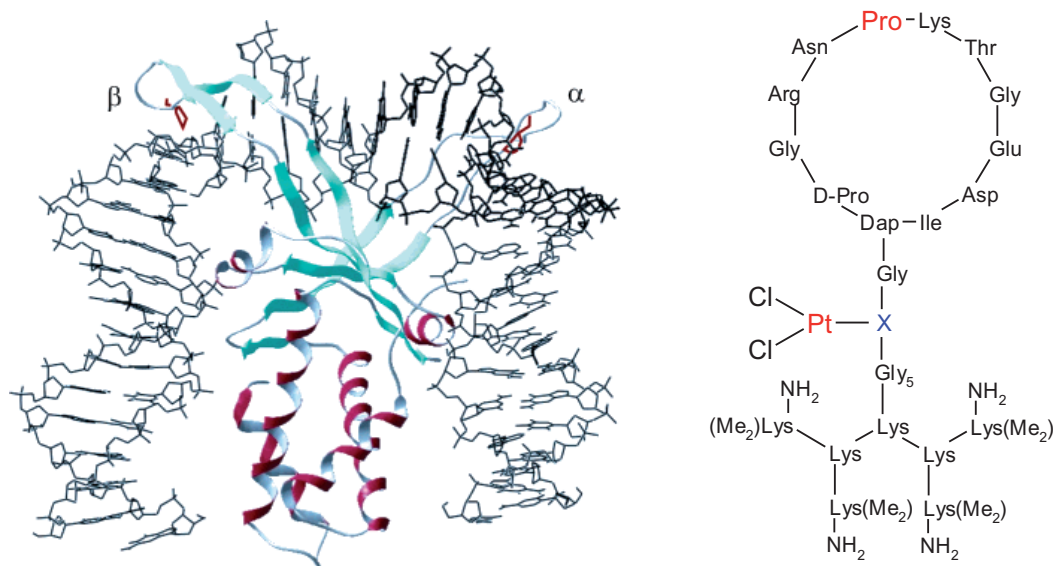


Figure 1.3 DNA-IHF cocrystal structure (left).^[44] Schematic representation of *platinated IHF mimicking peptide* (right) with DNA interacting residues (red) and unnatural amino acids containing the platinum coordinating site (blue).

In the current study are discussed the following tasks:

- DNA-metal complex interaction, in particularly the case of cisplatin.
- The design, synthesis and DNA binding studies of cisplatin analogs modified with nonspecifically DNA binding peptides.
- The design, synthesis and DNA binding studies of cisplatin analogs modified with specifically DNA binding peptides derived from IHF.

2. DNA – Model System for Drug Interaction

2.1 DNA Properties

Considering the role of DNA as functional key and hereditary unit for all living organisms, the discovery of the secondary structure of DNA in 1953 is a landmark in molecular biology.^[46] Knowledge of the chemical structure has allowed a better understanding of DNA interactions at molecular level in biological processes.^[47]

DNA is a biopolymer of monomeric units called nucleotides, a combination of base, sugar and phosphate groups. The genetic key of DNA is given by the sequence of the four bases (adenine – A, thymine – T, guanine – G, cytosine – C).^[48] Base stacking and base pairing contributes to the thermal stability of the DNA double helix.^[49,50]

The DNA molecule can adopt different conformations depending on the base sequence and chemical environment (Figure 2.1).^[51] A-, B- (right-handed) and Z-DNA (left-handed) are the most common forms. The glycosidic bond between the deoxy-ribose ring can undergo different ring "pucker" and ring/base conformations (B to A DNA transition corresponds to modification of the purine bases induced by cisplatin^[11]). The classical model of *Watson* and *Crick* corresponds to B-DNA, thermodynamically the most stable form and, therefore, the most common one.^[46,52] The base pair asymmetry induces in the DNA helical conformation a major (wide) and minor (narrow) groove pattern.

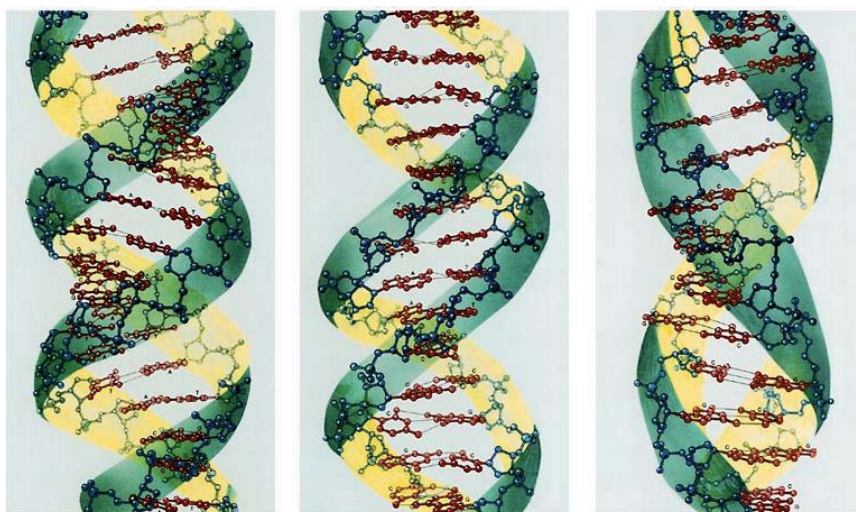


Figure 2.1 DNA conformations: side view of A-DNA (left), B-DNA (middle), Z-DNA (right).^[51,53]

2.2 Major and Minor Groove Site Binding

The DNA bases are accessible through the minor and major grooves, each with a different hydrogen bonding pattern (Figure 2.2.A). These patterns are important as they allow specific DNA sequence recognition by different molecules like proteins e.g. without having to open and thereby disrupt the double helix.^[48] The major groove is easier accessible compared to the minor groove due to its larger width and distinguishable hydrogen bonding properties between G:C and C:G, respectively A:T and T:A (Figure 2.2.B).

These features can be considered as a code of hydrogen bond donors (D)/acceptors (A), nonpolar sites (H), and methyl groups (M), AADH stands for G:C base pair, HDAA for C:G, respectively ADAM for A:T and MADA for T:A. In the minor groove such differences cannot be easily distinguished, the pattern differs only when comparing G:C/C:G to A:T/T:A, respectively ADA to AHA.

Major and Minor Groove Site Binding

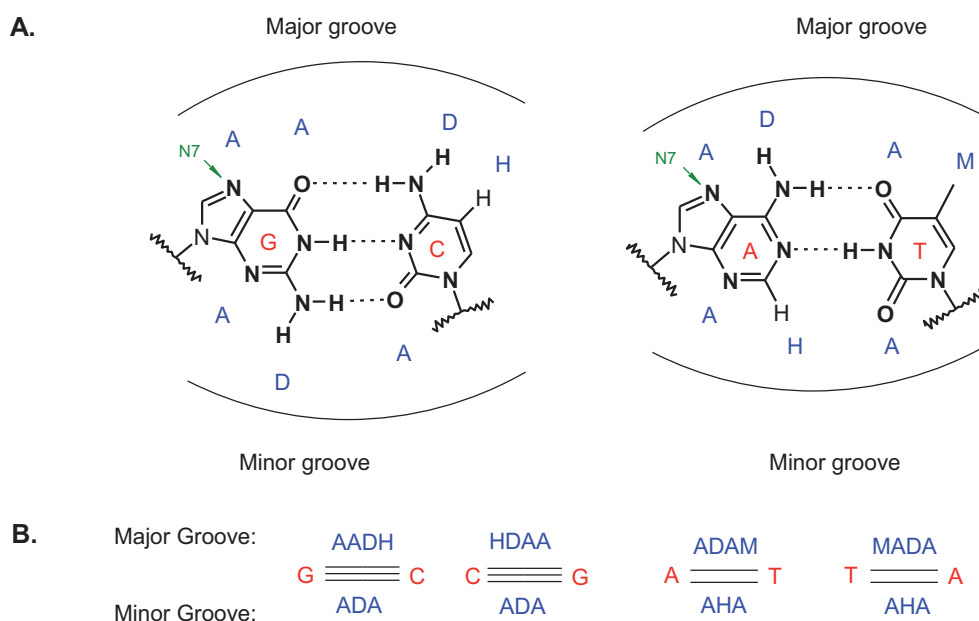


Figure 2.2 **A.** Hydrogen bonds between the edges of the base pairs in the major and minor groove (A – hydrogen bond acceptor, D – hydrogen bond donor, H – nonpolar hydrogen, M – methyl group for the van der Waals interaction). The *platination site* is shown in green at the N7 position of the purine bases. **B.** Hydrogen bond coding between the base pairs along the faces of the major and minor groove.

The function of DNA is influenced by its dynamic mobility.^[54] It has the ability to twist, unwind and supercoil, stretch, bend, induce tertiary (three dimensional) or quaternary structures. Thus DNA can bind, specifically or nonspecifically, covalently or non-covalently, to small inorganic or organic molecules, to peptides and proteins, causing interference in different steps of biological processes such as transcription or replication.^[7,47,55-58]

In general, small molecules bind B-DNA in the minor groove of the double helix, while the DNA binding proteins or gene targeted nucleotides interact with the major groove.^[59] Minor groove DNA binding drugs usually need to be small, flat and cationic molecules in order to represent suitable candidates in terms of size, flexibility, Van der Waals interaction and electrostatic potential.^[60] They may contain several aromatic heterocycles linked by amide or vinyl groups with cationic groups at their ends and have a preference for AT rich sequences (electronegative potential at the floor of the groove, less steric hindrance, more hydrophobic)

compared to the GC ones (electropositive potential).^[57,61] Determining the sequence recognition profile of DNA binding molecules is a major challenge.^[62]

Although it is accepted the preference of the groove binding molecules for the minor groove, there are classes of small molecules which are fitted better by the major groove.^[59] For example, antitumor platinum complexes such as cisplatin bind in the major groove specifically to the purine bases. By unstacking the bases at the platinum binding site it causes bending of the helix inducing a duplex kink of *ca.* 50°. ^[7,11]

2.3 DNA-Metal Interaction

The physical nature of DNA is an important parameter for any ligand interaction, especially when metal ions are involved. Due to the low *pKa* of the phosphate backbone DNA is highly charged, and therefore, addressable by electrostatic interactions with cations.^[63] It is known that a minimum of ions is needed to stabilize the biopolymer through ion complex formation. Therefore, some metal ions such as Na⁺, K⁺, Mg²⁺, Ca²⁺ *etc.* are fundamental elements in the human body. Other cationic species except metal salts include histone proteins or polyamines.

In the helical duplex the metal binding sites are within the phosphate backbone, sugar moiety, but mostly atoms of the heterocyclic bases are addressed by the metallo-complexes such as cisplatin and analogs.^[50,58]

There are three major ways to describe the DNA-metal ion interaction:

i) The ***diffuse binding*** mode describes strong electrostatic interactions between the anionic polymer and cations resulting in a delocalized positive charge sphere around the polyanionic DNA backbone. This pattern considers the DNA *Polyelectrolyte Model* based on the *Counterion Condensation Theory*, in which DNA is assumed to be a linear polyanionic chain of infinite length.^[64,65] The cations can move freely along the backbone, but remain always in close proximity (few angstroms distance). Thereby, concentration of condensed counter ions depends on the charge density of

the polyelectrolyte and is almost independent to changes of the bulk salt concentration. The condensed counter ion population neutralizes a certain fraction of the polyanionic charge (up to 76% in case of DNA), especially in the center of the oligomer. As an effect the charge density of the oligomer diminishes to the ends of the oligomer (“end effect”). The remaining counter ions reside in the bulk phase and its distribution can be modeled using *Poisson-Boltzmann* (PB) and *Grand Canonical Monte Carlo* (GCMC) calculations.^[66-68]

ii) Binding to DNA can also be described in a *site-bound outer sphere association* when water mediates the interactions between the metal ions and its ligand through hydrogen bonding. Metal ions, especially transition metals, have at least a solvation sphere and may have explicitly coordinated solvent molecules making them larger molecules.

iii) A third pattern includes *site-bound inner sphere association*, when the metal ion interacts directly with DNA via irreversible covalent binding by exchanging one or more aqua ligands, e.g. cisplatin.

The study of metal complex-DNA interactions is a wide research area.^[63,69] Considering the specific properties of the metal ions, their pattern of tissue uptake and distribution, and their preferred coordination properties in complexes, a variety of complexes have been developed to address different biological targets.

Platinum chemistry is a very wide research field because of its role in the antitumor therapy.^[70] Features of platinum(II)/peptide conjugates based on the anticancer active cisplatin are discussed in the present work. Our approach includes covalent metal-DNA interaction combined with the electrostatic interaction mediated by polycationic peptides derived from proteins, containing positively charged residues (lysine, arginine, histidine).^[40,41]

2.4 DNA Intercalation

DNA can not only be targeted by covalent or electrostatic binding, but also by intercalation. Intercalators induce significant structural changes of the DNA duplex when compared to the helix groove binding agents. Intercalation is considered as an important criterion in studying or/and designing new platinum based drug candidates.^[71]

The intercalation mode involves ligands with specific size and chemical pattern as cationic, planar, aromatic, polycyclic molecules corresponding to provide a geometry fitting between the DNA base pairs, specifically or nonspecifically. Many intercalators are known to preferentially bind to CG rich sequences.^[72] *Mainwaring et al.* defined DNA intercalation like “sandwiching of a molecule between two adjacent base pairs in the double helix”.^[73]

Intercalators like ethidium bromide (EtBr), propidium iodide (PI), (Figure 2.3) bind to the purine or pyrimidine bases of DNA just like nucleobases binding or stacking with each other in the double helix. The intercalation into DNA induces unwinding of the duplex to a degree dependent on the type of intercalator. The unwinding causes DNA structural changes, mostly reversible, such as lengthening of the strands, or twisting of the bases.^[71] Nevertheless, based on the *Neighboring Exclusion Principle* one ligand may intercalate approximately every second base pair.^[65,74]

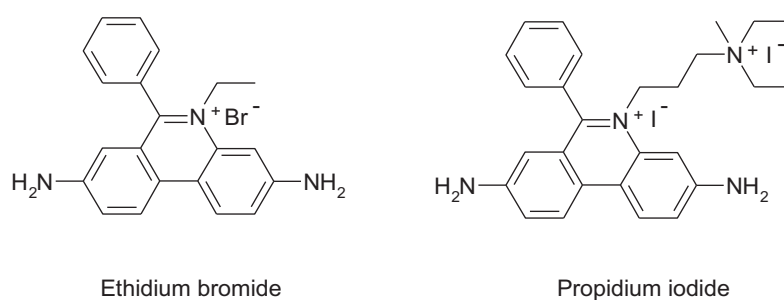


Figure 2.3 The chemical structures of DNA intercalators used in this work.

The mechanism of intercalation proposed by Lerman involves attraction of the cationic intercalator to the polyanionic DNA and the formation of a weakly electrostatic complex on the duplex surface.^[75] The differences in the DNA

environment (hydrophilic outer surface, hydrophobic inside the cavity between the base pairs) and the collisions between solvent molecules and the base pairs thermodynamically favor the insertion of the ligand between the base pairs. The binding is stabilized by the resulting π - π stacking interactions between the ligand and the planar, aromatic DNA bases.^[76]

DNA binding by intercalators is mostly reversible if the DNA structure is not affected while removing the ligand. Intercalators can be used as stains in biochemistry and medicine, e.g. fluorescent tagging of nucleic acids in gel electrophoresis (EtBr was used in this work to stain DNA). The fluorescence measurements of propidium iodide intercalating into the double stranded DNA in the presence of different platinum analogs is also discussed in the present work.

Nevertheless, the structural modifications during binding of the ligand through the duplex can induce functional changes, which make intercalators potential mutagens. They can be used as chemotherapeutic drugs due to their ability to inhibit replication, transcription and DNA repair processes. For example, quinoxaline antibiotics are potent bisintercalators.^[77]

Metal complexes can function as intercalators if they are planar or have an extended planar component which can insert between the base pairs.^[58] Based on the high binding affinity of intercalators towards DNA, the combination of intercalation and Pt-binding was approached.^[78] Such complexes derived from cisplatin showed impressive cytotoxic abilities.^[79,80] Some platinum intercalators show fluorescence properties, making them suitable for cellular tracking of the complexes.^[81]

3. DNA Binding Pt(II) Molecules and Analogs

3.1 Cisplatin

3.1.1 What is Cisplatin?

Cisplatin is the first clinically introduced metal based anticancer drug.^[70] Since the discovery of its pharmaceutical potential by *B. Rosenberg* in the 1960's, although first described 160 years ago, the compound has proven to be particularly efficient for the treatment of testicular and ovarian tumors.^[6,7] Today, three different platinum compounds, cisplatin, carboplatin, oxaliplatin are widely used in cancer treatment.^[8] However, the toxic side effects, combined with poor solubility, low selectivity towards tumor cells, and resistance development highlight the need for new and improved metal based anticancer drug candidates.^[12,13,70,82,83]

Therefore, most of the research activity was focused on understanding molecular events involved in the action mechanism of this drug, from cellular uptake, nucleic acid binding mechanism to platination effects, platinum-DNA damage repair and protein interaction.^[84] Basic characteristic of all platinum drugs with antitumor activity is covalent binding of DNA in a way of an "alkylating-like agent" leading to consequences on DNA replication and transcription.

3.1.2 Mode of Action

Upon administration to the bloodstream as an intravenous injection, cisplatin circulates primarily as a chloride due to high concentration of chloride ions (~100 mM), then the neutral compound enters the cell by passive or even active cellular uptake *via* specific receptors. There is evidence that the copper(II) transporter by constitutive triple response 1 (CTR1) receptor mechanism assists the platinum drug

to enter the cell. The excretion process involves an adenosine triphosphate (ATP) dependent pathway.^[3,12]

Inside the cell, the uncharged drug undergoes hydrolysis, the so-called aquation process, due to the low concentration of chloride ions (~4–12 mM) and higher concentration of water. It leads to formation of positively charged mono- or diaquated species, $[\text{Pt}^{\text{II}}(\text{NH}_3)_2\text{Cl}(\text{H}_2\text{O})]^+$, respectively $[\text{Pt}^{\text{II}}(\text{NH}_3)_2(\text{H}_2\text{O})_2]^{2+}$, followed by transfer to the nucleic acids (Figure 3.1). It seems that mostly the monoaquated complexes are responsible for the platinum-DNA adduct formation, and therefore, for the antitumor activity. Platinum(II)-OH₂ adducts are more reactive towards DNA than either Pt-Cl or Pt-OH species.^[85,86] Considering that the physiological *pH* is 7.4, secondary products of the aquation process are formed: the less reactive monohydroxy form $[\text{Pt}^{\text{II}}(\text{NH}_3)_2\text{OH}(\text{H}_2\text{O})]^+$ and the unreactive fully hydroxylated form $[\text{Pt}^{\text{II}}(\text{NH}_3)_2(\text{OH})_2]^{2+}$. To avoid formation of hydroxy forms, *pH* has to be considered, thus, most of the mechanistic studies are done in slightly acidic conditions as indicated by the *pK_a* values calculated for the cisplatin hydrolysis species.^[85]

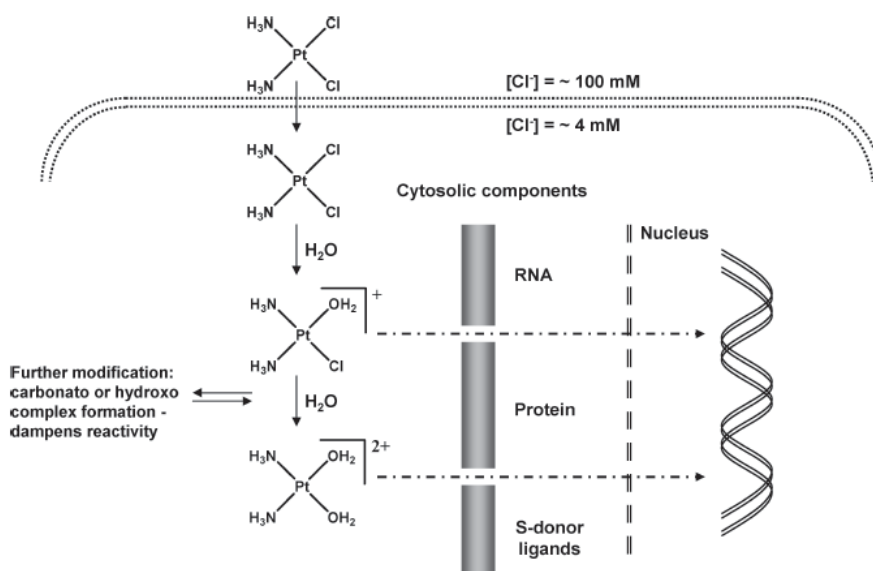


Figure 3.1 Schematic representation of the cellular uptake and the aquation process of cisplatin inside the cell, including the main active hydrolyzed species responsible for targeting the nuclear DNA.^[13]

Nevertheless, competitiveness between the nitrogen donors (e.g. N7 position of the purine bases) and sulfur donors (thiol containing peptides and proteins, e.g. the glutathione (GSH), metallothionein), but also the formation of the hydroxy species, induce only a DNA-Pt binding rate of *ca.* 10%. Coordination by sulfur containing biomolecules is mostly associated with the resistance and toxicity effect of the drug, but also, to a certain extent, as an intermediate mechanism step for DNA-drug binding in cases where a transfer from a thioester S ligand to guanine N7 does occur.^[87,88]

3.1.3 DNA – Final Target for Active Cisplatin Binding

Different cellular components, such as RNA, proteins, DNA, membrane phospholipids or microfilaments can be targeted by cisplatin.^[8] Among these, DNA binding has proven to be the main biological event related to the anticancer properties of the platinum drugs.^[89] Studies, like platinum distribution in the cancer cells, have indicated nuclear DNA as major target for cisplatin.^[90]

Platinum binds especially at the N7 position of the purine bases, guanine or adenine, in a variety of 1,2- and 1,3-intra- or interstrand crosslinks between the double stranded DNA, depending on the kinetics of the chloride ligand displacement reactions (Figure 3.2.A).^[9,10,83,89] There is a preference (~65%) for 1,2-intrastand crosslink binding at two neighbouring guanine bases with the formation of platinated d(GpG) adducts. This selectivity effect can be explained by increased basicity of the G-N7 site and by the kinetically favored hydrogen bonding of the Pt amine group with the O6 of guanosine (Figure 3.2.B).^[3] Furthermore, it has to be considered that most of the other functional groups of the bases are involved in structural DNA base pairing (see Figure 2.2). Platinum-AG intrastrand crosslinking has a rate of *ca.* 25% and has proven to be kinetically preferential over the formation of the GA adducts as an initial complex stabilization effect.^[91-93]

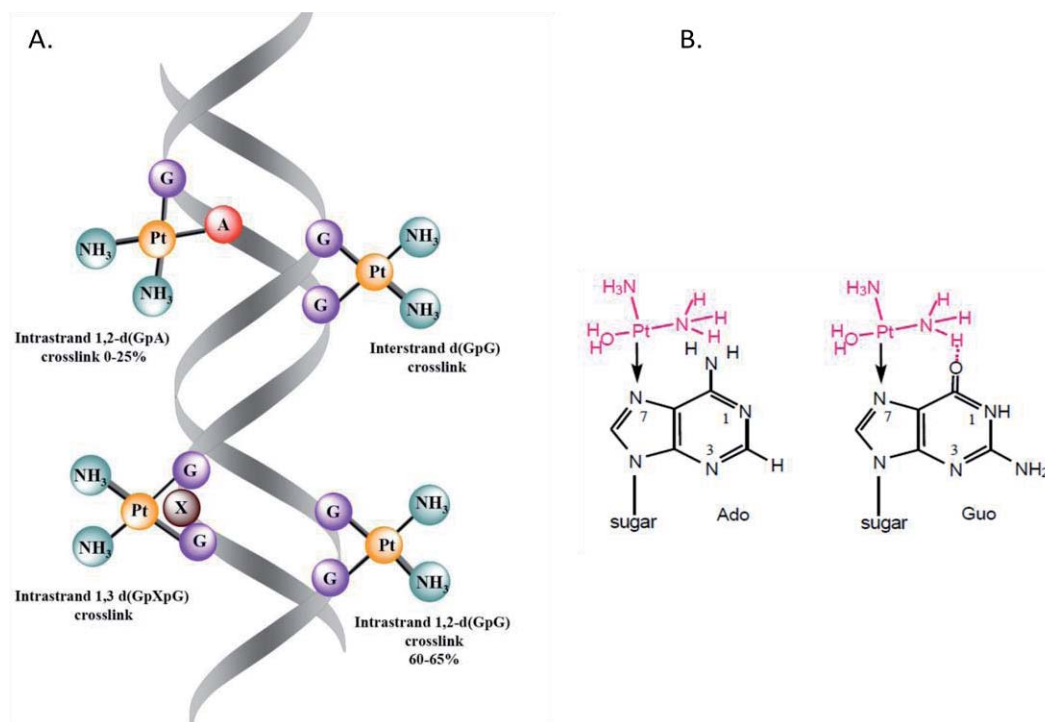


Figure 3.2 A. DNA-cisplatin adduct formation pathways.^[83] B. Platinum binding at N7 site of adenosine (Ado) and guanosine (Guo) favored by the hydrogen bonding with the O6.^[3]

3.1.4 Structural Changes Induced by Pt-DNA Adduct Formation

The DNA platination causes destacking of the purine bases, followed by kinking of the dsDNA with bending of the helical structure as elucidated by X-ray crystallography^[11,18] and NMR studies (Figure 3.3).^[16,17,94,95] For 1,2-d(GpG) the X-ray crystallographic analysis showed a DNA bend by 35–40° and a duplex unwinding of ~25°. Thereby, the major groove is mostly compacted and the minor groove is widened and flattened, the platinum ion lies out of the guanine planes with a roll angle of *ca.* 25°. As an overall effect, the DNA changes conformation at the 5' side from B-DNA to A-DNA. However, the NMR structures revealed bending by angles of 60–70° and an exaggerated roll of 49°, whereas only the B-DNA form was detected.

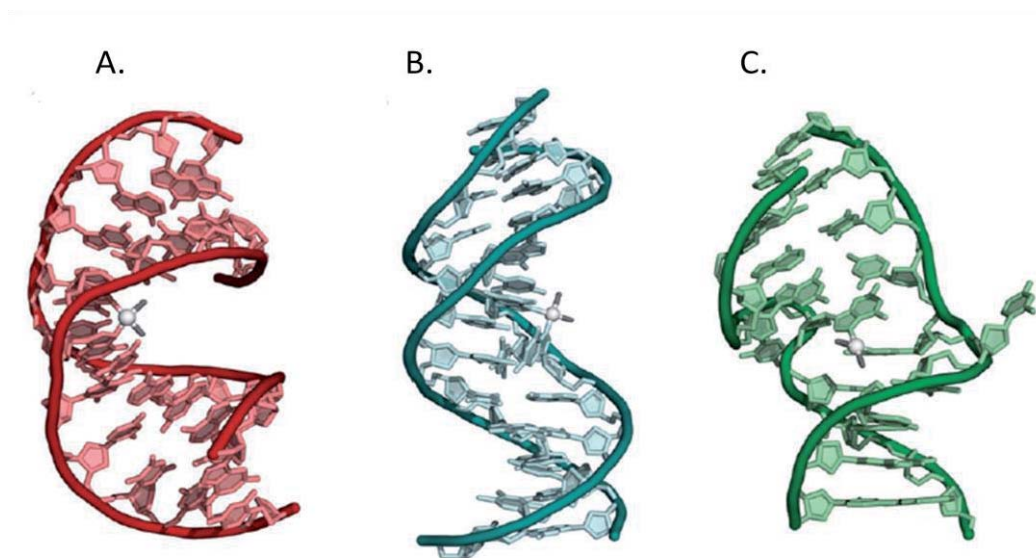


Figure 3.3 Molecular structures of cisplatin-dsDNA derived by X-ray and NMR studies: **A.** Cisplatin1,2-d(GpG) intrastrand crosslink; **B.** Cisplatin1,3-d(GpTpG) intrastrand crosslink; **C.** Cisplatin interstrand crosslink.

3.1.5 Consequences of Distorted DNA: Protein Binding of the Pt-DNA Adducts

Platinum chelation of the 1,2-d(GpG) site distorts the helix and significantly bends DNA towards the major groove, leaving the minor groove surface available for different proteins, that seem to bind to Pt-DNA adducts with greater affinity than to unmodified DNA, such as *high-mobility group (HMG) domain proteins*, DNA repair proteins, transcription factors (e.g. p53 protein) and others.^[12,13,16,96]

The HMG proteins, particularly HMG box protein 1 – HMGB1, have the property to bend DNA upon binding, but also to recognize both unwound and locally bent DNA, like in the cases of the cisplatin adducts.^[19-21,97-100] Thus bent DNA is recognized by the HMG proteins, the so-called damage recognition proteins, in the widened minor groove to the 3' end of the platinated strand (Figure 3.4). A phenylalanine residue intercalates into a hydrophobic notch created at the cisplatin crosslink (between the G bases) and binding of the domain is dramatically reduced when this residue is

substituted by alanine.^[20,21] As a result the bending of the helix increases significantly and the binding of DNA repair proteins is prevented or retarded.^[84]

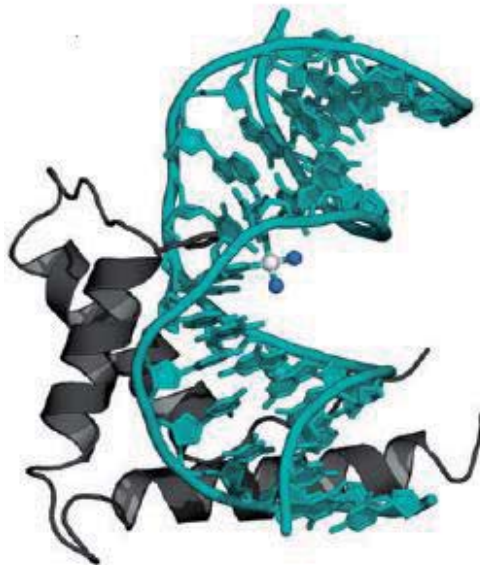


Figure 3.4 Molecular structure derived by the X-ray crystal structure of HMGB1 domain A bound to cisplatin 1,2-d(GpG) intrastrand crosslinked DNA (PDB accession code – 1CTK). The intercalating Phe residue plays an important role in substrate recognition.

It seems that HMG proteins have greater affinity towards Pt-damaged DNA than unmodified DNA suggesting that GG or AG sites resemble with naturally occurring DNA (recognized by HMG sequences) and escapes repair reactions.^[98]

Direct cellular responses to the formation of platinated DNA include replication or transcription inhibition (associated with transcription-coupled repair TCR), cell cycle arrest, DNA repair and apoptosis (Figure 3.5),^[13] for example p53 pathway.^[101] P53 is an important tumor-suppressor with crucial role in many cellular processes; in particular, it inhibits cell-proliferation by inducing either cell-cycle arrest or apoptosis.^[102]

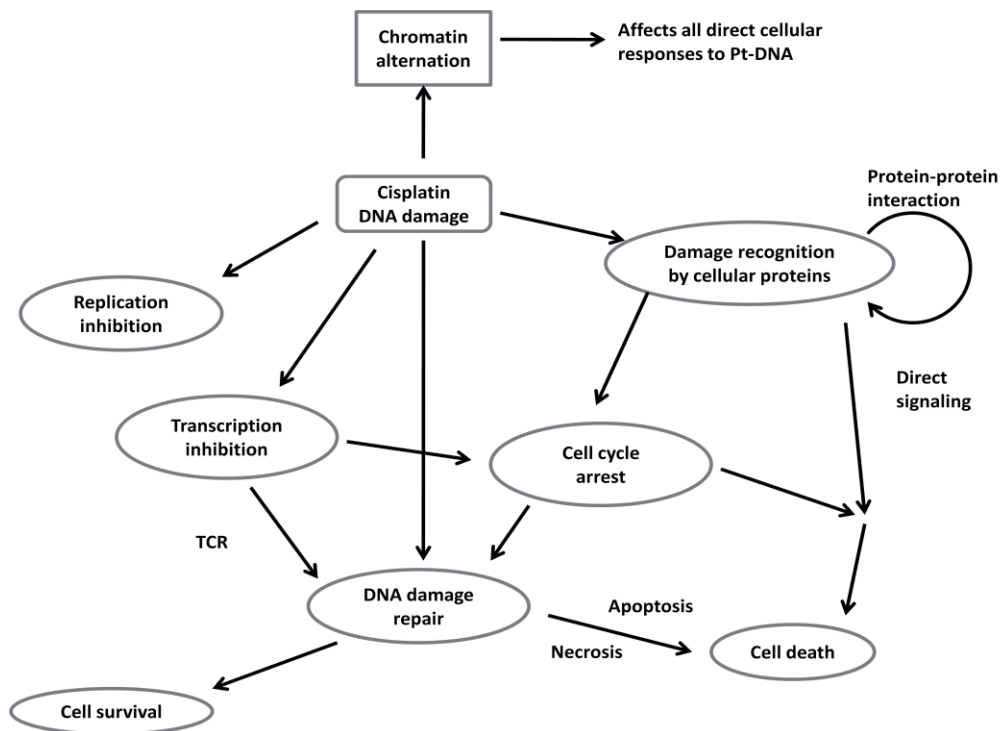


Figure 3.5 Overview of direct cellular responses to the formation of platinum-DNA adducts.

3.1.6 Cisplatin Resistance

However cisplatin activity is also associated with toxic side effects (e.g. nausea, ototoxicity, nephrotoxicity, neurotoxicity), but also with increased or spontaneous drug resistance effects.^[8] Resistance to platinum drugs can be intrinsic or acquired and can be mediated by factors outside or inside the cancer cell or at its cell membrane (Figure 3.6). The molecular mechanisms of resistance against cisplatin can be divided in two groups: mechanisms that prevent cDDP reaching DNA, its main therapeutic target (low solubility, reduced accumulation, and increased deactivation due to S donor biomolecules) and mechanisms that block the induction of cell death, apoptosis or necrosis.^[84,103,104] Several transcription factors (p53/p73, c-Myc, YB-1, CTF2, ATF4, ZNF143, mTFA) are involved in resistance to cisplatin.^[105]

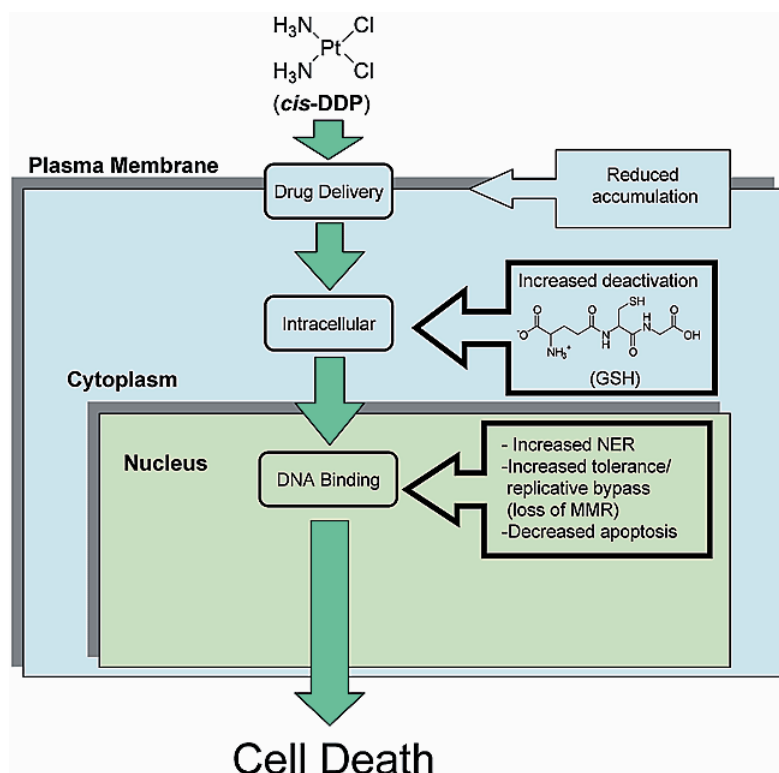


Figure 3.6 Schematic drawing of the major biochemical mechanisms of resistance to cisplatin. Resistance mechanisms may operate prior to or after binding of *cis*-DDP to DNA. MMR – mismatch repair; NER – nucleotide excision repair; GSH – glutathione.

In general, damaged DNA can be repaired by nucleotide excision repair (NER), mismatch repair (MMR), double-strand break repair, base excision repair and direct repair. It seems that tumor cells mostly have intrinsic differences in DNA repair mechanisms if compared to the healthy cells.^[106]

Nevertheless, mechanistic studies have directed research to a better understanding of cisplatin activity, but also to the discovery of improved new platinum drugs.

3.2 New Improved Platinum Drugs

3.2.1 General Classical Considerations

The strategy for developing potential platinum-anticancer drugs involves that the candidate should carry into the tumor cell both the DNA binding warhead and a molecular fragment that can interfere with a specific cellular pathway.^[12] Structure-activity relationship studies of the platinum compounds have determined a set of rules specific for these compounds; mainly such compounds should be a neutral platinum(II) species with two ammine ligands or one bidentate chelating diamine, and two ligands that can be replaced by aquation reactions (Figure 3.7). *Cis* geometry of the two amines (since *trans*-platinum is inactive) and the presence of at least one NH group on the amine function (responsible for important hydrogen-bond donor properties) is preferred.^[22,107,108]

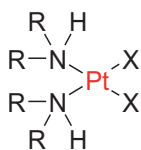


Figure 3.7. Lead structure for the design of platinum based drug candidates. X – leaving group (e.g. two chloro groups or bidentate malonate), R – H or an alkyl substituent.

3.2.2 Classical Platinum Compounds

Cisplatin is considered to be the “parent” of the platinum based drugs. First variations were derived by substituting different ammine and anionic ligands.^[83] Thus, the second generation platinum drug, carboplatin was introduced, by exchanging the chlorides in the cisplatin structure, exhibiting lower toxicity than cisplatin. Its lower reactivity allows the administration of a higher dose. The spontaneous, intrinsic drug resistance developed in certain tumors has led to new structural investigation and a new generation of platinum drugs. The third generation included compounds with different amine ligands, such as oxaliplatin (Figure 3.8).

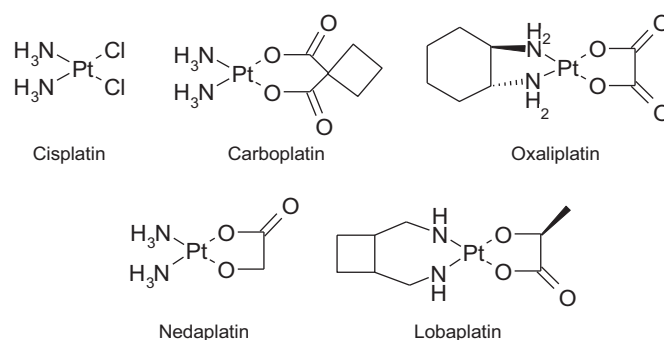


Figure 3.8 Structures of platinum compounds currently in clinical use.

Despite the huge number of platinum drug candidates, only *cisplatin*, *carboplatin* and *oxaliplatin* are used worldwide in the treatment of different types of cancer. Nedaplatin and lobaplatin are approved only in Japan, respectively China.^[25]

3.2.3 Non-Classical Platinum Compounds: New Approaches for Platinum Drug Design

The knowledge about the chemistry of the classical platinum drugs and correlation of their structures with anticancer activities has been the starting point for designing novel anticancer drug candidates based on the earlier mentioned mode of action (section 3.1.2).^[109,110] Modification of the leaving groups can influence tissue and intracellular distribution, whereas the carrier ligand usually determines the structure of adducts formed with DNA. The Pt-DNA adducts formed by cisplatin and the classical analogs are very much alike, and this can explain the similar patterns of tumor targeting and low resistance mechanism.

New approaches include active *trans* compounds, complexes with non-amine neutral ligands, such as aromatic systems, positively charged compounds, homo or hetero multinuclear compounds and even platinum(IV) compounds (Figure 3.9).^[22,25,83,111,112] The latter appears to be reduced to Pt(II) species inside the cell, but have improved cellular uptake and can address multiple intracellular targets (e.g. mitaplatin).^[113]

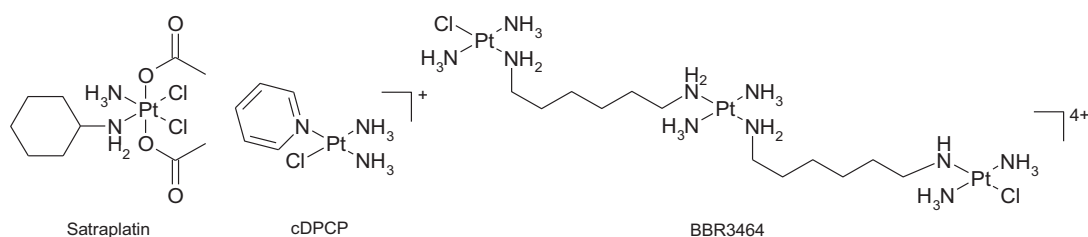


Figure 3.9 New non-traditional platinum compounds in clinical trials.

The major drawback of the platinum drugs is the poor capability to distinguish tumor cells from healthy ones. Identifying a special pathway for targeting only the tumor cells is unlikely, but it seems possible to increase the selectivity addressing e.g. solubility, cellular uptake. Compounds with bioactive carrier groups, such as aromatic intercalators, photoactivatable carriers, e.g. a benzophenone ligand, or antibodies that address special intracellular targets (increased rate of DNA cross-linking, mitochondria, proteins or combinations), are of major research interest.^[21,114] Nanotechnology is commonly used to build up target specific nanocarriers to deliver platinum into tumor cells with strong therapeutic effects.^[115,116] A variety of carriers including water soluble polymers, dendrimers, micelles and microparticles were introduced as eventually drug vehicles for a more efficient delivery of the drugs into the cells.^[5,117] Improving the delivery of platinum-based drugs may lead to reduced side effects at lower doses of drugs, and a possible way for a more specific tumor targeting.

The phosphodiester backbone seems also to play an important role in facilitating DNA platination.^[118] Polynuclear platinum complexes were designed as phosphate clamps and can be considered as another mode of DNA binding or as a preassociation step that facilitates covalent binding. TrisplatinNC, e.g. does not intercalate or bind in either groove, instead it binds to phosphate oxygen atoms, and thus, associates with the backbone.^[119] Electrostatic forces appear to even induce DNA bending. The charge of the internal platinum atom(s) is important to anticancer activity of the complex, being associated with increased cellular accumulations as proposed for the involvement of polyamine transporters.^[120] Therefore, metal centers

in molecules that are positively charged are favored to bind to the negatively charged biomolecules.

Another way of reducing side effects of platinum drugs is to increase their targeting property towards the nuclear DNA, still considered the “key” site to anticancer activity. Metallo-drugs, such as platinum based ones, have been conjugated to molecules with high affinity for DNA. Platinum(II) or (IV) compounds have been combined with oligonucleotides or PNA (peptide nucleic acid) sequences and have shown some ability to overcome cisplatin resistance and sequence specific inhibition of certain oncogens.^[114] Sequence specificity was also achieved using minor groove binders, like pyrrols and imidazole sequences that can direct the platinum complex towards particular DNA sequences.^[121,122]

To facilitate the comparison between platinum complexes, the following possible research parameters can be summarized: nature of non-labile ligand or carrier ligand; nature of the labile ligand or leaving group; type of atoms that link ligands to the platinum atom; oxidation state of platinum atom; nature of axial groups in Pt(IV) ligands; nuclearity or number of platinum atoms in the platinum complexes; formal charges present in the molecule; intrinsic bioactivity of some ligands or bioactivity induced by molecules attached to ligands by linkers.^[110]

As a general remark regarding the platinum drug design strategy it can be stated that, compared to the classical cisplatin, all ligand types coordinated to the metal center can be modified.^[110,123] Furthermore, combination with specific DNA targeting molecules is considered to be essential in order to obtain increased biological activity, concretized in possible new Pt-based anticancer agents. Nevertheless, cisplatin represents the most successful model as lead structure.

3.2.4 The Approach of This Study

DNA bending is a significant biological process. Structural studies of DNA bending proteins, such as the HMG proteins,^[20,124] a key factor in cisplatin efficiency, or the IHF proteins,^[38,44] a highly sequence specific DNA binder, have suggested an

important role for electrostatics in protein-mediated DNA bending. Charged peptides are known to induce bending.^[39,41,125] Targeting of polyanionic DNA by cisplatin and related compounds is known to be facilitated by the presence of positive charges on the metal center or closely related groups.^[12,25] Generally, the charged metabolites create an influx also for the non-charged drug, further contributing to the activity.

The approach of this study to achieve platinum drug analogs with enhanced selectivity and solubility makes use of the interaction of DNA with a positively charged peptide that is modified with a platinum chelating moiety. More precisely, the synthetic scheme involves building molecules that contain both a *DNA bending peptide* with positive charges to wrap around DNA and *an artificial (amino acid) side chain with Pt-chelating properties* (Figure 3.10).

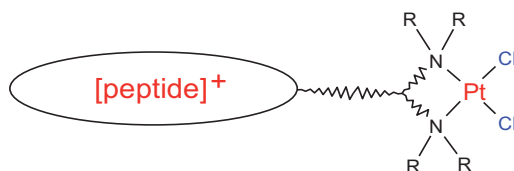


Figure 3.10. General research scheme for designing new platinum analogs. Dashed bond represents variability of the chain (aliphatic or aromatic) in the ligand structure, R – H or alkyl; in blue – the leaving groups, in red – the reactive centers of the molecule.

The two research directions, *nonspecific and specific DNA targeting* using peptides, make use of peptide constructs with the property of inducing structural distortions, such as bending and/or unwinding. A prebent DNA is supposed to facilitate covalent binding of platinum compounds to dsDNA.

We have synthesized platinum drug candidates derived from the cisplatin structure; more precisely, modifications were performed to the ammine ligands region, by chelating the platinum unity to bidentate (amino) acid functionalized building blocks, incorporated into peptides that can interact nonspecifically or specifically with the DNA, such as DNA bending peptides imitating the IHF. Binding to the dsDNA was investigated with encouraging positive results.

4. Synthesis and DNA Binding Studies of Cisplatin Analogues Modified with Nonspecifically DNA Targeting Peptides

4.1 Synthesis of Platinum Complex/Nonspecific Peptide

Chimera

Our research scheme for synthesis of new DNA-Pt binders involves on the one hand synthesis of platinum chelating building blocks, on the other hand the synthesis of peptides responsible for nonspecific electrostatic interaction, making use of classic organic synthesis and solid phase peptide synthesis (SPPS) employing the Fmoc (9-fluorenylmethyloxycarbonyl) protocol.

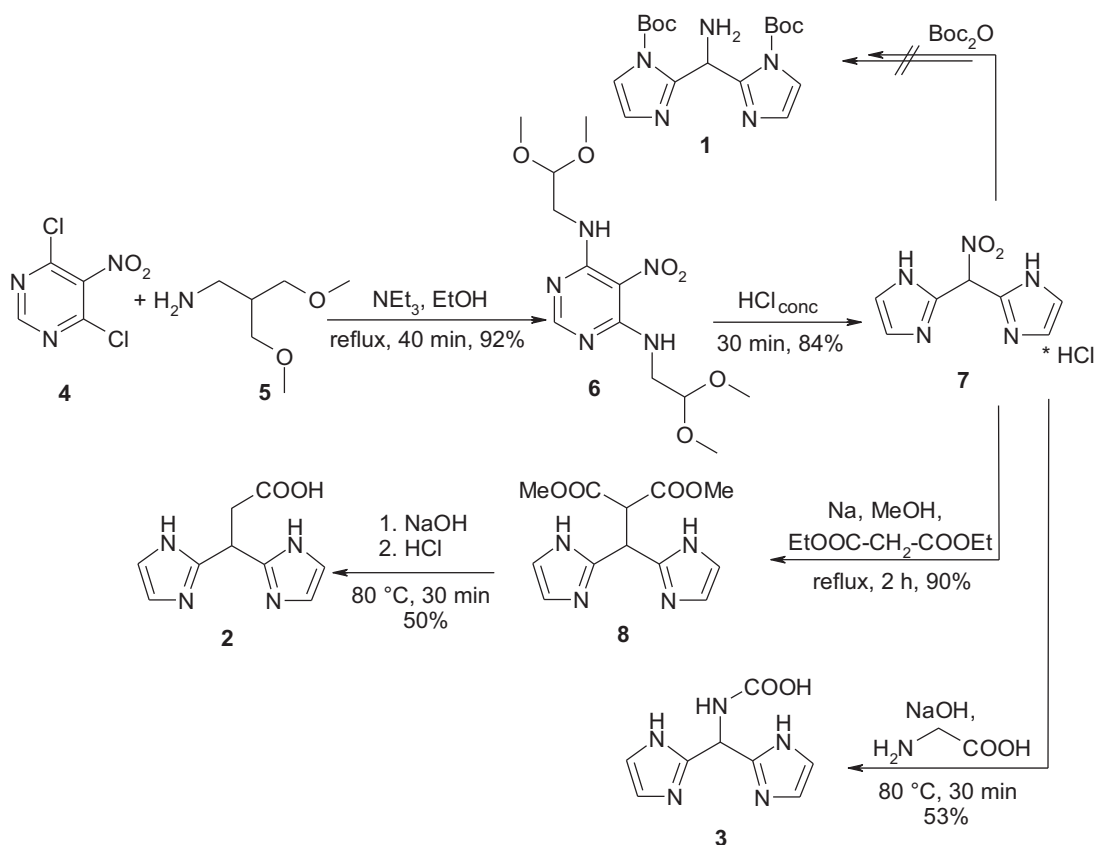
4.1.1 Synthesis of Platinum Chelating Building Blocks

Organic synthesis involved the design of aliphatic or aromatic building blocks that have a platinum coordination site, but also an additional amino or acid group for later peptide coupling.

Initially, a bisimidazole derivative was thought to be a suitable candidate since it was known that such aromatic systems do exhibit anticancer activities.^[126,127] Scheme 4.1 shows the approached synthetic pathway. Compounds **1**, **2** and **3** were the first considered targets that were matching our purposes. Compound **1** had an amino side chain, whereas **2** and **3** had carboxylic acid function. Synthesis was done according to literature procedures.^[128,129] Synthesis of compound **1** implied Boc protection of the corresponding nitrobisimidazole derivative **7**, followed by reduction to the amino function. Since Boc protection was unsuccessfully (possible steric hindrance), building block **1** could not be synthesized, although standard protocols (Boc₂O,

NaOH/KHCO₃ in dioxan-water)^[130] or other procedures (β -cyclodextrine, DMAP, NaH) were applied.^[131]

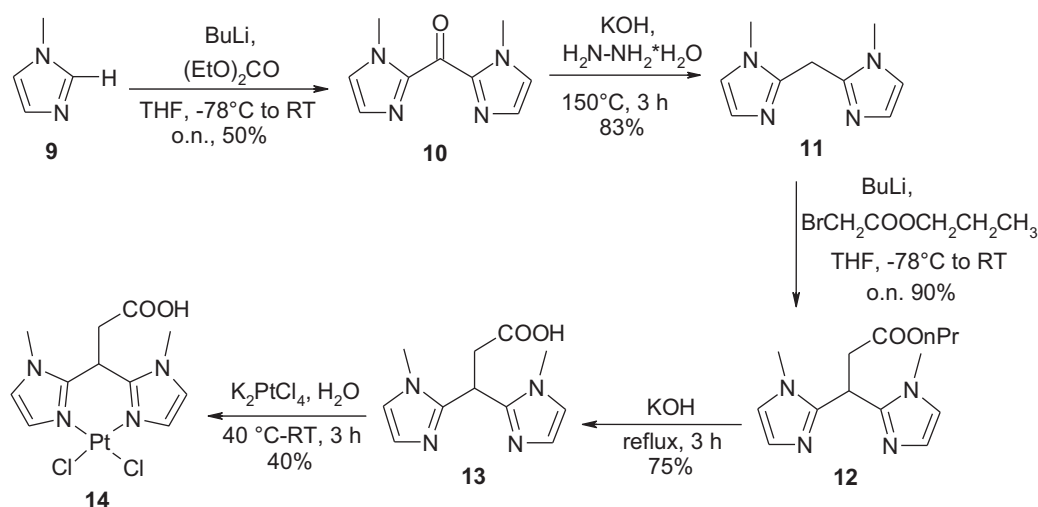
The building blocks **2** and **3**, bearing a carboxylic acid function, were designed so that after peptide coupling would result a target molecule having a free C-terminus (an amide dead end, with an increased stability) instead of an N-terminus.



Scheme 4.1 Synthesis route for the bisimidazole ligands **1**, **2**, **3**.

Compounds **2** and **3** were successfully synthesized (Scheme 4.1). Compound **2** experienced solubility problems since it was only soluble in hot water. Therefore, coupling with a peptide failed even at higher temperatures (50 °C). Boc protection^[132] or generating the active ester (with PFPOH–pentapfluorophenol)^[133-136] of compound **2** was not successful. Since Boc protection of the bisimidazole ligand has proved to be difficult, compound **3** was considered to have too many competitive platinum coordination sites.

Another approach (Scheme 4.2) was to synthesize the methylated bisimidazole building block in analogy to literature procedures by formation and then conversion of keto-bridged bisimidazole and subsequent reduction to the methylene-bridged compound.^[137,138] Cleavage of the ester **12** under alkaline conditions gave the desired ligand **13** in 75% yield and was used further for SPPS. As reference for DNA binding studies, the platinated analogue **14** (40% yield) was synthesized by heating for 3 h at 40 °C using K_2PtCl_4 as platination agent.

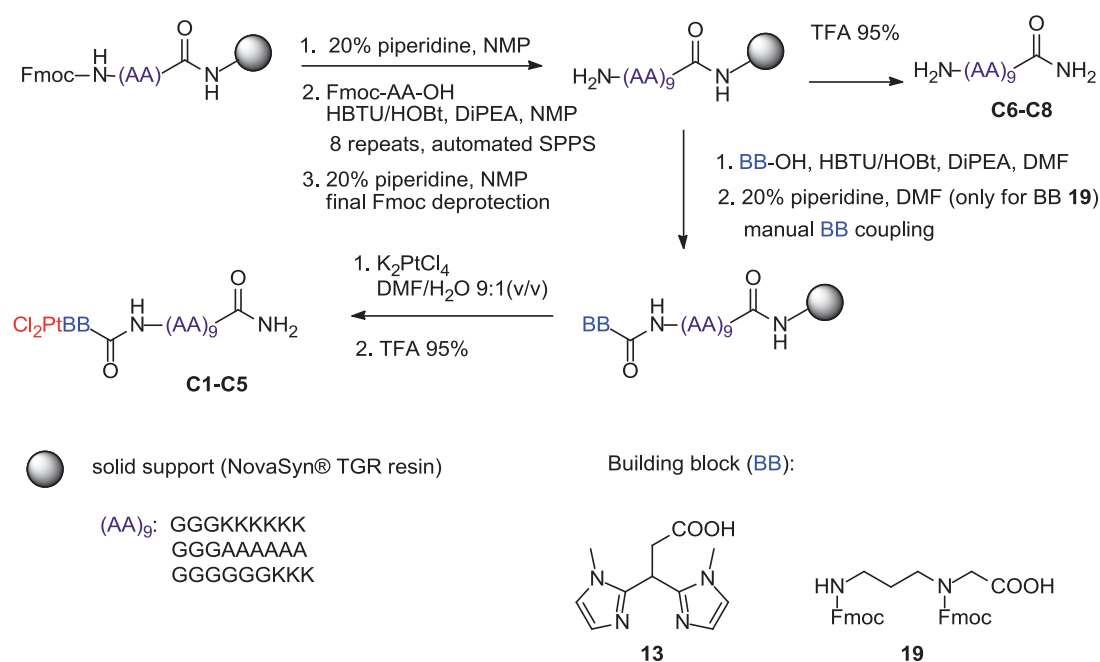


Scheme 4.2 Synthesis route for the bisimidazole building block **13** used for SPPS, and the respective cisplatin analog **14**.

The second type of building block with platinum chelating ability was an aliphatic system. Aminopropyl glycine was chosen as a flexible and sterically not demanding platinum binding site. The synthesis of building block **19** was obtained in analogy to the preparation of the respective ϵ -bisamine^[139] starting with the nucleophilic substitution of *tert*-butyl bromoacetate **16** by 1,3-diaminopropane **15** yielding amino acid **17** in 90% yield (Scheme 4.3). Fmoc protection of both amino groups gave **18** in 65% yield. Ester cleavage provided building block **19** (85% yield) that was directly introduced in the final SPPS coupling step. Synthesis of its cisplatin analog **21** implied standard Boc deprotection of **17** in quantitative yield, followed by platination using K_2PtCl_4 (30% yield).

peptide sequences with a various number of positively charged side chains were prepared: H-(GGGKKKKKK)-NH₂ (**C6**), H-(GGGGGGKKK)-NH₂ (**C7**), and H-(GGGAAAAA)-NH₂ (**C8**) (Scheme 4.4). Therefore, a gradual charge interaction with DNA was investigated. Furthermore, building blocks **13** and **19** were coupled to the *N*-terminus of the respective oligomers by manual SPPS also using HBTU/HOBt activation. The final assembly of platinum complexes was performed with the resin bound oligomers, with subsequent cleavage of the constructs from solid support by treatment with TFA. After purification by HPLC, the desired platinum complex/peptide chimera (**C1–C5**) were obtained and characterized by HR-MS.

To be mentioned also the complex between **21** and **C8** was synthesized (HR-MS evidence), that is the platinated propylenediamine-alanyl based complex, but it could not be purified due to limited solubility. Therefore, it was not used in the DNA binding studies.



Scheme 4.4 Preparation of peptides and platinum complex/peptide chimera by Fmoc-SPPS.

In conclusion, it was achieved the synthesis of five platinum complex/peptide chimera **C1–C5** that contain cisplatin analogs covalently linked to peptides varying with respect to the amount of positive charges in the amino acid side chains (Figure

4.1). The presumption was that the presence of charged peptides would facilitate in particular electrostatic DNA pre-association and bending of the DNA target. The newly synthesized platinum(II) complexes were based on bisimidazole ligands or propylenediamine and combined with nonapeptides containing six (**C1** and **C2**) or three lysinyl units (**C3** and **C4**) or non-charged alanyl units (**C5**).

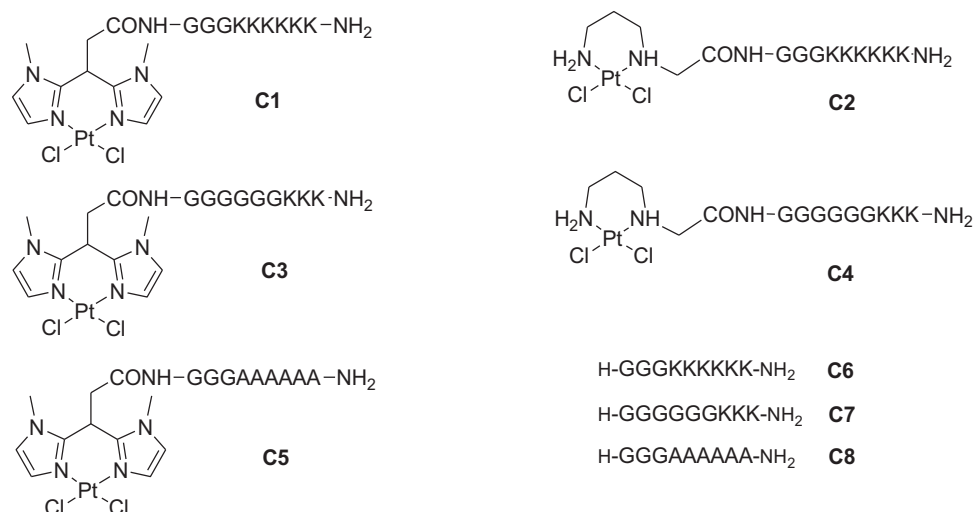


Figure 4.1 Platinum complex/peptide chimera **C1–C5** and the respective reference peptides **C6–C8**.

4.2 DNA Binding Studies of the Cisplatin Analogs

The DNA binding properties were investigated by agarose and polyacrylamide gel electrophoresis, propidium iodide intercalation and thermal denaturation studies. Typically, enhanced adduct formation was found to take place for platinum complex/peptide chimera and DNA in the presence of positively charged peptides. The observation sustains the suggested idea of using platinum complex/peptide chimera as novel DNA-modifying agents.

4.2.1 Plasmid Binding Studies

The DNA conformational changes induced by platination were visualized by agarose gel electrophoresis in a gel mobility shift assay of platinum exposed circular plasmid.^[142] After platinum binding, DNA unwinding takes place, and both supercoiled and relaxed forms can be visualized by agarose gel electrophoresis. The increase in the amount of platinum complex bound to DNA induces the decrease in the migration rate of the supercoiled plasmid band.

Considering the property of cisplatin and analogs as DNA unwinding agent,^[15] we investigated the DNA binding affinity of platinum complex/peptide chimera **C1–C5**, peptides **C6–C8** and the platinated building blocks **14** and **21** with the negatively supercoiled pUC18 plasmid. The ratio of nucleotide concentration (C_{DNA}) and concentration of platinum compounds (C_{Pt}) ($r_f = C_{\text{Pt}}/C_{\text{DNA}}$) was varied in the range of 0–0.3 (Figure 4.2).

As expected a pronounced effect was detected for the positively charged lysine-glycine containing complexes. Thus, the bisimidazole platinum complex/peptide chimera **C1**, which at *pH* 5.8 contains six positively charged lysinyl residues, led to unwinding of the plasmid already at low concentrations. However, smearing of the bands was observed, as well as complete retardation of the DNA migration at $r_f = 0.15$ – 0.2 , simply based on charge neutralization (Figure 4.2). A similar gel migration pattern was observed for the reference peptide **C6** which is in accordance with the charge neutralization effect. In general, for the lysinyl containing oligomers DNA precipitation was observed already at $r_f = 0.5$. Therefore, gel mobility shift assay was performed until $r_f = 0.3$. The propylenediamine platinum complex **C2** with the same peptide sequence as **C1** provided a similar result with respect to retardation, but more defined unwinding of the plasmid up to $r_f = 0.15$ was observed. A critical value was pointed around $r_f = 0.076$ for the lysinyl peptides **C1** and **C2**.

Decreasing the amount of charged lysinyl side chains within the peptide to three provided an interesting observation. In contrast, both platinum complexes in combination with the peptide sequence G₆K₃ (**C3** and **C4**) led to distinct plasmid

unwinding. For the propylenediamine platinum complex **C4** the coalescence point was almost reached at a platinum complex/DNA concentration of $r_f = 0.3$, whereas the peptide **C7** was not sufficient for plasmid binding. Without the platinum moiety attached to the peptides, no effect of binding was observed. Thus, the combination of platinum complex and positively charged peptide is indicated to provide improved DNA binding.

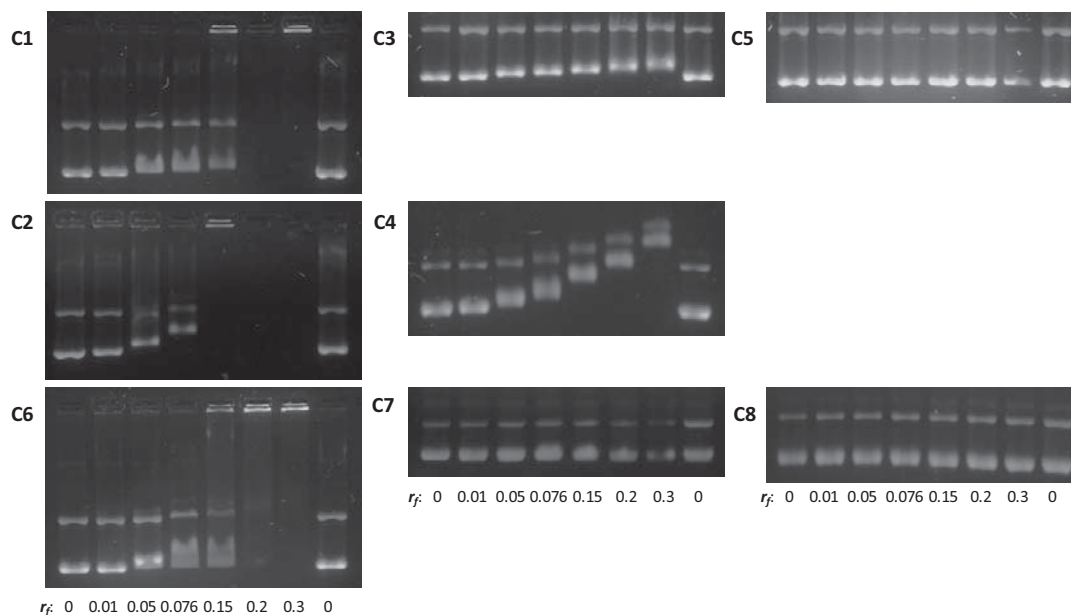


Figure 4.2 Gel mobility shift assay of platinum complex/peptide chimera **C1–C5** and peptides **C6–C8** with supercoiled and relaxed forms of the pUC18 plasmid (incubation for 2 h, 32 °C with r_f varying from 0 to 0.3, 10 mM $\text{Na}_2\text{HPO}_4/\text{NaH}_2\text{PO}_4$, pH 5.8, $[\text{pUC18}] = 0.15$ mM nucleobases).

Comparison of the two types of complexes with respect to binding efficacy clearly indicates the superiority of the propylenediamine ligand over the bisimidazolyl ligand. Platinum binding might be obstructed by the sterical hindrance and lower conformational flexibility of the aromatic ligand system compared to the more site accessible and smaller aliphatic diamine.

As a final proof of the charge requirement for improved platinum-DNA interactions, was the study of the platinum complex chimera containing the non-charged glycine-alanine peptide sequence **C5**, as well as the peptide **C8** binding to the plasmid. Thus,

no mobility shift in the gel up to $r_f = 1.0$ was induced when using non-charged peptides. Similarly, the platinated building blocks **14** and **21** lacking the peptide chain showed no gel mobility shift up to an $r_f = 0.8$ (Figure 4.3).

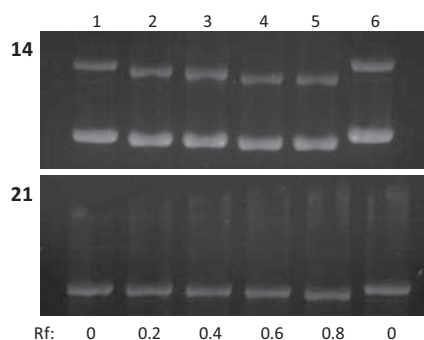


Figure 4.3 Gel mobility shift assay of platinated building blocks **14** and **21** with supercoiled and relaxed forms of the pUC18 plasmid (incubation for 2 h, 32 °C with r_f varying from 0 to 0.8, 10 mM $\text{Na}_2\text{HPO}_4/\text{NaH}_2\text{PO}_4$, pH 5.8, $[\text{pUC18}] = 0.15$ mM nucleobases).

4.2.2 Oligonucleotide Binding Studies

Another method to investigate DNA recognition and covalent binding of the cisplatin analogs was polyacrylamide gel electrophoresis. The single-stranded 22-mer DNA 5'-TCTCCTTCTTGGTTCTCTTCTC-3' was used as target. With only one d(GpG) site a defined binding stoichiometry was expected. The DNA was radio-labeled at the 5'-end using polynucleotide kinase and $[\gamma\text{-}^{32}\text{P}]\text{-ATP}$.

The respective platinum complex/peptide chimera and control peptides were added to the DNA (650 cps/reaction) in 10 mM phosphate buffer, incubated at room temperature for 18 hours, and analyzed under denaturing conditions. Titration studies were initially performed to allow formation of a single adduct. At 1 μM concentration for all complexes a shift in the gel was detected only for **C1-C4**, whereas 10 μM was needed for the rest of the complexes in order to give similar effect. Therefore, a concentration of 1 μM was used for the lysinyl containing complexes **C1-C4** and 10 μM for all other complexes and the peptides as shown in Figure 4.4.

It is known that both covalent binding and electrostatic association of larger molecules to DNA induce changes in gel migration patterns of the resulting structurally distorted DNA. Larger molecules and bent oligomers are expected to migrate slower in a polyacrylamide gel.^[41,76,143] The shifted bands can be correlated to the amount of charge neutralization, but the influence of the complex size or DNA bending might also contribute to the observed gel shifts.

The platinum complex/peptide chimera **C1–C4** were all found to give rise to a major reaction product with retarded gel mobility indicative of efficient platinum binding. Stronger migration retardation was observed for the platinum complex/peptide chimera with six lysinyl residues (**C1** and **C2**) as an effect of the influence of the positive charge of the lysinyl side chain. Nevertheless, the results show that the platinum moiety is indeed required for DNA binding, since the charged peptides **C6** and **C7**, lacking the platinum complex, did not cause any significant gel shifts under these conditions (Figure 4.4). The requirement of charged peptides for efficient binding is further indicated by the study of complex **C5** and **C8** which also do not interact with the DNA at any of the reaction conditions.

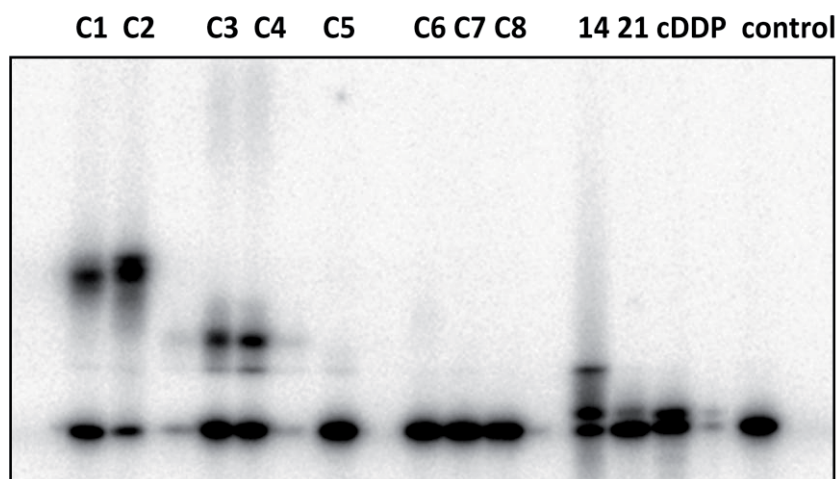


Figure 4.4 Autoradiogram of platinum complexes **C1–C5**, peptides **C6–C8**, platinum complexes **14** and **21** as well as cisplatin with radio-labeled DNA 5'-TCTCCTTCTTGGTTCTTCTC-3'. A 1.0 μ M complex concentration was used for **C1**, **C2**, **C3** and **C4**; all other derivatives were added in 10 μ M concentration. The samples were separated on a 0.2 mm, 20% denaturing polyacrylamide gel (PAA/8 M urea).

However, only at ten times higher concentration (100 μM) of **C5**, a slower migrating platinated product can be visualized (Figure 4.5). Even at this high concentration, no band retardation is seen in the gel upon addition of the unconjugated peptides, **C6–C8** (Figure 4.5).

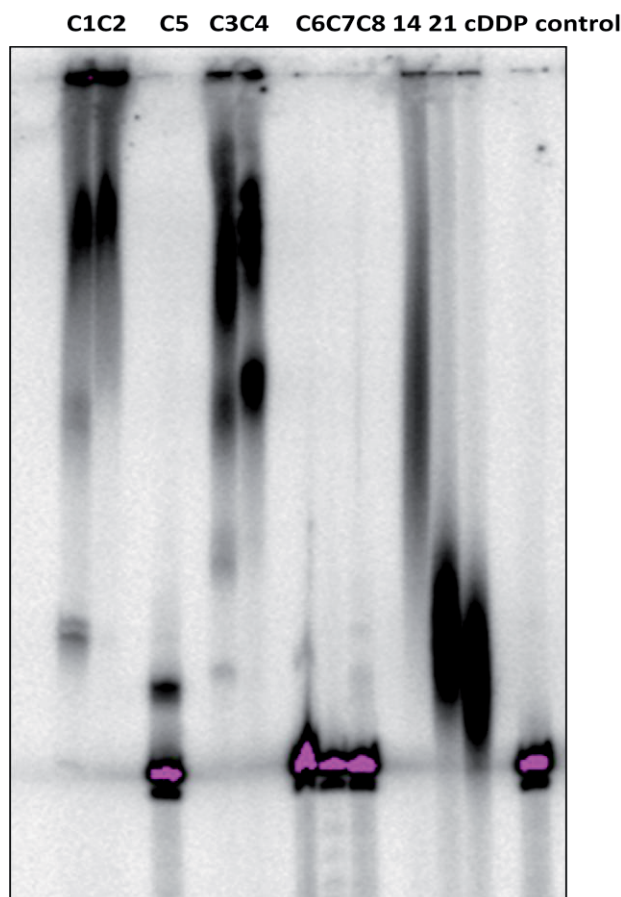


Figure 4.5 Autoradiogram of platinum complexes **C1–C5**, peptides **C6–C8**, platinum complexes **14** and **21** as well as cisplatin with radiolabeled DNA 5' TCTCCTTCTTGGTTCTCTTCTC-3'. All the complexes are in large excess at an end concentration of 100 μM . The samples have been separated on a 0.2 mm, 20% denaturing polyacrylamide gel (PAA/8 M urea).

At this high concentration the lysine complexes give rise to stable large aggregates. When the two different types of platinum coordination spheres are compared, it is obvious that the platinum complexes bound to the propylenediamine ligand (**C2** and **C4**) showed a significantly higher DNA binding compared to the corresponding bisimidazolyl ligand oligomers (**C1** and **C3**). The cisplatin analogs **14** and **21** lacking

the peptide moiety and cisplatin alone were also shown to interact with DNA, but ten times higher concentrations were needed to obtain distinct gel retardation.

In summary, the pronounced band shifts were obtained for the platinum complex/peptide chimera. It sustains the idea that attachment of charged peptides to the platinum moiety can be used to facilitate covalent nucleic acid binding. Regarding the platinum complexes **14** and **21**, it required ten times higher concentration compared to the platinum complex/peptide chimera for efficient DNA-binding, whereas no DNA interaction was indicated for the charged peptides lacking the metal binding site.

Therefore, it can be concluded that the ability of this platinum complex/peptide chimeras to preassociate and bend the DNA contributes with an influential reaction step in the mechanism of covalent DNA modification by these presently investigated compounds and related analogs.^[142]

4.2.3 Fluorescence Intercalation Studies

DNA structural changes induced by the platinum complex/peptide chimera were investigated by using propidium iodide (PI) fluorescence studies. Thus, the PI intercalation was monitored in the absence or presence of the different platinum complex/peptide chimera. As previously shown, the PI fluorescence increases during intercalation with double-stranded DNA due to π - π stacking interactions between the cationic dye and DNA nucleobases.^[144,145]

After pre-incubation of the platinum complexes **C1–C5** and peptides **C6–C8** (10 mM Na₂HPO₄/NaH₂PO₄, pH 5.8; $r_f = C_{\text{complex}}/C_{\text{nucleotide}} = 0.083$; samples were pre-incubated for two hours at 32 °C), with herring DNA, PI was titrated into the resulting solution. The r_f value was determined after titration studies (higher concentration induced precipitation). The fluorescence was measured as a function of r_f , and the corresponding experimental data are shown in Figure 4.6.

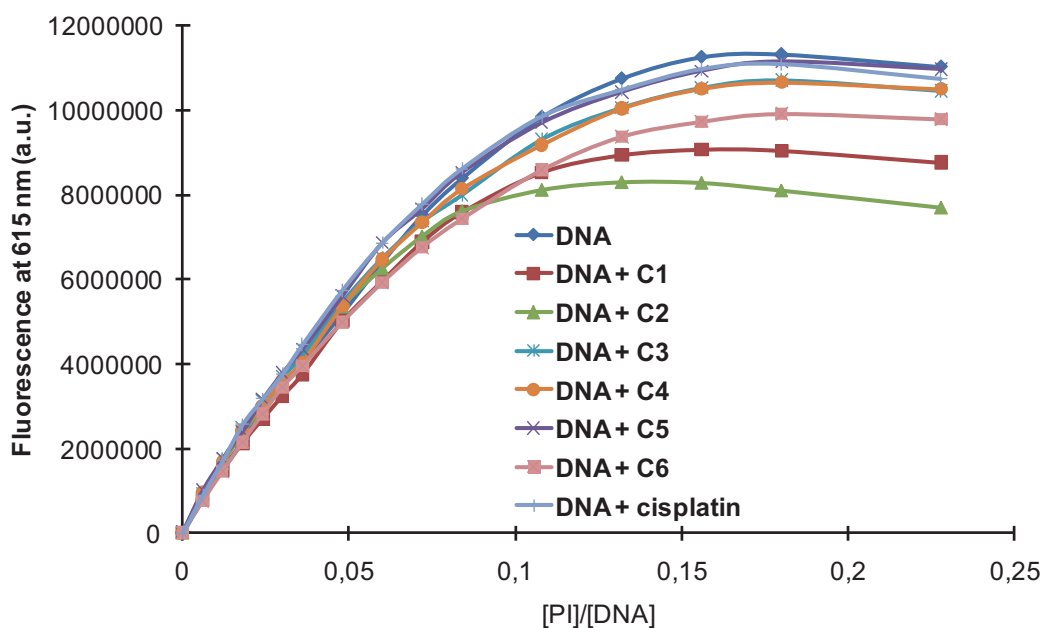


Figure 4.6 PI fluorescence as a function of r_f in the presence of C1–C6 and cisplatin with herring DNA as target.

It can be observed that all reaction mixtures exhibit similar features with an initial increase of fluorescence as a result of increasing r_f , but reaching a saturation fluorescence at r_f -values in the range 0.1–0.2. However some interesting differences can be observed. For example, it is strongly noticeable that the saturation fluorescence is influenced by the nature of the added compounds. The effect is particularly pronounced for compounds C1, C2 and C6, i.e. in the presence of the hexavalent nonapeptide, both unconjugated (C6) and conjugated to the platinum complexes (C1 and C2). Compound C2 gives rise to the largest reduction of PI fluorescence, *ca.* 30%.

Thus, these data suggest that the presence of these compounds on the DNA surface is enough to efficiently block the access of PI to intercalation sites on the DNA. Therefore, the flexibility of the double helix is decreased upon platination with these complexes. The observation is in line with the previously suggested structural effect observed e.g. during the plasmid binding studies (Figure 4.2). Additional support for a reduction of accessible PI intercalation sites on the DNA surface is also given by the fact that the plateau-value is reached earlier for the platinum compounds, with r_f -

saturation values at ca 0.14 and 0.16 for **C2** and **C1**, respectively, as determined by first-derivative analysis. It can be concluded that whereas the non- and trivalently charged platinum complex/peptide chimera still allow for PI intercalation in good agreement with the *Neighboring Exclusion Principle*,^[65,74] the presence of the hexavalent platinum complex/peptide chimera leads to an electrostatic contribution to the surface binding that is not readily displaced by PI. Furthermore, the platinum complex/peptide chimera **C3** and **C4** (three lysinyl units) caused only a minor effect, and the non-charged platinum complex/peptide chimera **C5** had no influence on PI intercalation.

Finally, very minor effect was seen for the peptides **C7** and **C8** or for the platinated building blocks **14** or **21** (Figure 4.7). These data are in agreement with the previously discussed evidence obtained from the pUC18 plasmid gel shift assays of the hexavalent lysinyl unit as the moiety with the largest binding affinity and ability to induce DNA structural changes.

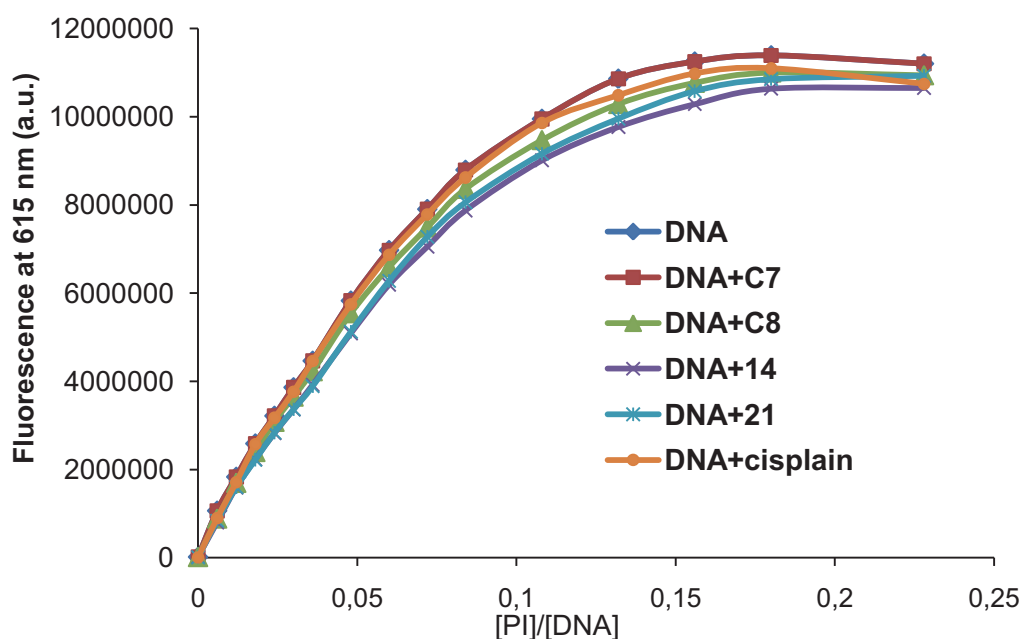


Figure 4.7 PI fluorescence as a function of r_f in the presence of **C7**, **C8**, **14**, **21** and cisplatin with herring DNA as target.

4.2.4 Thermal Melting Studies

Temperature dependent UV spectroscopy provided further insight into the interaction between the platinum complex/peptide chimera and DNA. Whereas covalent platinum binding can be expected to decrease the thermal stability of the duplex, its interaction with the charged peptides likely gives rise to the opposite effect.^[146,147] At the present reaction conditions (1.0 μM dsDNA 1, 10.0 mM $\text{Na}_2\text{HPO}_4/\text{NaH}_2\text{PO}_4$, pH 5.8) the double strand formed by DNA oligomers 5'-TCTCCTTCTTGTGTCTCTTCTC-3' and 3'-AGAGAGGAAGAACACAGAGAAG-5' provided a melting temperature of, $T_m = 37.0$ °C. The platinum complex/peptide chimera and peptides were added in a 4 μM concentration. The thermal melting values are given in Table 4.1.

System	T_m (°C)
Control, DNA only	37.0 (± 0.4)
C1, G ₃ K ₆ -Pt complex	44.5 (± 1.3)
C2, G ₃ K ₆ -Pt complex	50.5 (± 1.0)
C3, G ₆ K ₃ -Pt complex	36.7 (± 0.6)
C4, G ₆ K ₃ -Pt complex	37.9 (± 0.9)
C5, G ₃ A ₆ -Pt complex	36.1 (± 1.6)
C6, G ₃ K ₆ peptide	49.1 (± 1.0)
C7, G ₆ K ₃ peptide	46.1 (± 1.5)
C8, G ₃ A ₆ peptide	37.2 (± 1.5)

Table 4.1 Thermal melting studies of dsDNA (1.0 μM) in 10.0 mM phosphate buffer (pH 5.8). Platinum complex/peptide chimera and peptides were added in 4 μM concentration, T_m in °C with standard deviation.

It can be observed a comparable increase of the thermal melting temperature for the polylysinyll complexes **C1** ($T_m = 44.5$ °C), **C2** ($T_m = 50.5$ °C) and the respective peptide **C6** ($T_m = 49.1$ °C), thus indicating that the stabilization caused by positively charged peptides is dominating (Figure 4.8).

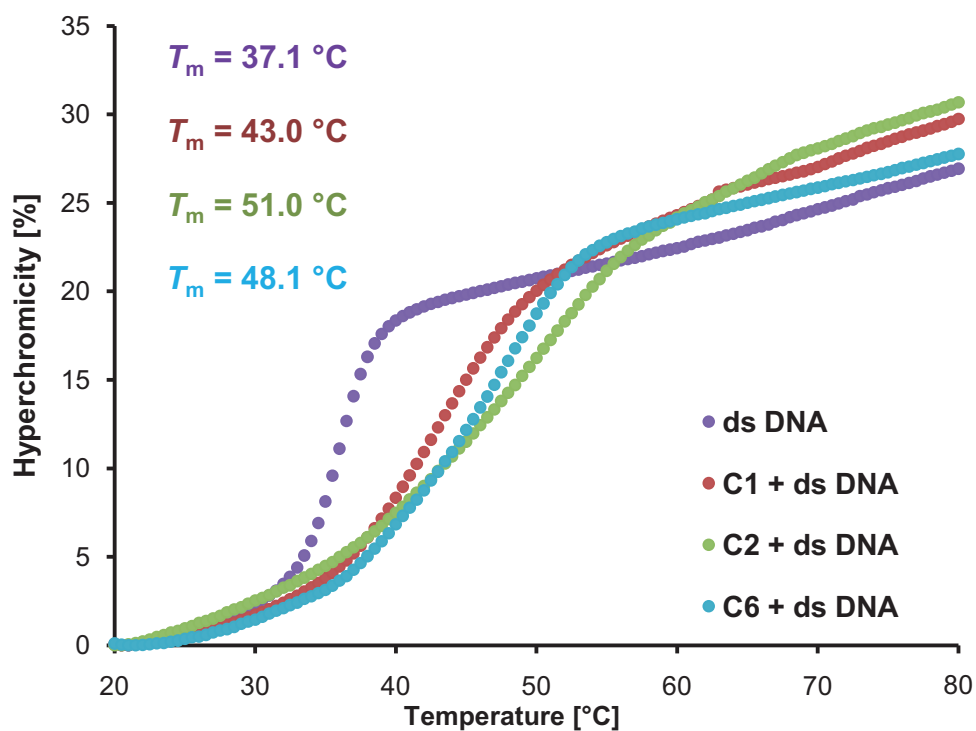


Figure 4.8 A representative thermal melting study of dsDNA, both before and after preincubation with platinum complexes **C1**, **C2** and the polypeptide **C6** ($C_{\text{dsDNA}} = 1.0 \mu\text{M}$, $C_{\text{C1,C2,C6}} = 4.0 \mu\text{M}$, $C_{\text{buffer}} = 10.0 \text{ mM}$, $pH 5.8$).

In accordance with gel electrophoresis and fluorescence results the propylenediamine platinum complex **C2** provided a stronger DNA stabilizing effect compared to the bisimidazolyl ligand system **C1**, i.e. indicating also an influence from the platinum binding moiety. Nevertheless, as indicated by the T_m obtained for DNA stabilization in the presence of peptide **C6**, the charge neutralization can be considered as the main contribution.

4.2.5 Conclusions

The *nonspecific DNA-peptide approach*, evaluated the potential of a novel type of extended, charged platinum complex/peptide chimera with respect to efficient DNA targeting. Covalent binding of cisplatin analogs to DNA was found to be directed by platinum coordination, as well as positive charges located at the platinum complex or in the ligation sphere. Evidence was given by electrophoresis, fluorescence intercalation studies and temperature-dependent UV spectroscopy.

Two different metal-chelating moieties, both linked to nonamer polypeptides, were successfully synthesized by coupling of the chelated metal complex to the polypeptide using solid phase peptide synthesis. The choice of the chelating moieties, the bisimidazolyl- and the propylenediamine-ligands, respectively, proved to influence the reactivity of these complexes. Thus, the propylenediamine complexes were found as the more reactive ones, most likely due to steric effect, where the more flexible polypropylene ligand allows for more suitable location of the platinum center in close vicinity of the reactive groups on DNA.

It was shown that an increased charge on the nonapeptide moiety (0, +3, and +6) indeed facilitates the interaction. It seems reasonable to assume that the improved binding observed, in particular for the hexavalent compounds **C1** and **C2**, is caused by a combination of i) maximized electrostatic attraction to the DNA surface and ii) increased flexibility of the DNA structure around the association site, both facilitating formation of the structurally distorted, platinated DNA structure. The most promising candidate was found compound **C2**, for which interactions with DNA were observed at a *ca.* 10-fold lower concentration compared to cisplatin. Further, for this compound the adduct formation was accompanied by a *ca.* 13 °C increase of the melting temperature, consequently suggesting formation of a DNA-adduct with high energetic demands during formation of the single-stranded DNA needed for e.g. efficient repair.^[13]

This study indicates the potential of cisplatin analogs as hybrids with charged peptides, especially since cationic amino acids might be combined with specific

recognition or DNA bending sequences. It can be stated that this synthetic strategy deserves to be explored further towards the goal of providing highly efficient drug alternatives to cisplatin.

5. Synthesis and DNA Binding Studies of Cisplatin Analogs Modified with Specifically DNA Targeting Peptides Derived from IHF

5.1 IHF – Integration Host Factor

5.1.1 General Structure

IHF of *Escherichia Coli* is a DNA-bending protein and belongs to the group of histone-like proteins.^[148] Bending is important in DNA packing and in regulating diverse cellular processes. Although first discovered as a host protein required for lysogeny by bacteriophage λ , IHF is involved in many processes that lead to high ordered protein-DNA complexes: e.g. in DNA replication by binding to *ori C*, in transcriptional regulation by binding upstream of many σ -dependent promoters, and in different site specific recombination systems.^[38,149] Like HMG domain proteins, IHF has architectural elements in the assembly of nucleoprotein structures.

The general structure shows IHF as a small heterodimeric protein made up of α and β subunits, ~10 kDa each, that are ~30% identical in sequence. Each IHF subunit contains 5 β -sheets (S) and 3 α -helices (H). The order of S and H is H1-H2-S1-S2-S'2-S'3-S3-H3 (Figure 5.1).

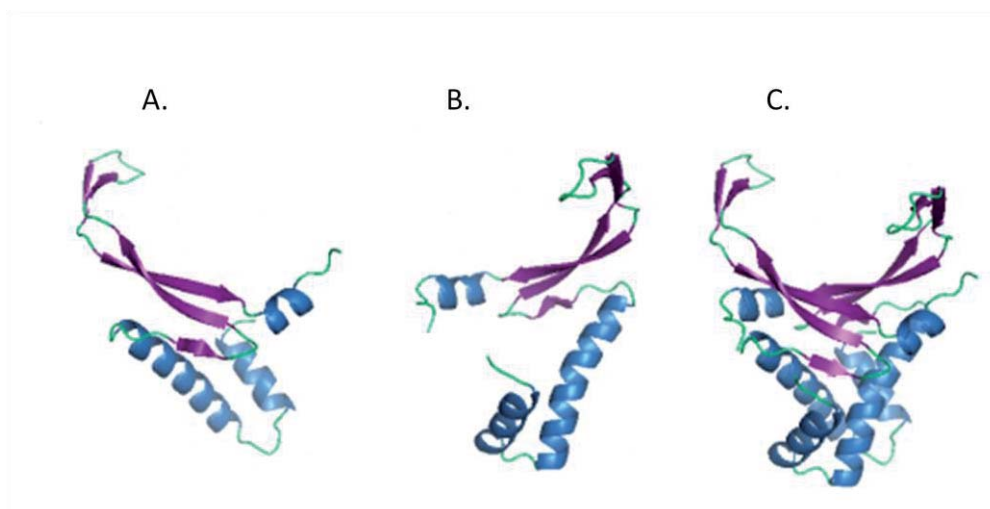


Figure 5.1. Molecular Structure of the IHF subunits α (A) and β (B) units and the overall structure (C).

The structure of IHF is closely related to the histone-like protein (HU), a nonspecific DNA binding protein that also bends the double strand and belongs to the same protein family.^[43,44,150] Despite the structural similarity (each subunit of IHF is nearly 40% identical in sequence to HU), IHF binds to DNA in a sequence specific manner, thus, facilitating both, biochemical and structural characterization of the complex.

5.1.2 Interaction with DNA – Binding and Bending

IHF was cocrystalized with a 35 base pairs (bp) DNA fragment containing the H' site of phage λ ^[43,44]. It revealed the two subunits to form a largely α -helical body, with certain content of basic amino acids (e.g. lysine, arginine), followed by β -sheets that are extending into two flexible β -ribbon arms (Figure 5.2). These arms recognize dsDNA in the minor groove and wrap around it, whereas the positively charged protein core interacts nonspecifically mainly with the polyanionic DNA phosphate backbone. A proline residue (P65- α /P64- β) is positioned at the tip of each arm, and intercalates into the DNA double strands, disrupting the stacking interactions between the base pairs and inducing a U-turn in the DNA structure by an overall bend of $\sim 180^\circ$. The majority of the bending occurs at two kinks nine bp apart. The bend is stabilized by electrostatic interaction with the positively charged body of the

protein (26 positively charged side chains, as well as the *N*-termini of the helices in the heterodimer body).^[44]

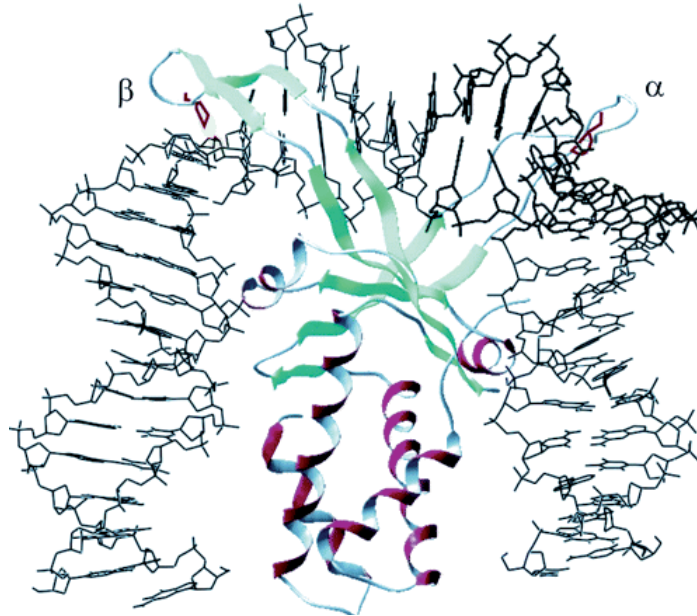
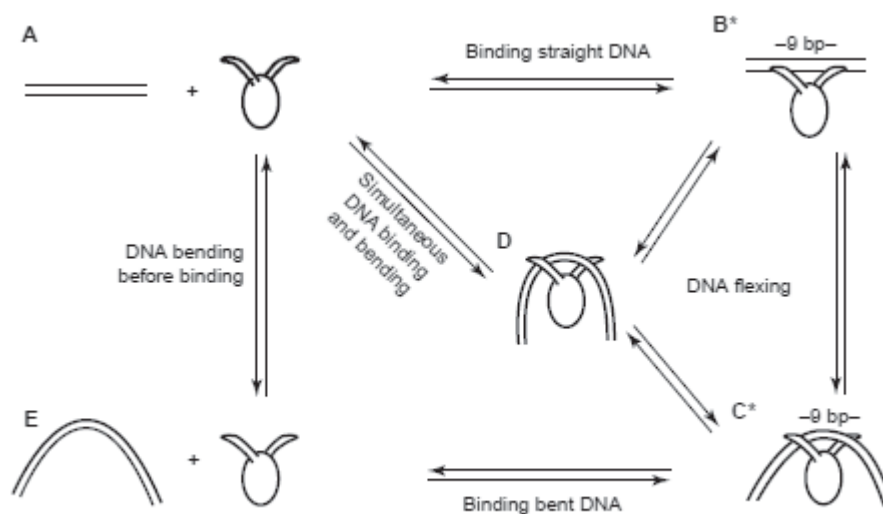


Figure 5.2 Molecular structure of IHF-DNA complex. The intercalating proline residues of each arm are highlighted in red.^[41,44]

Sequence specificity of IHF recognition is derived from indirect readout by shape recognition of the minor groove next to a negligible amount of hydrogen bonding.^[45] Specificity is assumed to result from the sum of many small interactions, such as two rigid arginines of the α -subunit (Arg⁶⁰, Arg⁶³) reaching into the minor groove and forming hydrogen bonds with conserved nucleobases or with the intercalating proline residues. The contribution to sequence specificity is much higher for the IHF α -arm extending more deeply into the minor groove than the β -arm.

Studies on binding and bending DNA by proteins such as IHF or HU (both DNABII family members), have led to the development of a general scheme for DNA binding and bending effects (Scheme 5.1).^[45] Proteins (C) can bind pre-bent substrates ($E \leftrightarrow C$) or they can bind B-form DNA and then bent ($A \leftrightarrow C$). Concerted binding and bending is showed in $A \leftrightarrow D$ transformation, whereas B^* , C^* are nonspecific complexes induced by the straight or lightly bent complexes with 9 base pairs between the active intercalating prolines.



Scheme 5.1 General scheme for DNA binding by the DNABII family members.^[45]

The intrinsic flexibility of both, DNA substrate and IHF protein (or HU), is source of the protein's ability to facilitate many different cellular processes, and thus, a model for designing small peptide mimics that are used to elucidate the native mechanism of action.

5.1.3 IHF Mimicking Molecules

The design and synthesis of a small peptide with specific DNA binding and bending characteristics derived from the IHF-DNA complex was firstly reported by *E. Liebler et al.* (Figure 5.3.B).^[41,151] The structure of the mimicking peptide involves three parts: 1) a *cyclopetide* – which imitates the minor groove binding loop of the IHF α -subunit, the lead structure for designing the mimicking peptide; 2) a three generation *lysine dendrimer* – imitates the positively charged body of the protein; it provides the water solubility characteristics for the IHF mimic considering that lysine residues are known to get protonated under physiological conditions;^[152] 3) a *glycine oligomer* – for linking the recognition unit with the dendrimer.

For specific recognition and bending the amino acid sequence of the IHF α -subunit was maintained around the intercalating Pro⁶⁵, but limited to 10 amino acids in order to cover only the contact area in the minor groove ('mimic' in Figure 5.1.3).

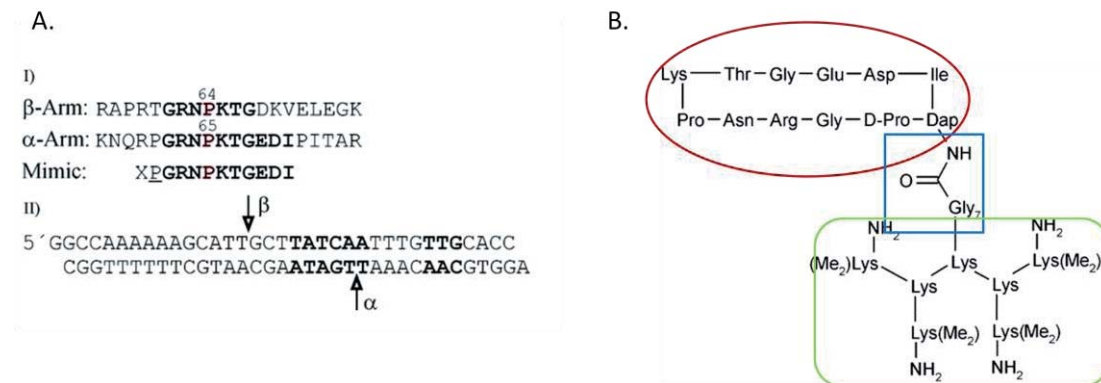


Figure 5.3 A. I) Part of amino acid sequences of the α - and β - subunits of the IHF protein. Conserved sequences are highlighted in bold, the intercalating prolines P65- α and P64- β in red. X – diaminopropionic acid (Dap). P – D-Pro. II) Model DNA sequence used for cocrystalization (Figure 5.2).^[44] The consensus sequence of IHF binding is depicted in bold; the arrows indicate the position of the intercalating prolines P65- α /P64- β . **B.** First IHF mimicking peptide reported by E. Liebler,^[41] containing the cyclopeptide (red), the linker (blue) and the dendrimer (green).

For additional cyclization and attachment of the linker, two amino acids were introduced: D-proline – induces cyclization by its β -turn effect and partially ensured conformational rigidity; diaminopropionic acid (Dap) – provides an additional amino group for attachment of the dendrimer.

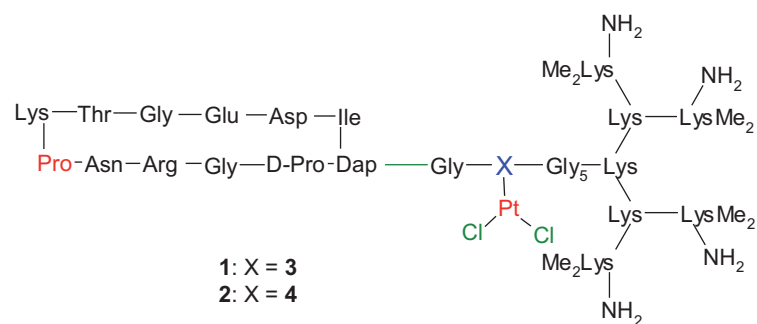
Other IHF mimicking approaches studied in the *Diederichsen* group include: disulfide bridge within the cyclopeptide sequence for conformational stabilization;^[151] the extension of the cyclopeptide, for inducing a larger kink; the replacement of three amino acids from the cyclopeptide area with histidine residues for the purpose of stabilizing conformational preorganization; the construction of dimeric IHF mimics to resemble the heterodimeric basic structure of the IHF or even modifications on the β -subunit of the protein.^[153] Moreover, variation of the intercalating proline was investigated in order to evaluate the influence of size of the side chain residue, aromaticity, conformation of the five-membered ring and the peptide backbone conformation on binding and bending the dsDNA.^[154]

5.1.4 Platinum Modified IHF Mimicking Molecules

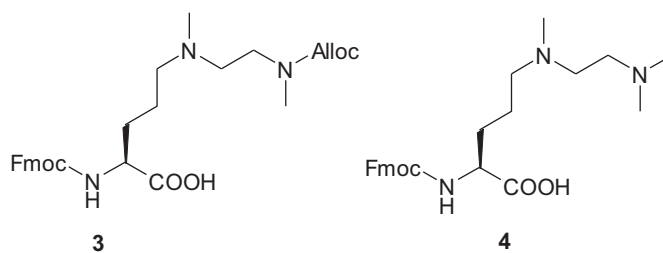
The approach presented in this study involves the synthesis of cisplatin analogs based on the IHF mimicking peptide developed by *E. Liebler* (Figure 5.3.B). The goal was to obtain new potential cisplatin drug derivatives with increased solubility and potential cellular uptake. Addressing sequence specific DNA binding, kinking and bending should be facilitated, with a stronger and more selective covalent platinum binding. Modifications were proceeded within the linker area of the IHF mimic to give the platinated IHF mimicking peptides **22**, **23** by introduction of different artificial amino acids, **24**, **25** providing the platinum coordination sites (Figure 5.4).

The design of the present platinum IHF mimics implied the synthesis of new unnatural amino acids, as well as the use of both, solid and solution phase peptide synthesis. New synthetic routes were approached in order to minimize the number of synthetic steps required in solution phase since SPPS has the advantage of time, yield and easier handling. Platination was carried out in solution. For latter DNA binding experiments, the cisplatin analog reference compounds **26**, **27** were synthesized.

Besides biological activity, modulating the interactions between DNA and peptide incorporated platinum moieties applying IHF mimics was thought to be a useful tool for further understanding of protein/DNA recognition on the molecular level.



X: unnatural amino acids used in the SPPS



→ cisplatin analog references



Figure 5.4 Platinum functionalized IHF mimicking peptides **22**, **23** and their cisplatin analog references **26**, **27**.

5.2 Synthesis of Unnatural Amino Acids

An artificial amino acid was needed for SPPS. Designing and synthesis involved building blocks with two functional sites (Figure 5.5): 1) the amino acid moiety responsible for integration within the peptide; 2) a diamino ligand system as platinum chelating site.

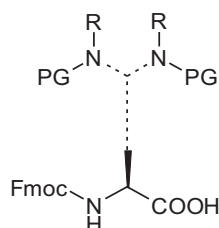
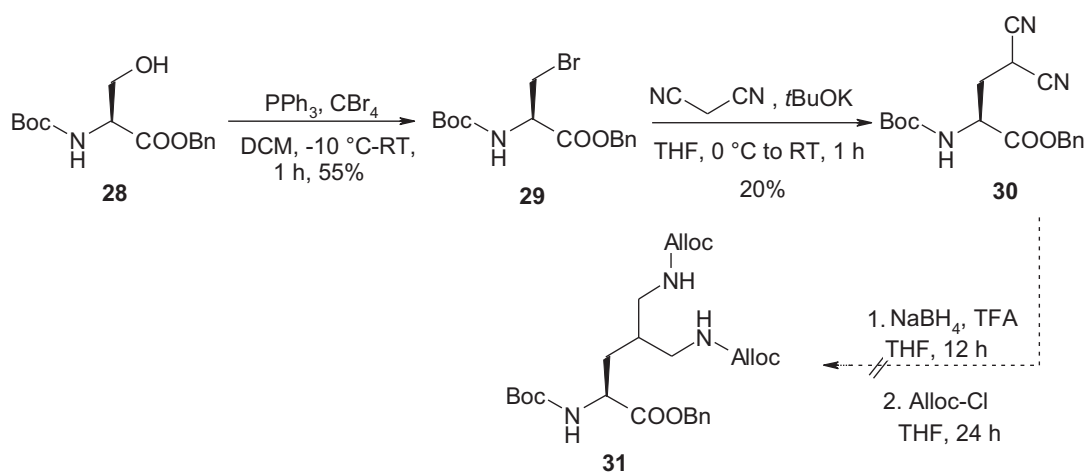


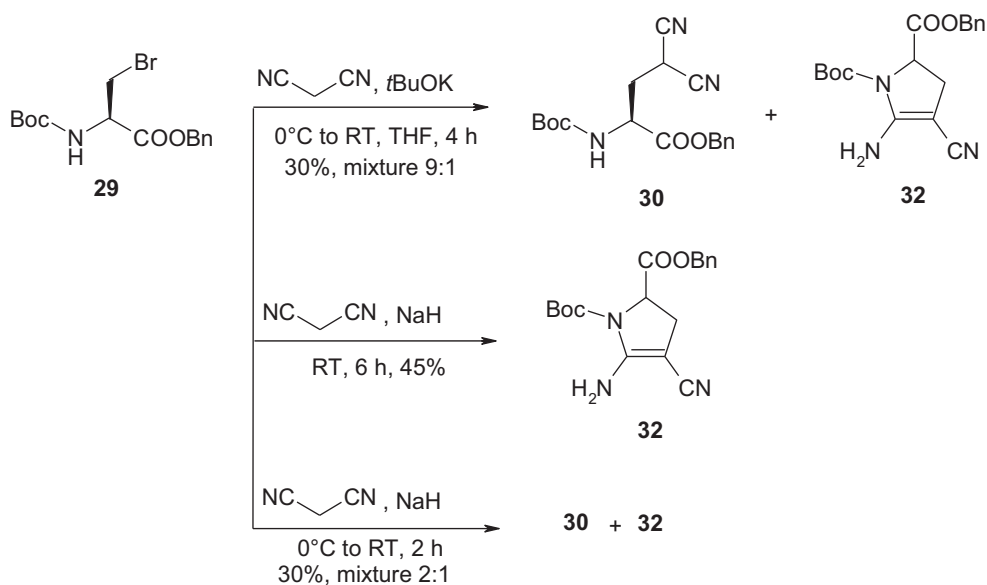
Figure 5.5 General scheme for building block synthesis providing an artificial amino acid backbone, as well as a platinum coordination site. PG – protecting group; R – hydrogen or methyl group.

One approach started from Boc-Ser-OBn (**28**) by performing an Appel Reaction to obtain the bromo derivative **29** in analogy with literature protocols.^[155,156] It was followed by a S_N2 reaction, obtaining the malonodinitril derivative **30** in 20% yield. Problems were experienced in the reducing step of the nitril groups to the amine and allyloxycarbonyl (Alloc) protection (Scheme 5.2).



Scheme 5.2 Synthetic route for compound **31**.

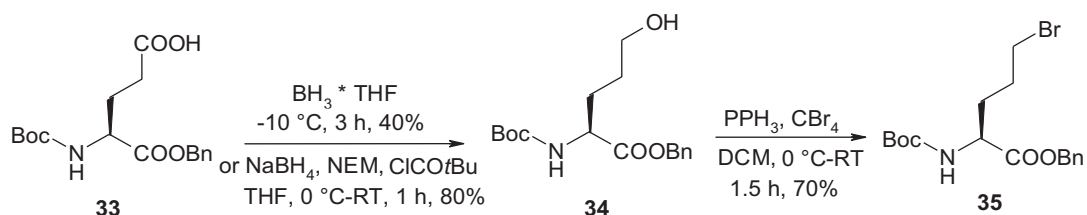
Synthesis investigation was directed on improving the yield of **30**, but also the reduction and Alloc protection conditions. By variation of reaction time, the formation of the cyclic product **33** was observed, thus, explaining the low yield for compound **30** (Scheme 5.3).



Scheme 5.3 Synthesis pathway for improving the yield of **30** with isolation of side product **32**.

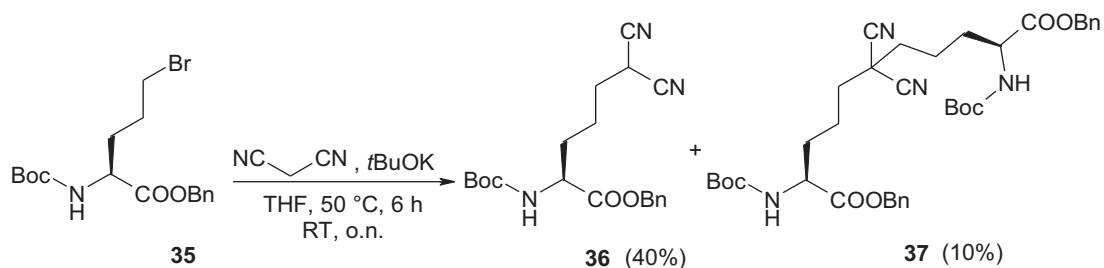
Compound **30** and the side product **32** had the same chromatographic behavior, mass spectra, only NMR revealed the differentiation. The use of a stronger base, such as NaH induced the complete formation of **32**. Nevertheless, when proceeding further with the reduction step, the same pattern of cyclization was observed (ESI-MS evidence). Cyclization was likely to occur by a combined effect of partial nitril reduction and nucleophilic attack by one of the amino centers. Other reduction methods of compound **30**, like hydrogenation using different catalysts (Pd/C, PtO₂·H₂O) indicated the similar cyclization pattern.

In order to avoid cyclization, a new approach involved the design of a monomer holding an extended side chain. Synthesis started with reduction of Boc-Glu-OBn (**33**) to the alcohol group resulting the compound **34**, followed by the Appel reaction in order to obtain the brominated analog **35** (Scheme 5.4).^[157]



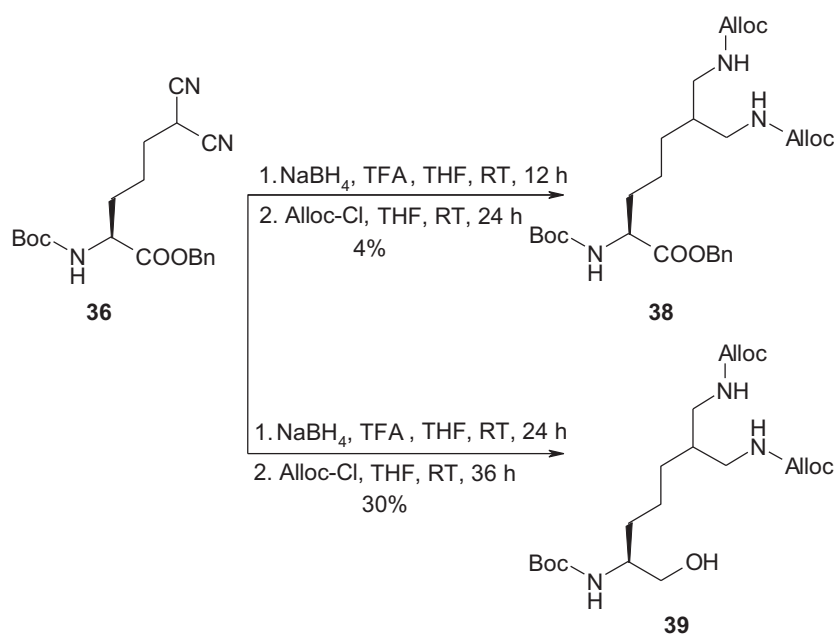
Scheme 5.4 Synthesis of monomer **35**.

Thus, following the same synthetic pattern as previously mentioned, compound **35** was reacted with malononitrile and gave product **36**, only when high temperature was applied, in a yield of 40% (Scheme 5.5). As further products the dimer **37** was isolated in 10% yield.



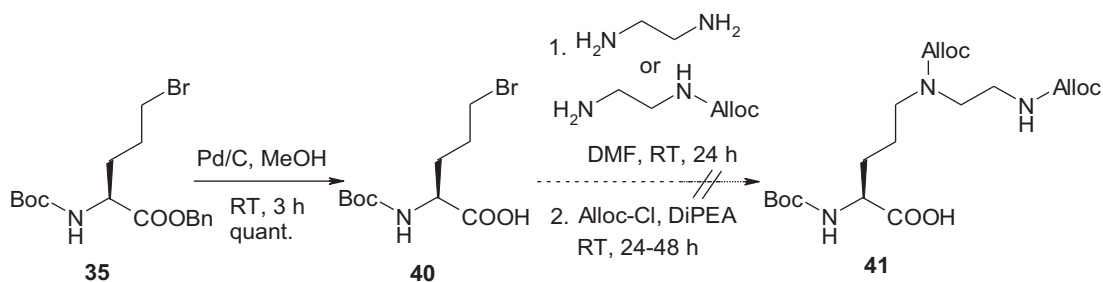
Scheme 5.5 Synthesis of the malononitrile derivative **36**.

Reduction of compound **36** with NaBH_4 and Alloc protection gave the desired product **38** in only 4% yield as observed in the NMR data, which could not be isolated from the adduct (Scheme 5.6). Longer reaction time induced the formation of the reduced alcohol form **39** (30%) which proved to be unstable after purification by column chromatography. By comparing NMR spectra in CDCl_3 and DMSO, side products were observed in DMSO. Also full and concise NMR assignment of the peaks was not possible. HPLC was used to determine the reaction time for NaBH_4 reduction to 24 h.



Scheme 5.6 Synthetic route for compound **38** with formation of the side product **39**.

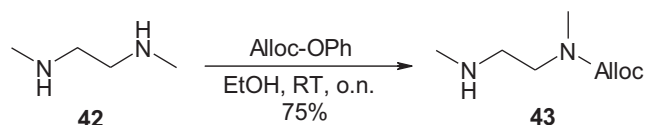
Considering the strong side reactions, a new route for the building block was developed with ethylenediamine/Alloc-ethylenediamine as the platinum chelating site. Synthesis started with ester deprotection using 10% Pd/C to give **40** in quantitative yield (Scheme 5.7). Ligation to the diamine derivatives showed only traces of the product **41**. We assumed the zwitterionic form of the intermediate products might inhibit Alloc protection.



Scheme 5.7 Synthetic route for compound **41**.

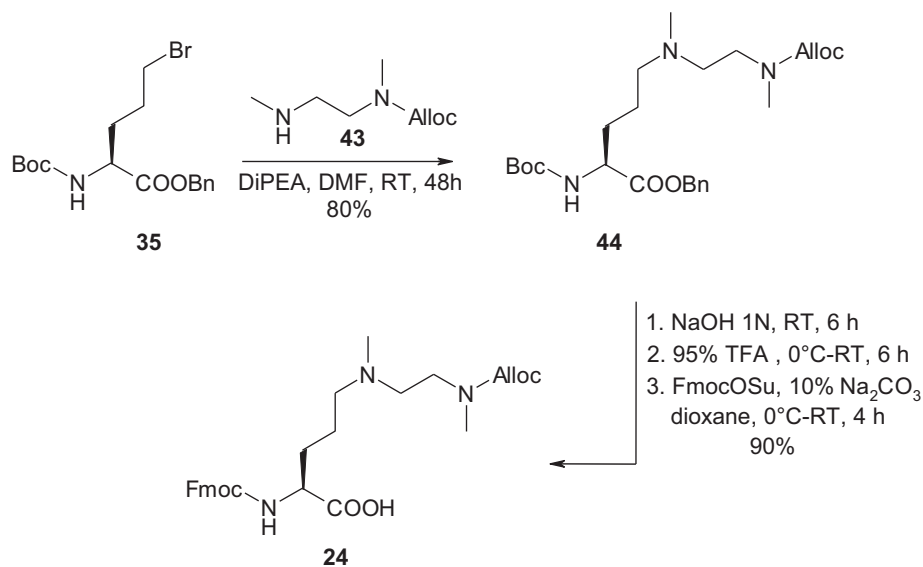
However, these results clearly indicated the need of using a differently protected ethylenediamine derivative. Therefore, N,N'-dimethylethylenediamine **42** was selectively protected to obtain **43** in 75% yield (Scheme 5.8) by modifying literature

protocols.^[158] The key to obtain a pure compound avoiding column chromatography was in the work up step by performing several alternative extractions at basic and acidic *pH*. This was the best method found for selective amine protection since standard protection with AllocCl or diphenyl carbonate gave a mixture of the mono and diprotected forms of **42**.



Scheme 5.8 Synthesis route for compound **43**.

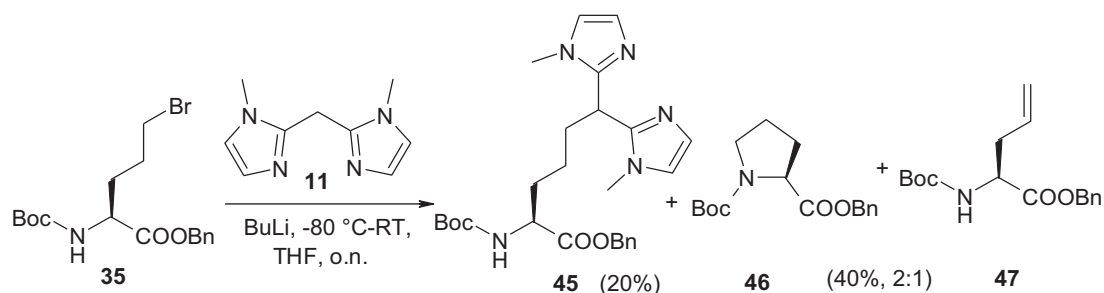
Attachment reaction of amine **43** to the monomer **35** gave compound **44** in a very good yield (80%), followed by a three step reaction that was performed without intermediate purification (Scheme 5.9). Benzyl deprotection with NaOH 1N, Boc deprotection with 95% TFA and Fmoc protection of the free amine group gave the unnatural amino acid **24** (90% yield) which was incorporated into the IHF mimicking peptide.



Scheme 5.9 Synthesis route for the target amino acid derivative **24** used in SPPS.

The synthesis of an aromatic bidentate amino acid ligand was prepared likewise. Therefore, compound **11** was reacted with monomer **31** (Scheme 5.10). The desired

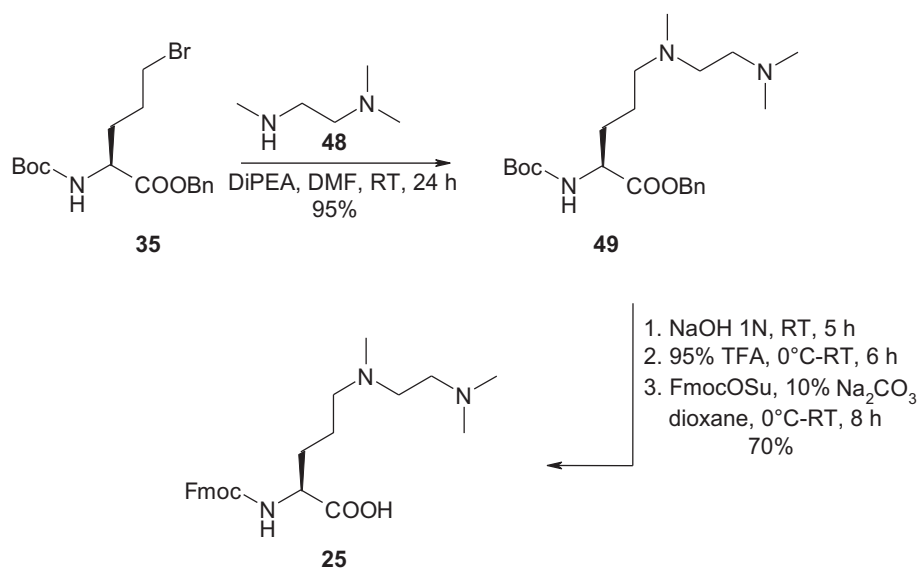
product **45** resulted in 20% yield and a mixture of the cyclic proline derivative **46** along with the alkene **47** (40% yield) as side products. Applying longer reaction time or bases alternation (BuLi, *t*BuOK), only the formation of the side products was induced.



Scheme 5.10 Synthesis route for compound **45** with formation of the side products **46** and **47**.

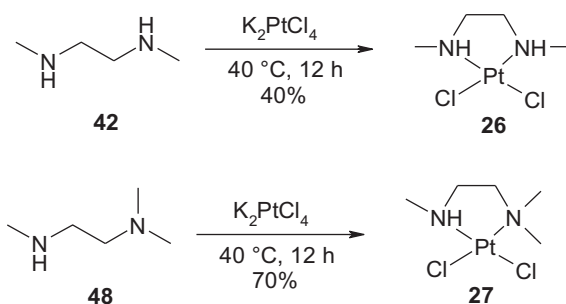
Another target amino acid **25** was synthesized by using *N,N,N'*-trimethylethylenediamine **48** as the platinum coordination site (Scheme 5.11). Applying a similar synthetic pattern as used for obtaining compound **24**, synthesis involved preparation of compound **49** in high yield (95%), but as a mixture of conformers caused by rotation effect of Boc or/and the tertiary amine. Benzyl deprotection with NaOH 1N, Boc deprotection with 95% TFA and Fmoc protection of the free amine group gave the unnatural amino acid **25** (70% yield) which was incorporated into the IHF mimicking peptide.

Compound **24** (minor effect), but especially compound **25** showed a certain degree of instability (cleavage of the fluorenyl group) by longer storage. Therefore, immediately after synthesis, they were incorporated into the peptides.



Scheme 5.11 Synthesis route for the target amino acid derivative **25** used in SPPS.

As references for the DNA binding experiments the cisplatin analogues **26** and **27** were synthesized using a method that differed from the one reported in literature (Scheme 5.12).^[159] Compound **26** was obtained as a mixture of diastereoisomers, whereas **27** proved to have stability problems in DMSO (possible hydrolysis) by prolonged storage. The aquation process specific to cisplatin might be considered here.



Scheme 5.12 Synthesis route for the cisplatin analogs **26** and **27**.

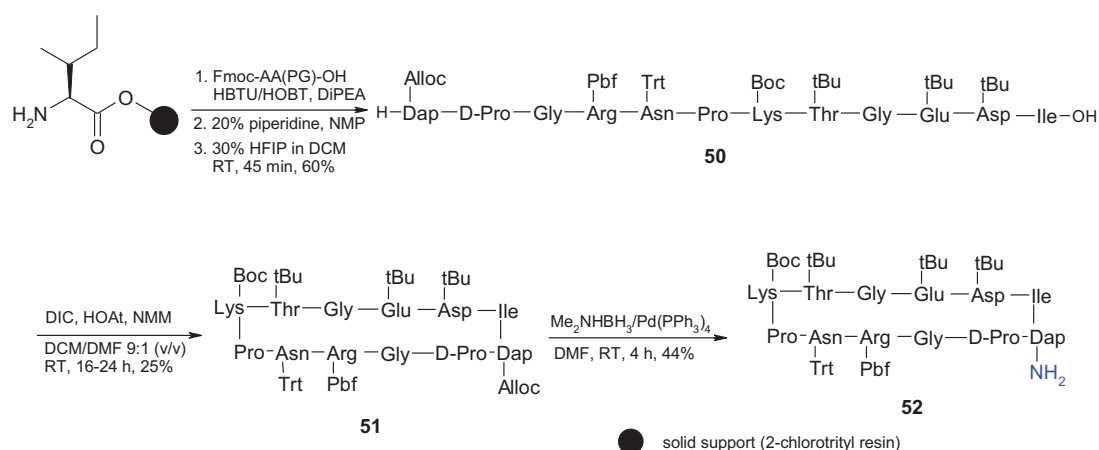
5.3 Synthesis of Platinated-IHF Mimicking Peptides

Synthesis of the platinated-IHF mimicking peptide using the building block **24** involved several steps: 1) Synthesis of the cyclopeptide; 2) Synthesis of the linker-lysine dendrimer; 3) Coupling of the cyclopeptide to the linker-dendrimer unit; 4) Alloc deprotection of the coordination site; 5) Platination and final deprotection of the peptide.

Another approach included complete synthesis of the IHF mimicking peptide backbone on the resin. For this purpose, building block **25** was designed (contains no free amine group) and incorporated into the peptide as the platinum coordination site.

5.3.1 *The Cyclopeptide Synthesis*

The cyclopeptide sequence was described in Section 5.1.3 (Figure 5.3). The synthesis was performed according to the protocol for the IHF mimic described by *E. Liebler*,^[41] which is considered as a model peptide for specific DNA binding with bending properties. The cyclopeptide was first prepared as the linear dodecamer **50** on a 2-chlorotrityl resin preloaded with isoleucine, using the Fmoc-SPPS protocol on an automated microwave synthesizer (Scheme 5.13). HBTU/HOBt was used as amino acid activation mixture. The Fmoc group was removed using 20% piperidine. Dap was introduced, Alloc side chain protected in order to have an orthogonal protection to Fmoc and the acid labile permanent side chain protecting groups. D-Pro was chosen to induce a β -turn in the cyclopeptide and to ensure a certain degree of conformational rigidity.^[160] Cleavage with 30% HFIP for 45 min gave compound **50**, thus, avoiding deprotection of the acid-labile Trt group.



Scheme 5.13 Synthesis route for cyclopeptide **52**.

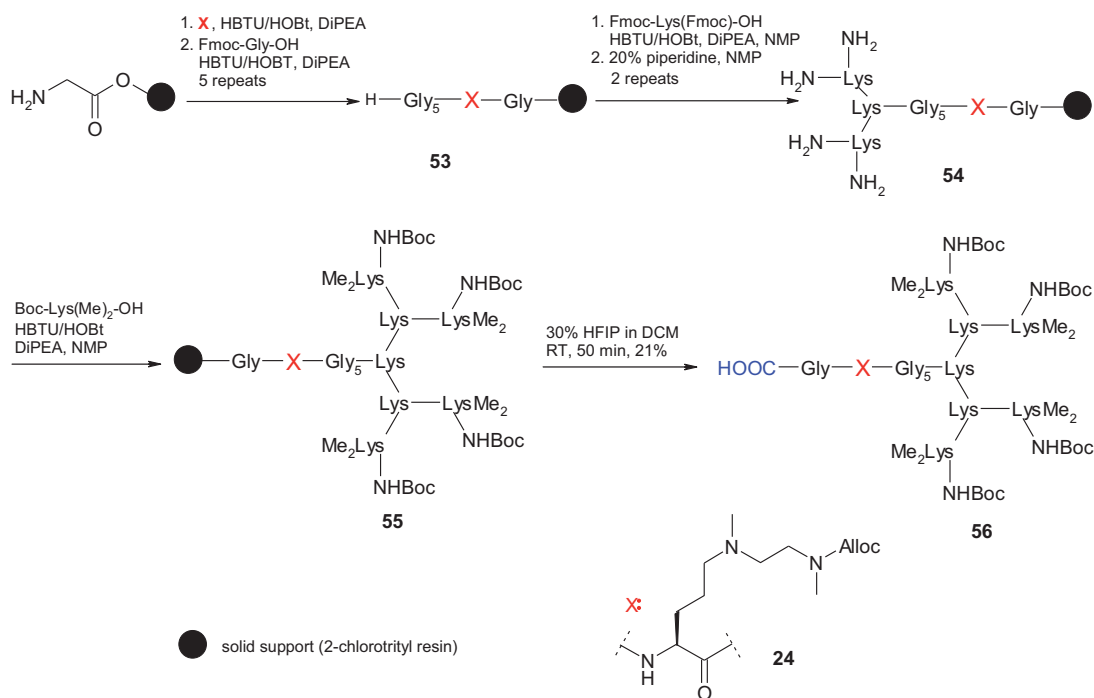
Cyclization using DIC/HOAt and NMM in DMF afforded peptide **51**, followed by selective Alloc deprotection using a Pd catalyst to give the cyclopeptide **52**.

5.3.2 The Linker-Lysine Dendrimer Synthesis

The water soluble linker-lysine dendrimer **56** was prepared on a glycine preloaded 2-chlorotrityl resin by manual Fmoc-SPPS protocol (Scheme 5.14). HBTU/HOBT was used as amino acid activation. Fmoc deprotection was carried out with piperidine. The linker chain was kept at the same length (seven glycine units) as previously reported,^[151] based on MacroModel calculations for estimating the distance between the IHF α -subunit and its "body". The IHF-DNA crystal structure revealed the distance between the C α -atom of leucine (Leu⁵⁴) and arginine (Arg⁶⁰) of 17.7 Å.^[44] Therefore, the linker length was set up to seven glycine residues summarizing a length of 22.2 Å. Glycine was chosen in order to minimize linker-DNA interaction since glycine is less reactive and can form only hydrogen bonds. The platinum coordination building block was inserted in the next to last position of the linker region (nearby the peptide C-terminus), so that after cyclopeptide coupling would be in the proximity of the DNA intercalating proline.

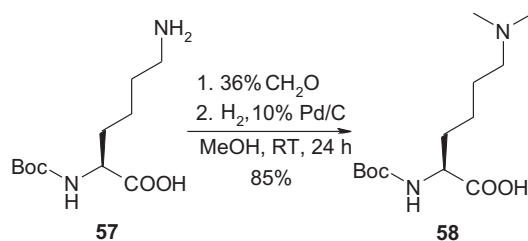
Synthesis of Platinated-IHF Mimicking Peptides

The three-generation lysine dendrimer was build up using Fmoc-Lys(Fmoc)-OH as monomeric unit up to the second generation and Boc-Lys(Me₂)-OH as the third layer. Mild deprotection with 30% HFIP in DCM afforded peptide **56** in 21% yield.



Scheme 5.14 Convergent synthesis of the lysine dendrimer connected to an oligoglycine linker modified with the building block **24** as platination site.

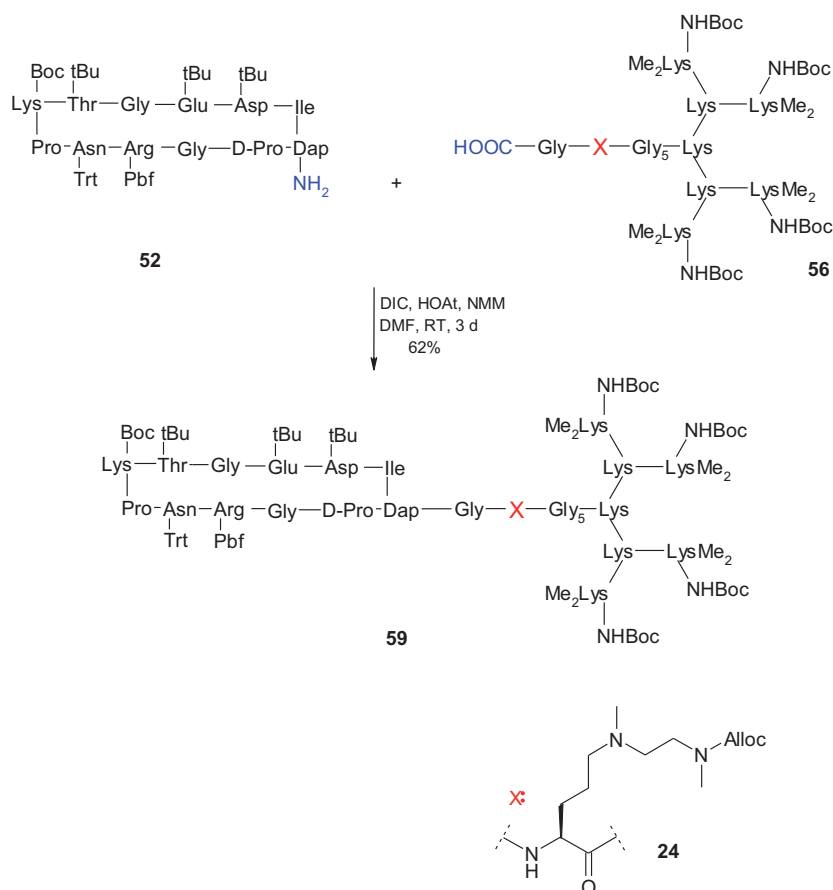
N-Bismethylation provides protonation at *pH* 7, and the terminal lysine amine is also assumed to contribute to phosphate neutralization.^[41] Boc-Lys(Me₂)-OH (**58**) was prepared in analogy to ornithine based on literature reference (Scheme 5.15).^[161] Purification by column chromatography was achieved using acetone/water 4:1, v/v.



Scheme 5.15 Synthesis route for compound **58**.

5.3.3 Assembly of the IHF Mimic and Platination

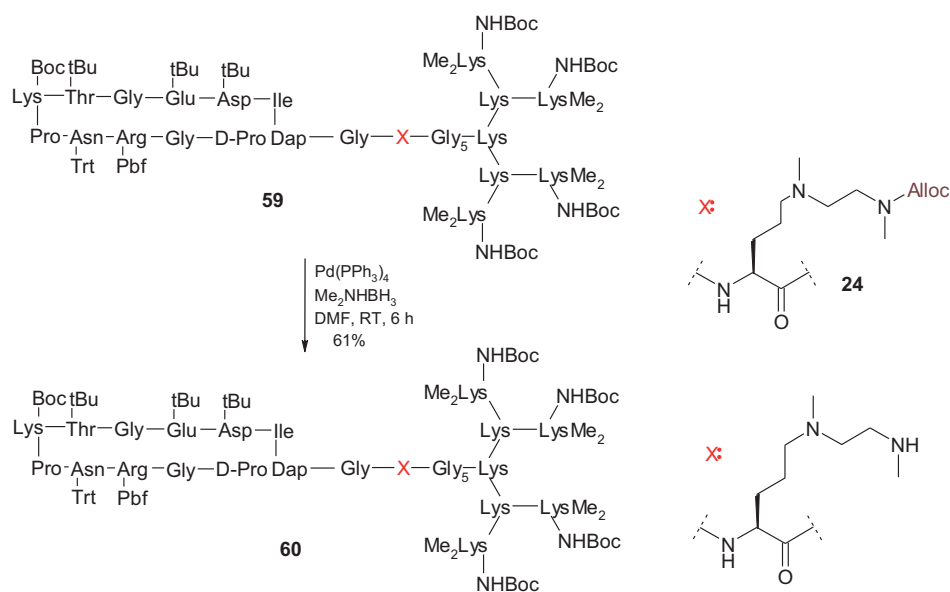
Coupling of the cyclopeptide **52** via Dap side chain to the C-terminal position of the linker-dendrimer **56** proceeded using DIC/HOAt and NMM activation in DMF to give compound **59** in 62% yield (Scheme 5.16). It was a key reaction step. Different conditions were applied with respect to reaction time and equivalents.



Scheme 5.16 Synthesis of compound **59**.

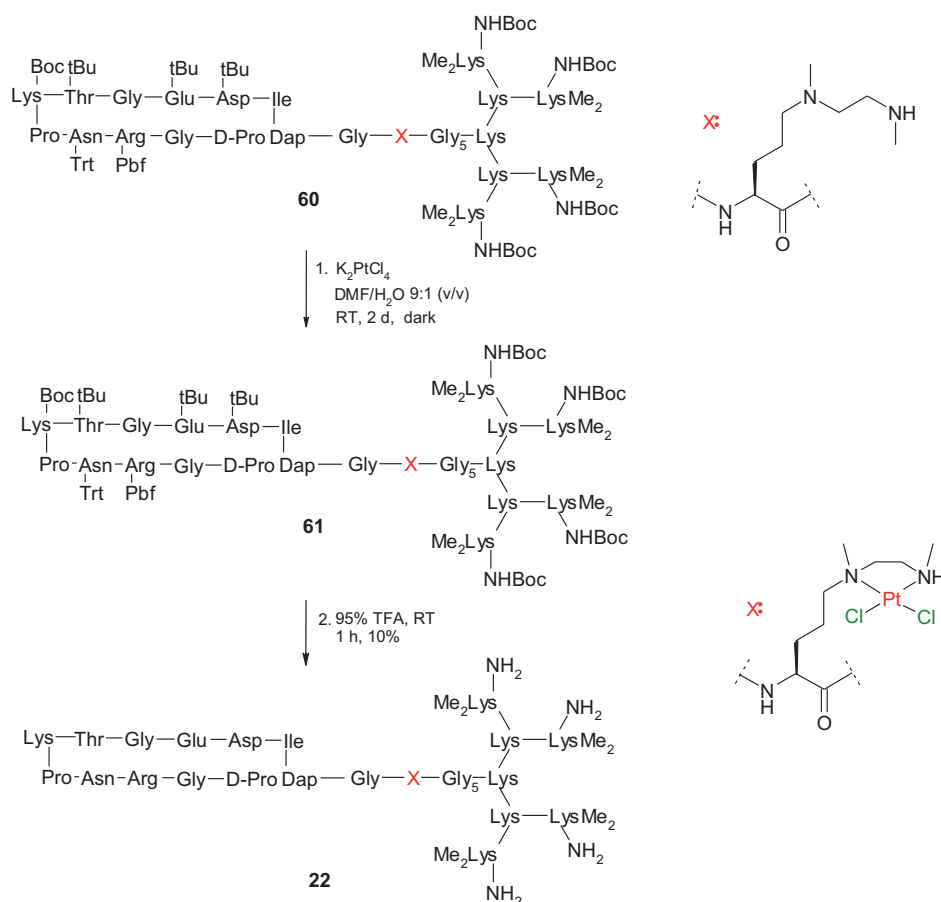
Orthogonal deprotection of the Alloc moiety was carried out using the same Pd catalyst mentioned earlier under reduction conditions giving compound **60** in 61% yield (Scheme 5.17).

Synthesis of Platinated-IHF Mimicking Peptides



Scheme 5.17 Synthesis route for compound **60**.

After purification of the Alloc-deprotected peptide **60**, platination was accomplished with K_2PtCl_4 for 2 days at room temperature in the dark. ESI and HRMS mass spectra evidenced the formation of platinated IHF mimicking peptide **61** (Scheme 5.18). Considering that the HPLC diagram showed a high purity of the compound (one major peak) and in order to avoid possible loss of product during HPLC purification, it was proceeded further without preparative purification. All side chain protecting groups were cleaved with 95% TFA in H_2O and the target peptide **22** was obtained in 10% yield.



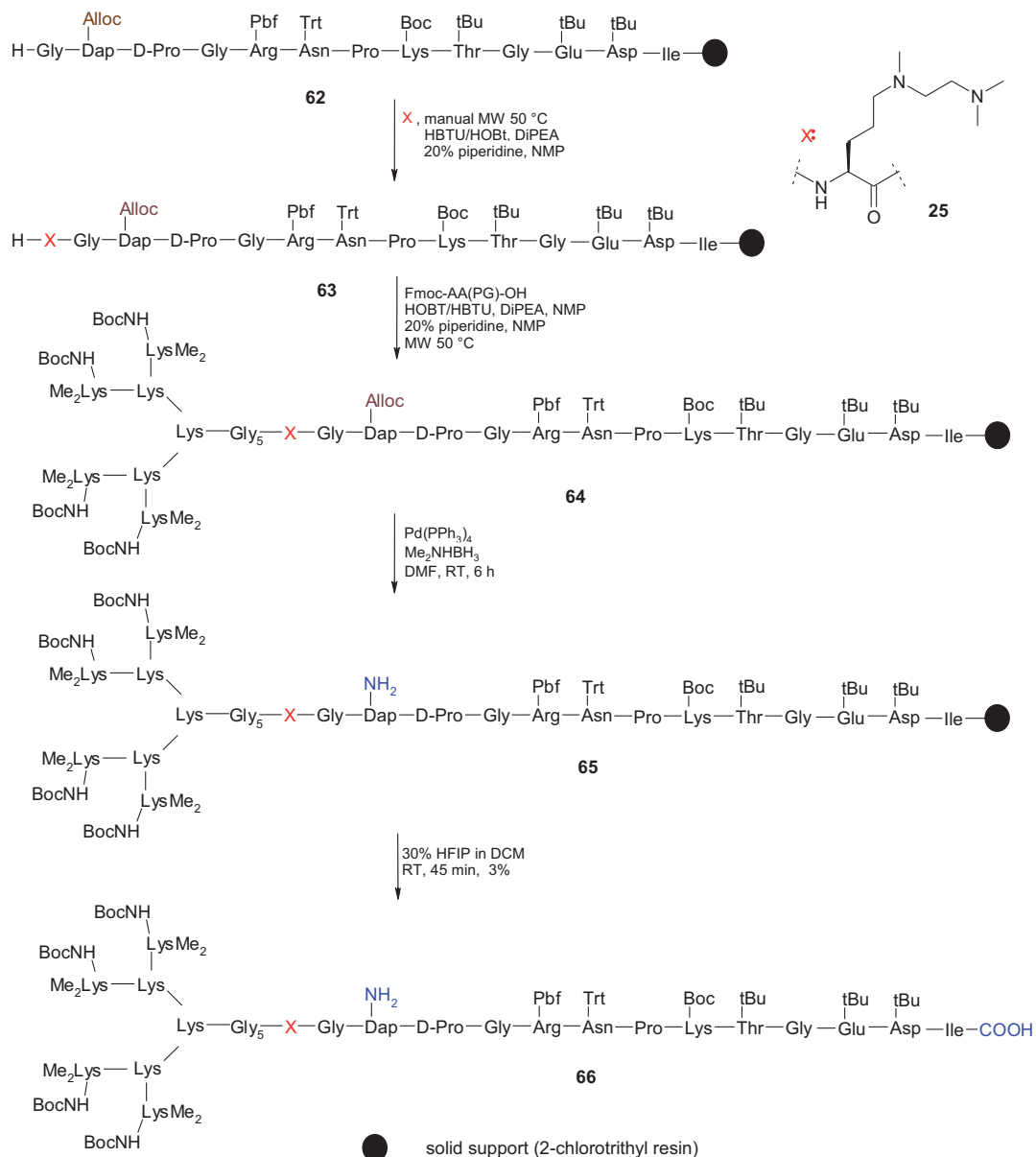
Scheme 5.18 Synthesis route of the target platinum-IHF mimic peptide **22**.

5.3.4 Complete Synthesis of the IHF Mimic on the Resin

A new approach for synthesis of platinated-IHF mimicking peptides was considered by using building block **25** as coordination site for platinum (Scheme 5.19). This artificial amino acid contains no free amino group, therefore cyclization can be performed on the resin. In order to maintain the same conformation pattern of the IHF peptide as described in Section 5.1.3., cyclization was induced by using Alloc-Dap(Fmoc)-OH prepared according to literature.^[162] Peptide **62** was generated on a preloaded isoleucine resin using an automated microwave Fmoc-SPPS protocol. Further coupling was achieved by manual microwave SPPS. Double coupling with longer reaction time was needed for the amino acid **25** to give peptide **63**. Orthogonal

Synthesis of Platinated-IHF Mimicking Peptides

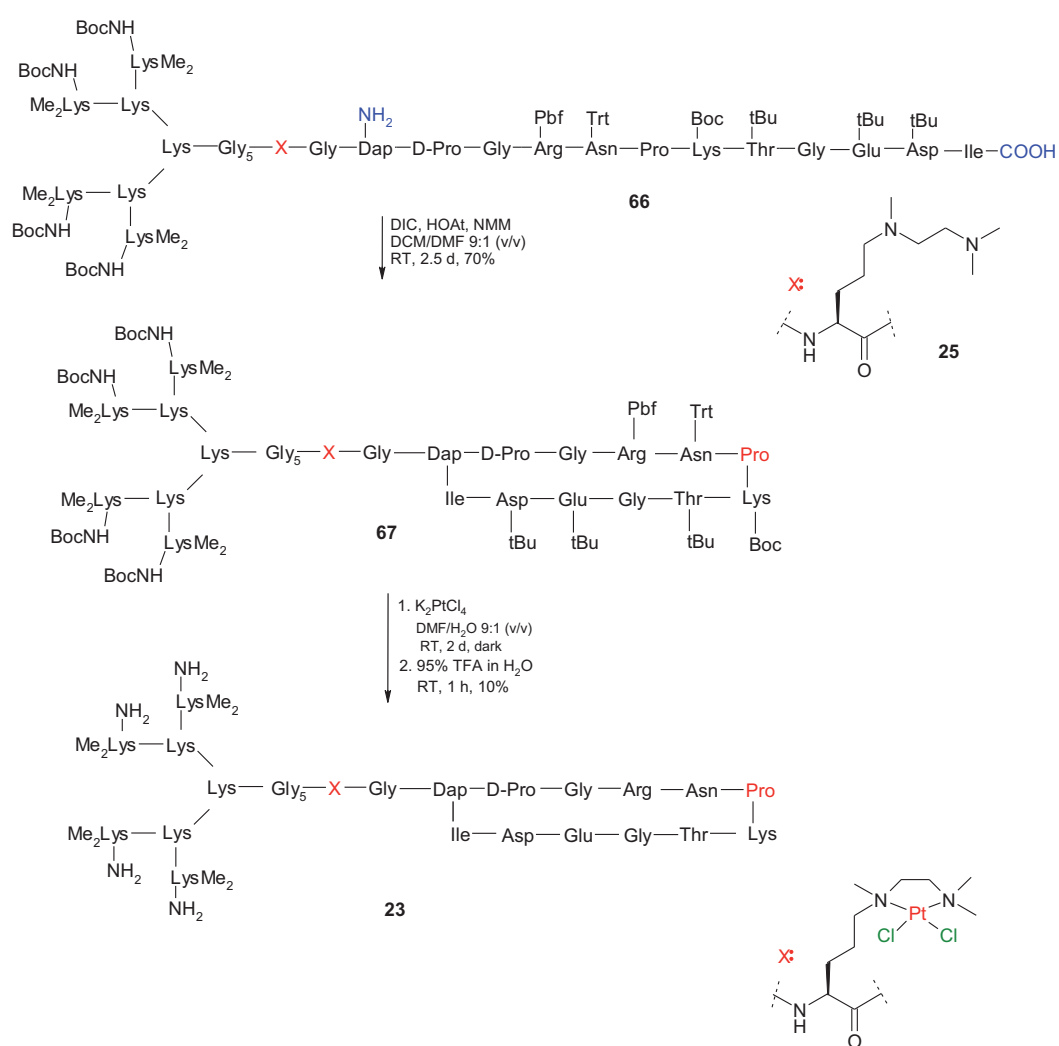
removal of the Alloc protected Dap amino acid and cleavage from the resin provided peptide **66**.



Scheme 5.19 Synthesis route for peptide **66**.

Cyclization using DIC/HOAt and NMM in DMF afforded compound **67**, followed by platination and full deprotection of the peptide to give the final target peptide **23** (Scheme 5.20).

DNA Specifically Binding Molecules – Platinated IHF



Scheme 5.20 Synthesis route of the target platinum-IHF mimic peptide **23**.

5.4 Preliminary DNA Binding Experiments

Preliminary DNA binding studies of the potential IHF mimics to the dsDNA were investigated by agarose gel electrophoresis, using 200 or 55 base pairs DNA, both containing the λ phage consensus sequence ($^5TAAAAAGCATTGCTTATCAATTTGTTGCAACGA^3$) for the IHF protein (the *H'*-binding site).^[45] We based our investigations on the specificity of previously reported IHF mimic peptides for this binding site.^[41,154] The 55 bp DNA was commercially available

($^5CCCACGGCATTATAAAAAAGCATTGCTTATCAATTTGTTGCAACGAACAGGTCGG^3$), whereas the 200 bp DNA was synthesized using the polymerase chain reaction (PCR) technique (the 34 bp *H'*-binding site sequence was amplified from the 502 bp attP site with the additional base pairs).

The 200 bp DNA double strands were used containing the *H'*-binding site either in a central (*H'*-middle) or in a terminal position (*H'*-edge). Specific binding and bending of one of the mimics leads to differentially shaped DNA-peptide complexes (Figure 5.6). Binding to the *H'*-edge site results in a more linear shaped complex compared to the *H'*-middle binding. The linear complex moves faster through an agarose gel than bent DNA,^[163] but both complexes should migrate slower than dsDNA.



Figure 5.6 DNA-IHF mimic peptide complex. Binding can occur to the *H'*-binding site placed in the middle (left) or terminal position of DNA (right).

The competitive DNA binding ability of the three peptides **C4**, **68** and **69** was investigated (Figure 5.7). Cisplatin was used as reference. Peptides **68** and **69** are IHF mimics and were provided by *Stefanie Scholz*. Compound **69** is the first mimicking peptide described by *E. Liebler*,^[41] whereas **68** contains 3,4-dehydroproline (Dh-Pro) with a nearly planar conformation of the five-membered ring, as the intercalating amino acid.^[154]

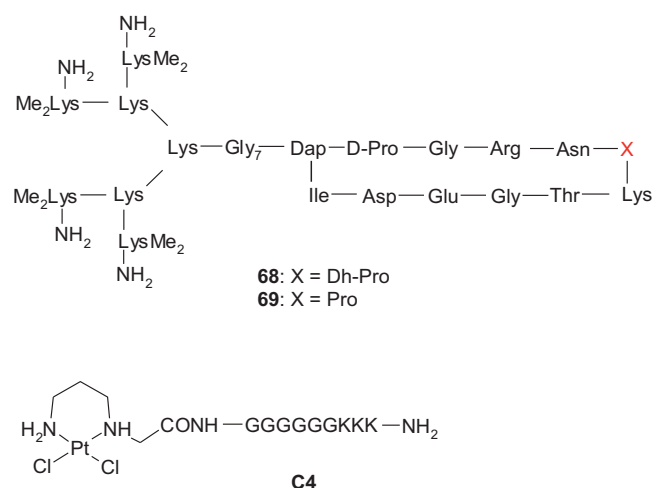


Figure 5.7 Peptides used in the DNA binding experiments.

Gel electrophoresis of the 200 bp DNA H'-middle was performed in Tris HCl buffer (10 mM HCl, 10 mM EDTA, 100 mM NaCl, 1 mM dithiothreitol, *pH* 7.5) with an incubation time of 3 h at RT. All three bands of **C4**, **68** and cisplatin were shifted (Figure 5.8, lanes 3, 4, 5), whereas a significant retardation was noticed for **C4** (lane 3) and **C4** + **68** (lane 6). The presence of the platinum unit in **C4** or in cisplatin combined with the peptide **68** (lanes 6 and 7) induced a higher DNA binding effect compared to the unplatinated IHF mimic (lane 4). The difference in retardation might be associated with the presence of multiple binding sites (H'-middle recognition unit, but also the GG sites responsible for platinum binding).



Figure 5.8 Agarose gel electrophoresis (2%). lane 1: 50 bp DNA ladder; lane 2: 200 bp DNA H'-middle; lane 3: **C4**, lane 4: **68**; lane 5: cisplatin; lane 6: **68** + **C4**; lane 7: **68** + cisplatin. The samples were incubated for 3 h at RT in Tris HCl buffer with $r_f = 200$. [DNA] = 0.248 μM . For mixtures a 1:1 ratio was used.

Furthermore, an inhibitory effect was observed when combining the peptide **68** (lanes 6 and 7 compared with lane 3) with **C4** or cisplatin. The presence of the IHF mimic diminishes extremely the binding ability of **C4**. This can be assumed as an effect of both, DNA binding and bending characteristics of the IHF peptide **68**.

Gel electrophoresis of the 200 bp DNA H'-edge with **C4** and **68** revealed a similar inhibitory effect of the IHF mimic (Figure 5.9). Keeping the same r_f of compound **68** (lanes 3–7) an increasing concentration of the peptide **C4** was added until 1:1 ratio (lane 7). Then, the r_f of compound **C4** was maintained and the r_f of compound **68** was decreased (lanes 8, 9). The presence of the IHF mimicking peptide **68** blocks/reduces the binding ability of **C4** even at double concentration of the platinum peptide (lane 8 compared to lane 7). Only **C4** shows a high DNA binding ability (lane 9).

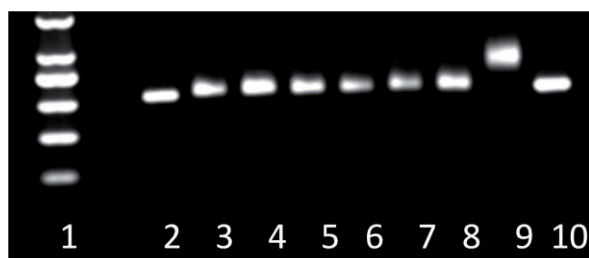


Figure 5.9 Agarose gel electrophoresis (2%). lane 1: 50 bp DNA ladder; lane 2, 10: 200 bp DNA H'-edge; lane 3: **68** r_f = 200, [DNA] = 0.312 μ M; lane 4: **68** r_f = 200, **C4** r_f = 50; lane 5: **68** r_f = 200, **C4** r_f = 100; lane 6: **68** r_f = 200, **C4** r_f = 150; lane 7: **68** r_f = 200, **C4** r_f = 200; lane 8: **68** r_f = 100, **C4** r_f = 200; lane 9: **C4** r_f = 200. The samples were incubated for 3 h at RT in Tris HCl buffer.

Decreasing the incubation time of the peptide **68** compared to cisplatin (lanes 3, 4) or **C4** (lanes 5, 6) provided the same proof of inhibitory effect of the IHF mimic (Figure 5.10).

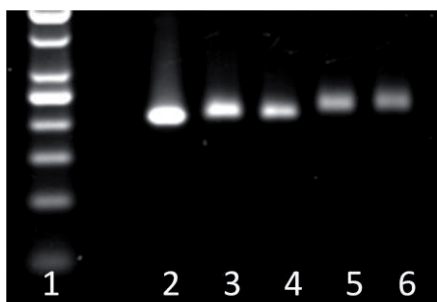


Figure 5.10 Agarose gel electrophoresis (2%). lane 1: 50 bp DNA ladder; lane 2: 200 bp DNA H'-edge; lane 3: cisplatin + **68** added 30 min later; lane 4: cisplatin + **68** added 1 h later; lane 5: **C4** + **68** added 30 min later; lane 6: **C4** + **68** added 1 h later. [DNA] = 0.312 μ M. The samples were incubated for 3 h at RT in Tris HCl buffer with $r_f = 200$. For mixtures a 1:1 ratio was used.

Similar experiments were performed using 55 bp dsDNA (Figure 5.11) having both 5'-terminal ends labeled with fluorescein (FAM) and tetramethylrhodamine (TAMRA), respectively, also used for fluorescence resonance energy transfer (FRET) analysis. The peptide **68** was added to cisplatin (lanes 4–7) or **C4** (lanes 9–12) at different times ranging from 30 min to 1.5 h.

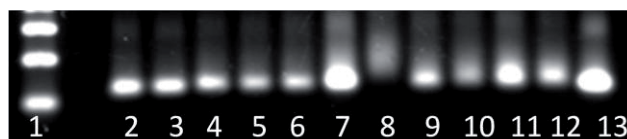


Figure 5.11 Agarose gel electrophoresis (2%). lane 1: 50 bp DNA ladder; lane 2, 13: 55 bp dsDNA; lane 3: cisplatin; lane 4: cisplatin + **68**; lane 5: cisplatin + **68** added 30 min later; lane 6: cisplatin + **68** added 1 h later; lane 7: cisplatin + **68** added 1.5 h later; lane 8: **C4**; lane 9: **C4** + **68**; lane 10: **C4** + **68** added 30 min later; lane 11: **C4** + **68** added 1 h later; lane 12: **C4** + **68** added 1.5 h later. [DNA] = 0.8 μ M. The samples were incubated for 3 h at RT in Tris HCl buffer with $r_f = 200$. For mixtures a 1:1 ratio was used.

The platinum peptide **C4** induces high band retardation when IHF mimicking peptide **68** is not present (lane 8) and exhibits a better effect compared to cisplatin (lanes 8–12 compared to lanes 3–7).

DNA binding ability of **68**, **69**, **C4** and cisplatin (aqua form)^[164,165] was investigated using 55 bp dsDNA (Figure 5.12). The same pattern as previously described was observed. Furthermore, the presence of Pro instead of Dh-Pro (**69** compared to **68**)

seemed to induce a higher shift, both alone and in combination with platinum compounds, especially with **C4** (lanes 7, 9); therefore a higher inhibition rate can be associated with the IHF mimic **68**. A certain degree of smearing was noticed when using 55 bp DNA compared to 200 bp DNA. This effect seems to be more pronounced when the platinum unit is present, most likely as an effect of multiple binding sites.

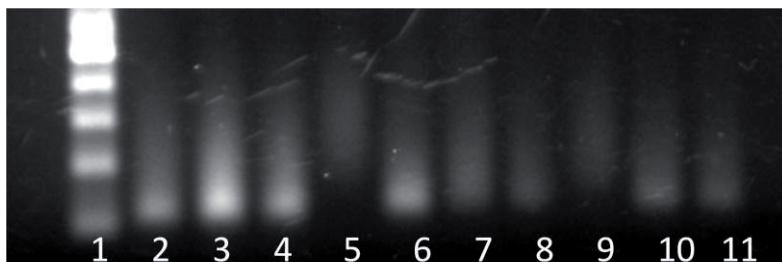


Figure 5.12 Agarose gel electrophoresis (2%). lane 1: 50 bp DNA ladder; lane 2, 11: 55 bp dsDNA; lane 3: **68**; lane 4: **69**; lane 5: **C4**; lane 6: cisplatin(aq); lane 7: **68** + **C4**; lane 8: **68** + cisplatin(aq); lane 9: **69** + **C4**; lane 10: **69** + cisplatin(aq). The samples were incubated for 3 h at RT in Tris HCl buffer with $r_f = 200$. $[DNA] = 0.8 \mu M$. For mixtures a 1:1 ratio was used.

The intermolecular competitive effect between the IHF mimics **68**, **69** and the platinum peptide **C4** is a favorable indication of the possible combined effect that can be provided by the platinated IHF mimicking peptides **22** and **23**. DNA binding studies of these constructs were not performed yet due to time limitation, but it is considered further outlook of this work.

6. Summary

Cisplatin is one of the most effective metal-based anticancer drugs. Biological activity derives from its capacity to preferentially bind DNA at the N7 position of two neighboring guanine bases. However, its low solubility and poor selectivity between healthy and sick cells has generated resistance, as well as toxic side effects. Molecular design of new cisplatin analogs with increased DNA binding ability and selectivity is a challenging task and target for developing such drugs.

In this study, we report new cisplatin constructs based on chimera of platinum complexes and peptides. The mixture of cationic metal complexes with charged peptides was chosen as a strategy to facilitate DNA binding induced by DNA pre-association and bending of the DNA target. The two research approaches make use of cationic polypeptides as drug carriers, which in general bind DNA in a *nonspecific* or *specific* manner.

The *first approach* included the synthesis of five new cisplatin analogs (Figure 6.1) based on propylene or bisimidazole platinum ligands attached to variable charged (+6, +3, 0) *nonspecific* nonapeptides. DNA binding experiments were investigated by agarose and polyacrylamide gel electrophoresis, fluorescence intercalation and UV thermal melting studies. The formation of covalently bound platinum DNA adducts was shown to be facilitated by the cationic peptides. An increased binding was observed for the complexes **C1** and **C2**, as a combined effect of ligand flexibility and peptide electrostatic effect. Less sterical hindrance indicated **C2** and **C4** as promising candidates, a possible drug alternative strategy to cisplatin.

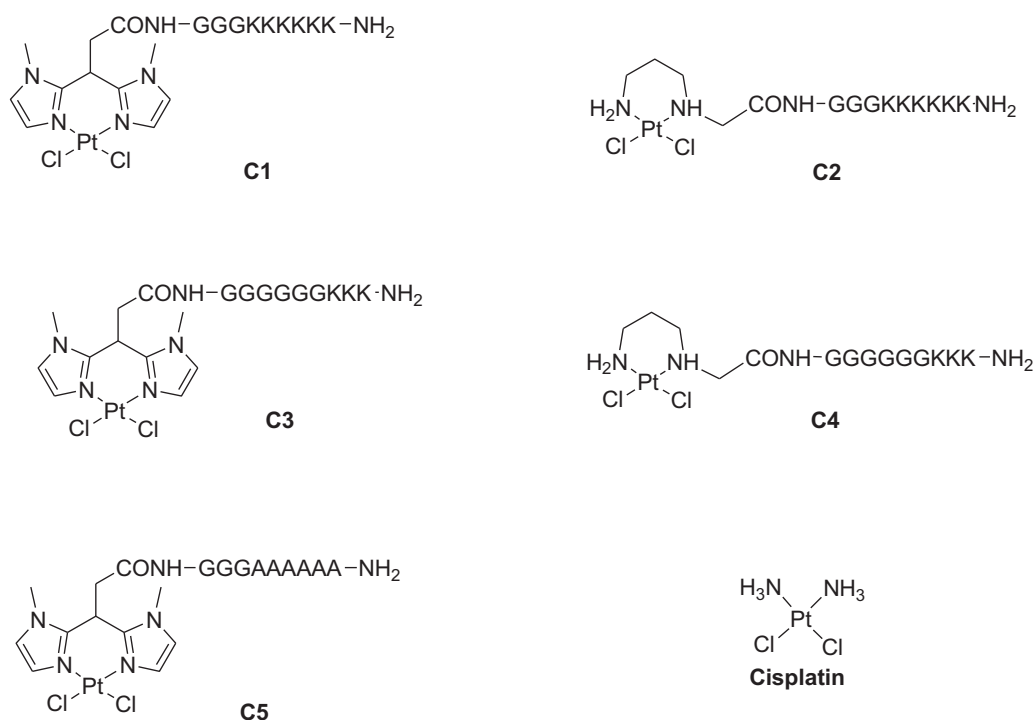


Figure 6.1 Platinum complex/*nonspecific* peptide chimera **C1–C5**.

The *second approach* involved the design and synthesis of *specifically* binding peptides that mimic the IHF, a known DNA binding and bending protein, modified with a covalently bound platinum binding site.

These constructs (Figure 6.2) included the synthesis of a cyclopeptide linked via a glycine linker to a small lysine-based dendrimer. Specific DNA recognition is provided by the cyclopeptide moiety reaching into the minor groove and inducing bending of the helix, stabilized by the non-specific charge-charge interactions of the dendrimer. A second DNA binding center was introduced into the linker region by incorporation of the newly synthesized unnatural amino acids **24** or **25** providing the coordination site for covalently binding of the *cis*-dichloro platinum moiety. Two platinated IHF mimicking peptides **22** and **23** were synthesized (Figure 6.2).

7. Zusammenfassung

Cisplatin ist eines der wirksamsten Metall-basierten Zytostatika, dessen biologische Aktivität auf der bevorzugten Bindung an die N7-Position zweier benachbarter Guanin-Basen der DNA beruht. Jedoch, sind die geringe Löslichkeit und schlechte Selektivität bezüglich gesunder und bösartiger Zellen Nachteile in Hinblick auf Resistenz sowie toxische Nebenwirkungen dieses Medikaments. Für die Entwicklung neuer Medikamente ist die Verbesserung der Bindungseigenschaften, der Selektivität und des molekularen Designs der Cisplatin-Zytostatika eine anspruchsvolle und herausfordernde Aufgabe.

Im Rahmen dieser Arbeit wurden neue Cisplatin-Derivate entwickelt, die aus Chimären von Platin-Komplexen und Peptiden bestehen. Die Verbindung aus einem kationischen Metallkomplex mit geladenen Peptiden wurde gewählt, um durch Präassoziation und Knicken der DNA ein gezieltes Binden der Moleküle an die DNA zu erreichen. Dabei wurden zwei Ansätze verfolgt, die kationische Polypeptide als *drug carriers* nutzen, welche die DNA *spezifisch* oder *nicht-spezifisch* binden können.

Der erste Ansatz beinhaltet die Synthese von fünf neuen Cisplatin-Analoga (Abbildung 7.1), die auf Propylendiamin- bzw. Bisimidazol-Liganden basieren, die mit verschiedenen geladenen (+6, +3, 0) *unspezifischen* Nonapeptiden funktionalisiert wurden. Mit diesen Molekülen wurden DNA-Bindungsstudien mittels Agarose- und Polyacrylamid-Gelelektrophorese, Fluoreszenz-Interkalation sowie temperaturabhängiger UV-Spektroskopie durchgeführt. Die Bildung kovalent gebundener Platin-DNA Addukte vermittelt durch die kationischen Peptide konnte gezeigt werden. Für die Komplexe **C1** und **C2** konnte eine höhere Bindungsaffinität als Folge der besseren Ligandenflexibilität und der elektrostatischen Effekte der Peptide beobachtet werden. Die Moleküle **C2** und **C4** stellen durch ihre geringe

sterische Hinderung vielversprechende Kandidaten als mögliche Alternative für die Cisplatin-Strategie dar.

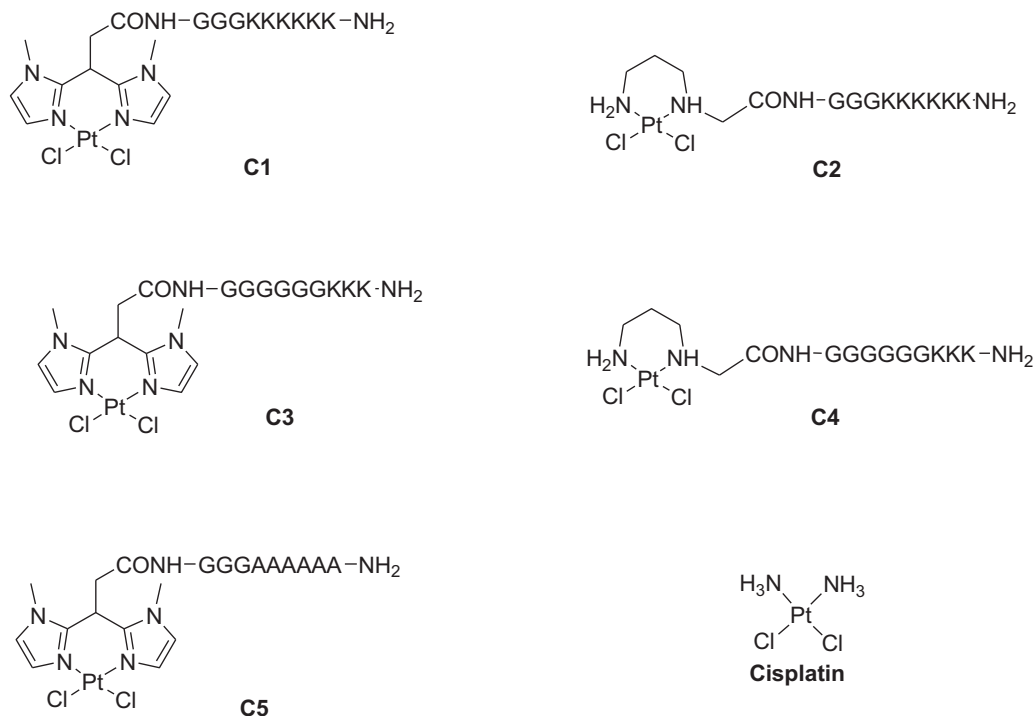


Abbildung 7.1 Platin-Komplex/*unspezifische* Peptid-Chimäre **C1–C5** und Cisplatin.

Der zweite Ansatz beinhaltet das Design und die Synthese von *spezifisch* an die DNA bindenden Peptiden mit einer Platin-Bindungsstelle. Die Peptide wurden dem IHF (*Integration Host Factor*) nachempfunden einem Protein, dessen Bindungseigenschaften und Fähigkeit die DNA zu knicken, bekannt sind.

Diese hier entwickelten Verbindungen bestehen aus einem Zyklopeptid, das über einen Glycin-Linker mit einem Lysin-Dendrimer verbunden ist. Die spezifische Erkennung der DNA wird über das Zyklopeptid erreicht, das in die kleine Furche der DNA ragt und einen Knick in der Helix induziert. Dies wird durch die Ladungswchselwirkung des Dendrimers mit dem Phosphatrückgrat unterstützt. Des Weiteren wurden mit den Molekülen **24** und **25**, neue unnatürliche Aminosäuren, synthetisiert, die in ihrer Seitenkette *cis*-Dichlorplatin komplexieren können. Diese Aminosäuren wurden in die Linkerregion der zuvor beschriebenen Moleküle

eingbracht und bilden so ein zweites DNA-Bindungszentrum. Die synthetisierten Verbindungen **22** und **23** sind in Abbildung 7.2 dargestellt.

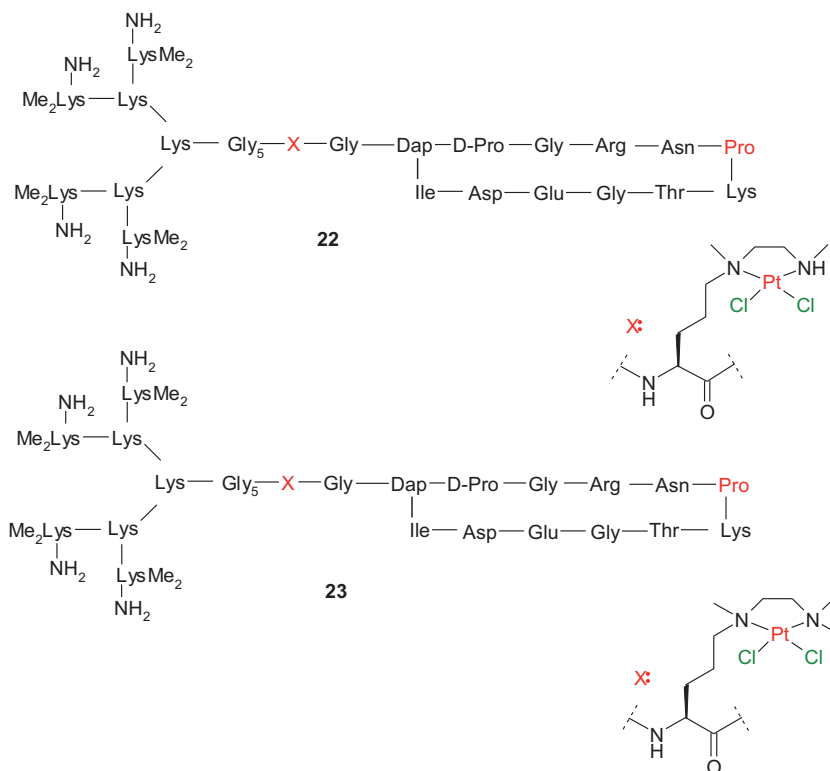


Abbildung 7.2 Platin-Komplex/spezifische Peptide-Chimäre **22**, **23**.

Vorläufige DNA-Bindungsstudien wurden durchgeführt, um die intermolekularen Auswirkungen der IHF-Referenzverbindungen **68** und **69** kombiniert mit den Platin-Verbindungen Cisplatin sowie **C4** zu untersuchen. Für die Platin-Komplexe wurde eine starke Bandenverschiebung beobachtet, während die von IHF-abgeleiteten Verbindungen einen inhibierenden Effekt aufwiesen. Dies ist ein positives Anzeichen für die möglichen synergistischen Effekte, die die Verbindungen **22** und **23** auf DNA ausüben können. Eine Optimierung der Synthese der IHF Mimetika **22** und **23** sowie Studien ihrer DNA-Bindungseigenschaften sind in zukünftigen Arbeiten weiterzuverfolgen.

8. Experimental Part

8.1 General

8.1.1 Solvents

All technical solvents were distilled prior to use. The solvents of analytical and HPLC grade were used as supplied from *Fluka*, *FisherScientific GmbH* or *Acros Organics*. Dry solvents were stored over molecular sieves (4 Å). Ultra pure water was derived using a water purification device *Simplicity* (*Millipore*, Bedford, UK).

8.1.2 Reagents

All reagents were of analytical grade and used as supplied. All amino acid derivatives as well as coupling reagents and the resins for solid phase synthesis were obtained from *NovaBiochem*, *IRIS Biotech*, *GL Biochem*, *Bachem*, *Merck*, *ABCR*. All other chemicals were purchased from *Sigma-Aldrich*, *Fluka*, *Acros Organics*, *Merck*, *Lancaster*, *Alfa Aesar* and *ABCR* in analytical grade. DNA oligomers were purchased from *IBA*, *PURIMEX*, *Sigma-Aldrich*. Biochemical reagents were obtained from *Fermentas*, *Perkin Elmer*, *GERBU*.

8.1.3 Reactions

All air sensitive and dry reactions were carried out under argon/nitrogen as inert gas using standard schlenk technique. For the extremely moisture sensitive reactions, the glass apparatus was dried using a heat gun under vacuum followed by purging dry argon (Ar) (3 x).

8.1.4 Lyophilization

Lyophilization (freeze-drying) of peptides or building blocks from aqueous solutions and mixtures containing minor amounts of acetonitrile or dioxane was performed using a *Christ Alpha-2-4* lyophilizer equipped with a high vacuum pump. Small amounts stored in *Eppendorf* caps were lyophilized using an evacuable *Christ RVC 2-18* centrifuge connected to the lyophilization device.

8.1.5 Chromatography

a) Thin Layer Chromatography (TLC)

Merck silica gel 60 F254 (layer thickness 0.25 mm) aluminium plates were used for the analytical thin layer chromatography (TLC). The substances were detected under UV light at 254 nm and/or dipping 3% ninhydrin solution (3.0 g ninhydrin, 100 mL EtOH) followed by heating with a heat-gun.

b) Flash Column Chromatography

The chromatographic separations were performed by the fritted glass column using *Merck* silica gel 60 (40–63 μm) at 0.4–1.0 bar pressure. The columns were packed with wet silica gel (50–100 fold weight excess). All compounds were either adsorbed on silica gel before loading or loaded as a concentrated solution in the same solvent, used as an eluent.

c) High Performance Liquid Chromatography (HPLC)

Reverse Phase (RP)-HPLC analyses were performed on a *Pharmacia Äkta Basic* instrument (pump type P-900, variable wavelength detector, GE Healthcare, London, UK).

UV absorption was detected at 215 nm, 280 nm, and 254 nm with a linear gradient of

- A (0.1% TFA in H₂O) to B (0.1% TFA in MeCN/H₂O 8:2, v/v)
- A (0.1% TFA in H₂O) to B' (0.1% TFA in MeOH)
- A (0.1% TFA in H₂O) to B'' (0.1% TFA in MeCN/H₂O 9:1, v/v).
- A' (0.1% HCl in H₂O) to C (0.1% HCl in MeCN/H₂O 9:1, v/v).

Peptides were analyzed using a *YMC J'sphere* column ODS-H80, RP-C18, 250 × 4.6 mm, 4 μm, 80 Å or a *YMC J'sphere* column ODS-A, RP-C18, 250 × 4.6 mm, 5 μm, 120 Å with a flow rate of 1 mL min⁻¹.

Purification was performed with a *YMC J'sphere* column ODS-H80, RP-C18, 250 × 20 mm, 4 μm, 80 Å or with a *YMC J'sphere* column ODS-A, RP-C18, 250 × 20 mm, 5 μm, 120 Å with a flow rate of 10 mL min⁻¹.

The fractions containing the desired product were collected and lyophilized.

8.2 Characterization

8.2.1 Mass Spectrometry

Electrospray-ionization mass spectras (ESI-MS) were obtained with a *Finnigan* instrument (type *LGC* or *TSQ 7000*) or *Bruker* spectrometers (*Apex-Q IV 7T* and *micrOTOF API*). High resolution spectra were obtained with the *Bruker Apex-Q IV 7T* or the *Bruker micrOTOF*, respectively. Spectra were provided in the form of relative intensity vs. *m/z* plots, where *m* is the total mass of the molecule and the ions added and *z* is the total charge on the molecule.

8.2.2. Nuclear Magnetic Resonance Spectroscopy (NMR)

¹H and ¹³C NMR spectra were recorded with a *Varian Unity 300*, a *Varian Inova 500* or *600* or a *Bruker 300* or *400* spectrometer. Chemical shifts are quoted in parts per million (ppm) downfield of TMS (δ_{TMS} = 0 ppm). Abbreviations for multiplicities are: s, singlet; d, doublet; t, triplet; q, quartet; m, multiplet; br, broad. Coupling constants ⁿJ_{X,Y} are in Hertz (Hz), where *n* is the order of coupling. 2-D NMR experiments, [¹H,¹H]-COSY, HSQC and HMBC, assisted to further characterize the complex structures. Signals were referenced to the following residual solvent peaks: [D₆]DMSO (¹H: δ = 2.49 ppm; ¹³C: δ = 39.5 ppm); CDCl₃: (¹H: δ = 7.26 ppm; ¹³C: δ = 77.2 ppm); C₂D₂Cl₄: (¹H: δ = 5.31 ppm; ¹³C: δ = 53.73 ppm).

8.2.3 Optical Rotations

Perkin-Elmer 241 polarimeter (path length =1 dm, Na **D**-line at wavelength 589 nm) was used to measure the optical rotations. These values were calculated according to the following equation:

$$[\alpha]_D^{20} = \frac{\alpha \cdot 100}{c \cdot l}$$

α = observed rotation in degree, l = cell path length in decimeter, c = concentration [mg/100 mL].

8.3 Solid Phase Peptide Synthesis (SPPS)

8.3.1 Loading of the Resin

Loading of *NovaSyn*[®] TGR resin (0.2–0.3 mmol/g resin loading capacity) with the first amino acid (Fmoc-Lys(Boc)-OH, Fmoc-Ala-OH) was carried out manually in a syringe equipped with a PE-frit; the resin was pre-swollen in DCM (1.5 h) and NMP (3 h). DIC (5 eq.) was added to a solution of the amino acid derivative (5 eq.) and HOBt (5 eq.) in NMP (2 mL per 100 mg resin) and allowed to react at room temperature for 5 min. The resulting suspension was added to the resin and the reaction mixture was shaken at room temperature for 1.5 h. After washing, the resin with NMP, DCM, NMP, the loading procedure was repeated using a solution of amino acid derivative (5 eq.), HOAt (5 eq.), DiPEA (5 eq.) in NMP (2 mL) at room temperature for 2 h. Finally, the resin was thoroughly washed with NMP, DCM and dried over KOH in a desiccator. Estimation of loading density was performed gravimetric or via UV absorption measurements.^[166]

8.3.2 Automated SPPS

Peptides were automatically synthesized via Fmoc solid phase peptide synthesis (Fmoc-SPPS) using either the peptide synthesizer 433 A (*Applied Biosystems*) by

applying the FastMoc 0.10 mmol (amount of resin) Fmoc standard protocol in an 8 mL reaction vessel or the ‘Liberty’ microwave peptide synthesizer (*CEM*, Kamp-Lintfort, Germany) equipped with a ‘Discover’ microwave reaction cavity (*CEM*), applying 0.1 mmol. Standard reagents, protocols and procedures were used for deprotection (20% piperidine/NMP), coupling (3.9 eq. HBTU/4 eq. HOBt, activator base (10 eq. DiPEA in NMP 0.5 M) and capping (2 M Ac₂O/0.6 M DiPEA/60 mM HOBt in NMP). For peptides synthesized on Cl-Trt resin by automated microwave synthesis a maximum temperature of 50 °C was applied without capping.

8.3.3 Manual SPPS

Manual SPPS was usually carried out at 0.05–0.1 mM scale using a frit equipped syringe as reaction vessel.

- The resin was swollen for 30–60 min in DCM.
- Fmoc-deprotection: a mixture of 20% piperidine in NMP was given to the resin and agitated for 10 min (2 mL per 100 mg resin); the procedure was repeated two times.
- Washing: the resin was washed successively with NMP, DCM, NMP, each 3 x 2–3 min;
- Activators for coupling HBTU/HOBt (4.9 eq./5.0 eq.) were dissolved and stirred together with the respective building block (5 eq.) in a minimum of NMP for 5 min (preactivation). As activator base DiPEA (10 eq.) was added prior to transfer of the reaction mixture to the solid phase. Standard coupling time was 40 min.
- Washing: NMP, DCM, NMP, each 3 x 2–3 min.

After the last amino acid was coupled, a final washing with DCM or Et₂O was applied, followed by drying in *vacuo*.

8.3.4 Kaiser Test

The *Kaiser* test was used to detect free amino groups after a coupling step. Three solutions were used: 5 g of ninhydrin in 100 mL of ethanol, 80 g of liquefied phenol in 20 mL of ethanol and 2 mL of a 0.001 M aq. KCN to 98 mL pyridine.

A few beads of resin were washed several times with ethanol and placed in a small glass tube. Two drops of each solution described above was added. The suspension was heated at 120 °C for 5 min. Resulting blue color resin beads indicated positive test (free amino groups), whereas yellow color indicated no free amino groups (negative test). The Kaiser test is not accurate in the case of peptides containing proline, asparagine or serine.

8.3.5 Manual MW-SPPS

General procedure as mentioned above was applied. Deprotection program: 1) 50 °C, 25 W, 30 sec; 2) 50 °C, 25 W, 3 min. Coupling program: 50 °C, 25 W, 15 min. Double coupling was needed for building block **25** for 30 min (1 x in DMSO, 1 x in DMF).

8.3.6 Cleavage

a) Cleavage from NovaSyn[®] TGR resin

The resin was placed in a PE-frit equipped syringe and agitated with a mixture of TFA/TES/H₂O (95:2.5:2.5, v/v/v) for 2 h at RT. For peptides containing the platinum unit cleavage was performed with TFA/H₂O (95:5, v/v). Afterwards the cleavage mixture was filtered.

b) Cleavage from 2-chlorotrityl resin

The resin was placed in a frit equipped syringe and agitated with a mixture of 30% HFIP in DCM for 45 min at RT. Afterwards the cleavage mixture was filtered.

8.3.7 Post-Cleavage Work-Up

After cleavage the resulting solution was concentrated under reduced pressure. The crude product was precipitated with cold Et₂O and centrifuged at -5 °C. The liquid phase was removed and the procedure was repeated 3 times. Afterwards the crude product was dried *in vacuo* and purified by RP-HPLC.

8.4 Binding Studies

8.4.1 Fluorescence Spectroscopy

The reactions were studied on a *SPEX FluoroMax-2 (Jobin Yvon)* spectrofluorimeter. The excitation wavelength was fixed to 535 nm and the emission was monitored between 550–650 nm. DNA (DNA sodium salt from herring testis, *Sigma-Aldrich*) at a final concentration of 150 µM nucleotide was mixed with the different complexes at a final complex concentration of 12.5 µM giving a complex/nucleotide ratio (r_f) of 0.08 in 10 mM phosphate buffer (Na₂HPO₄/NaH₂PO₄, *pH* 5.8). All complex samples were incubated at 32 °C for 2 h before being transferred to a 1 cm cuvette and titration of propidium iodide.

8.4.2 UV-Thermal Melting Analysis

A *Cary 4000 UV-Vis* spectrophotometer (*Varian*) was used equipped with a temperature control unit and 1 cm cuvettes. Data were collected every 0.5 °C from 20 °C to 95 °C with an increasing temperature of 0.2 °C per minute. The thermal melting temperature, T_m , was determined by the first derivative method. All experiments were performed in triplicates at three independent occasions.

Two complementary strands of 22-mer DNA oligomers 5'-TCTCCTTCTTGTGTCTCTTCTC-3' and 3'-AGAGAGGAAGAACACAGAGAAG-5' (*IBA GmbH, Göttingen, Germany*) were mixed in 10.0 mM phosphate buffer (Na₂HPO₄/NaH₂PO₄, *pH* 5.8) and annealed by heating to 100 °C for 2 min and then slowly cooled to room temperature over 20

min. After the two strands had annealed, the complexes **C1–C8** were directly added in the cuvettes. All melting studies were performed at a duplex concentration of 1.0 μM and a complex concentration of 4.0 μM .

8.4.3 5'-³²P-end DNA Labeling

5'-DNA radio-labeling was performed in T4 polynucleotide kinase (PNK) buffer (50 mM Tris-HCl, *pH* 7.6, 10 mM MgCl₂, 5 mM DTT, 0.1 mM spermidine, 0.1 mM EDTA) (*Fermentas*) with 10 U PNK (*Fermentas*) 1.11 MBq [γ -³²P]-ATP (*Perkin Elmer*), 200 pmol DNA (single-stranded 22-mer 5'-TCTCCTTCTTGGTTCTCTTCTC-3' of HPLC grade quality, *IBA GmbH*, Göttingen, Germany) in a total reaction volume of 20 μL at 37 °C. After incubation for 30 min, another 10 U PNK was added and the reaction proceeded for 30 min. The labeled DNA was purified on denaturing PAGE (20% acrylamide M-bis 24/1 (*GERBU*, Germany)/8 M urea). The bands were visualized by lumino-radiography using a *Bio-Image Analyzer* (*Fujifilm*), excised and eluted at 4 °C overnight in 1.0 M NaOAc, *pH* 5.5 and then recovered by ethanol precipitation.

8.4.4 Radio-labeled DNA Gelshift Studies

Radio-labeled DNA, typically 650 cps/reaction or 950 cps/reaction when using large excess conditions, was mixed with different platinum-peptide complexes in 10 mM phosphate buffer (Na₂HPO₄/NaH₂PO₄, *pH* 5.8). The platinum-peptide complexes or peptides alone were added to give a final concentration of 1 μM or 10 μM , which corresponds to at least equimolar concentrations of the complex and labeled DNA or 100 μM the latter corresponding to at least a 100-fold excess of the complex over nucleotide concentration. The samples were incubated at room temperature for 18 h and then analyzed on denaturing PAGE (20% polyacrylamide/8 M urea, TBE buffer). The bands were visualized by lumino-radiography using a *Bio-Image Analyzer* (*Fujifilm*).

8.4.5 Platinum Induced Agarose Gel Mobility Shift Assays

The gel mobility shift assays were analyzed on 1% agarose-TAE gel containing 0.6 µg/mL ethidium bromide. The gels were run for 2 h at 6 V/cm. The gel image was visualized by UV light and a photo was taken using a *MP-4 Polaroid* camera and analyzed by *DiMAGE Capture A2*.

All experiments were performed in 10 mM phosphate buffer *pH* 5.8. Platination of plasmid DNA (pUC18 plasmid, purified by use of a midi-prep kit from Sigma-Aldrich) was performed at different r_f ratios ($r_f = C_{\text{complex}}/C_{\text{nucleotide}}$ from 0 to 0.3, with constant concentration of DNA, 0.15 mM as determined by a *Nanodrop ND-1000* spectrophotometer. All samples were incubated at 32 °C for 2 h. Reaction volume was 10 µL. The reactions were quenched by addition of 5 µL loading dye with NaCl (1.1 M urea, TBE, 33% (v/v) formamide, 0.025% (w/v) bromophenol blue, 0.025% (w/v) xylene cyanol, 500 mM NaCl).

8.4.6 Agarose Gel Mobility Shift Assays-IHF Preliminary Studies

The gel mobility shift assays were performed by electrophoresis on 2% agarose/TBE gel run containing 0.11 µg/ml ethidium bromide. The gels were run for 1.5 h at 60 V in 1 x TBE buffer using a horizontal standard gel electrophoresis device *MIDI* (Roth). The gel image was visualized by UV light.

All experiments were performed in Tris HCl buffer (10 mM HCl, 10 mM EDTA, 100 mM NaCl, 1 mM dithiothreitol, *pH* 7.5) with an incubation time of 3 h at RT. Total volume of reaction was 5 µL. The reactions were quenched with 3 µL loading dye (Roti^R Load DNA, *Carl Roth GmbH&Co*). A 8 µL volume of DNA Ladder 50 bp (0.1 µg/µL, Gene RullerTM, *Ferments*) was used.

8.4.7 Polymerase Chain Reaction (PCR)

PCR was performed using a *MWG Biotech* thermal cycler *Primus 96 Plus*. A mixture of 1 µL template DNA, 1 µL primer-up, 1 µL primer down, 1 µL dNTP's, 5 µL Taq

Experimental Part

buffer and 40 μL H_2O was placed in small reaction tubes (0.2–0.5 mL). The samples were covered with a layer of 30 μL *chillout-wax*.

PCR program: 3 min 95 °C, 2 min 85 °C, then Taq polymerase (1 μL) was added; (1 min 95 °C, 1 min 50 °C, 1 min 72 °C), 30 repeats; 10 min 72 °C.

The PCR products were analyzed via 1% agarose gel electrophoresis. The generated DNA fragments were combined and 1/10 part (by volume) of 7M NH_4Ac and 3 parts (by volume) of 96% EtOH were added to precipitate the DNA. The sample was vortexed and the probe was centrifuged (2 x 3 min). The supernatant was removed. The resulting pellet was dried in a heating block at 42 °C and re-suspended in water. The DNA was cut out of a 1% agarose gel and isolated with a *Prep EaseTM Gel Extraction Kit* (Promega). The DNA concentration was determined with a photometer and the purity was analyzed via 1% agarose gel electrophoresis.

Sequence primers: *H'-middle up*: 5'-CATGC ATCTG TCGCA GTAGG ACTCA CGACT GATCT AGTCG ACGTA G\GTTT CTCGT TCAGC TTTTT TATAC-3'; *H'-middle down*: 5'-TCACA GTATC GTGAT GACAG AG-3'; *H'-edge up*: 5'-CATTAA TAAAA AAGCA TTGCT TATC-3'; *H'-edge down*: 5'-TCTGC AAGAC TCTAT GAGAA GC-3'.

Sequence 200 bp DNA H'-middle: 5'-CATGC ATCTG TCGCA GTAGG ACTCA CGACT GATCT AGTCG ACGTA GGTTT CTCGT TCAGC TTTTT TATAC TAAGT TGGCA TTATA AAAAA GCATT GCTTA TCAAT TTGTT GCAAC GAACA GGTCA CTATC AGTCA AAATA AAATC ATTAT TTGAT TTCAA TTTTG TCCCA CTCCC TGCCT CTGTC ATCAC GATAC TGTGA-3'.

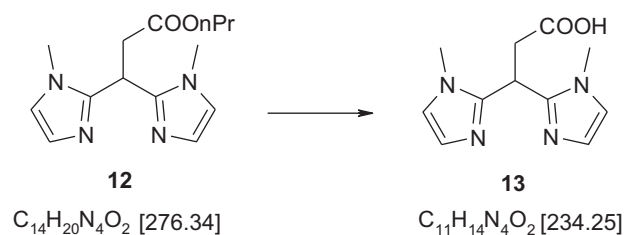
Sequence 200 bp DNA H'-edge: 5'-CATTAA TAAAA AAGCA TTGCT TATCA ATTTG TTGCA ACGAA CAGGT CACTA TCAGT CAAAA TAAAA TCATT ATTTG ATTTT AATTT TGTCC CACTC CCTGC CTCTG TCATC ACGAT ACTGT GATGC CATGG TGTCC GACTT ATGCC CGAGA AGATG TTGAG CAAAC TTATC GCTTA TCTGC TTCTC ATAGA GTCTT GCAGA-3'.

8.5 Synthesis of Platinum Complex/Nonspecific Peptide

Chimera

8.5.1 Synthesis of Platinum Chelating Building Blocks

8.5.1.1 3,3-Bis(1-methylimidazol-2-yl)propionic Acid (**13**)



To a solution of propyl-3,3-bis(1-methylimidazol-2-yl)propionate **12** (1.74 g, 6.29 mmol, 1 eq.) in THF (16 mL) a solution of KOH (1 M, 6.29 mL, 6.29 mmol, 1 eq.) was added, the solution was refluxed for 3 h and then allowed to cool to room temperature over a period of 1 h. The mixture was neutralized with HCl (1 M, 6.29 mL, 6.29 mmol, 1 eq.), the organic phase was evaporated, the aqueous phase was diluted with water (10 mL) and washed with DCM (2 x 20 mL) in order to remove traces of adduct. The water phase was collected and evaporated, then the residue was extracted three times with cold MeOH and the precipitated white KCl was removed by filtration. The organic phase was evaporated and the product was recrystallized from ethanol/water (19:1, v/v) to give **13** as white crystals (1.10 g, 4.69 mmol, 74.6%).

Analytical Data:

$^1\text{H NMR}$ (300 MHz, $[\text{D}_6]\text{DMSO}$): δ = 3.12 (d, $^3J_{\text{H,H}} = 7.3$ Hz, 2 H, CHCH₂), 3.50 (s, 6 H, NCH₃), 4.82 (t, $^3J_{\text{H,H}} = 7.3$ Hz, 1 H, CHCH₂), 6.84 (d, $^3J_{\text{H,H}} = 1.2$ Hz, 2 H, CH_{imid}NMe), 7.08 (d, $^3J_{\text{H,H}} = 1.2$ Hz, 2 H, CH_{imid}N=C).

$^{13}\text{C NMR}$ (125 MHz, $[\text{D}_6]\text{DMSO}$): δ = 31.83 (CHCH₂), 32.36 (NCH₃), 36.71 (CHCH₂), 121.99 (CH_{imid}N=C), 125.21 (CH_{imid}NMe), 145.22 (N=C-NCH₃), 171.81 (C=O).

MS (ESI) m/z : 233.1 $[\text{M}-\text{H}]^-$.

HRMS (ESI): $C_{11}H_{14}N_4O_2$ $[M-H]^-$ calcd. 233.1044, found 233.1043.

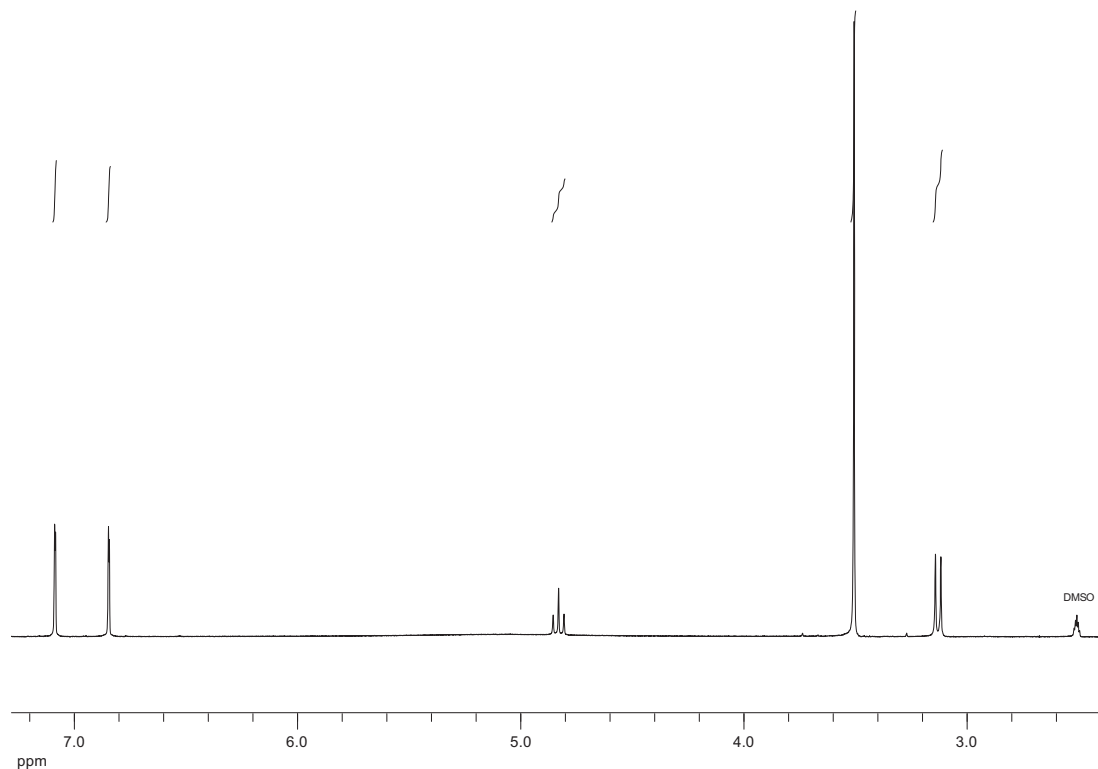
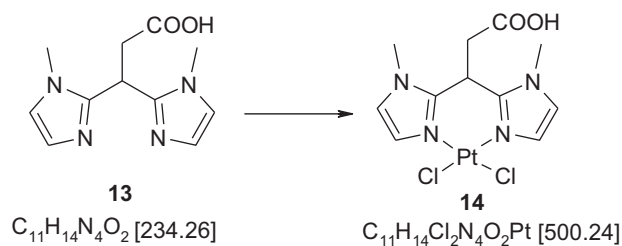


Figure 8.1 1H NMR Spectrum (300 MHz, $[D_6]$ DMSO) of compound **13**.

8.5.1.2 [3,3-Bis(1-methylimidazol-2-yl)propionic acid]dichloroplatinum(II) (**14**)



To a solution of K_2PtCl_4 (0.18 g, 0.43 mmol) in water (10 mL), a solution of 3,3-bis(1-methylimidazol-2-yl)propionic acid **13** (0.10 g, 0.43 mmol) in water (10 mL) was added at 30 °C and the resulting mixture was heated up to 40 °C and stirred at 40 °C for 3 h in the dark, then allowed to cool to room temperature over 1 h. The suspension was kept at 0 °C for 1 h and the formed precipitate was filtrated and washed with water to give **14** as a yellow solid (85 mg, 0.17 mmol, 40%).

Analytical Data:

^1H NMR (300 MHz, $[\text{D}_6]\text{DMSO}$): δ = 3.55 (d, $^3J_{\text{H,H}} = 7.4$ Hz, 2 H, CHCH₂), 3.84 (s, 6 H, NCH₃), 4.85 (t, $^3J_{\text{H,H}} = 7.4$ Hz, 1 H, CHCH₂), 7.26 (d, $^3J_{\text{H,H}} = 1.7$ Hz, 2 H, CH_{imid}NMe), 7.32 (d, $^3J_{\text{H,H}} = 1.9$ Hz, 2 H, CH_{imid}N=C), 12.00–12.36 (br s, 1 H, COOH).

^{15}N NMR (40.5 MHz, $[\text{D}_6]\text{DMSO}$): δ = -215.5 (NMe), -225.3 (N=C).

^{195}Pt NMR (64.5 MHz, $[\text{D}_6]\text{DMSO}$): δ = -2955.47.

MS (ESI) m/z : 523.0 $[\text{M}+\text{Na}]^+$, 545.0 $[\text{M}-\text{H}+2\text{Na}]^+$, 1067.0 $[2\text{M}-2\text{H}+3\text{Na}]^+$, 1236.9 $[3\text{M}+2\text{Na}-3\text{H}]^-$, 465.0 $[\text{M}-\text{Cl}]^+$, 499.0 $[\text{M}-\text{H}]$, 999.0 $[2\text{M}-\text{H}]^-$.

HRMS (ESI): $\text{C}_{11}\text{H}_{14}\text{Cl}_2\text{N}_4\text{O}_2\text{Pt}$ $[\text{M}+\text{Na}]^+$ calcd. 523.0031, found 523.0027, $[\text{M}-\text{H}]^-$ calcd. 499.0066, found 499.0052.

Elemental analysis: calcd. C 26.41%, H 2.82%, N 11.20%, found C 26.63%, H 3.01%, N 11.27%.

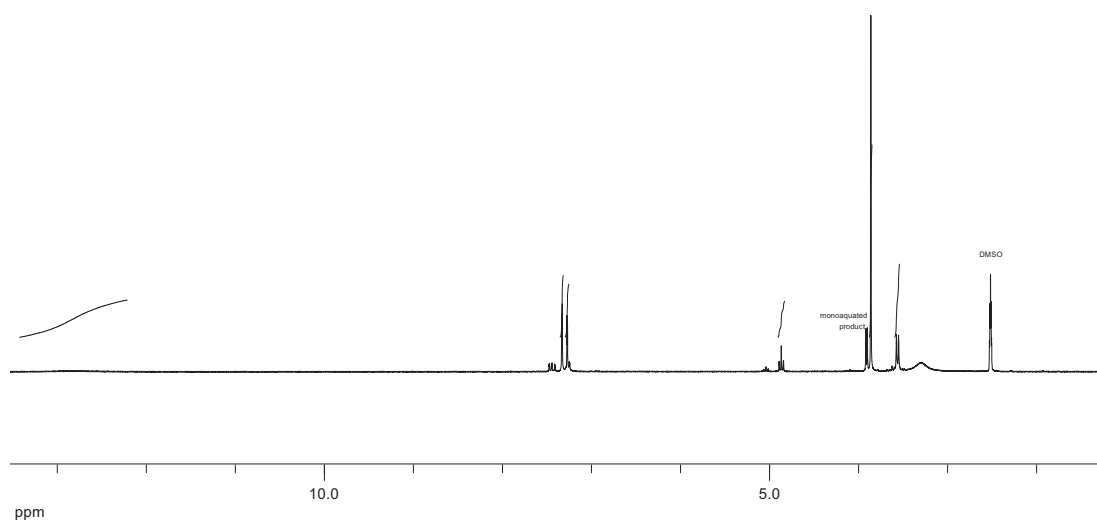
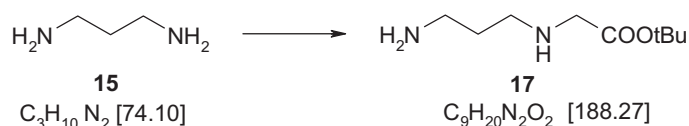


Figure 8.2 ^1H NMR Spectrum (300 MHz, $[\text{D}_6]\text{DMSO}$) of compound **14**.

8.5.1.3 *tert*-Butyl *N*-(3-Aminopropyl)glycinate (17**)**

To a vigorously stirred solution of 1,3-diaminopropane **15** (6 mL, 71.87 mmol, 8.78 eq.) in DCM (32 mL) *tert*-butyl bromoacetate **16** (1.2 mL, 8.18 mmol, 1 eq.) in DCM (6.5 mL) was added at 0 °C over 5 h. The resulting mixture was allowed to warm up to room temperature (approx. 3 h) and then stirred overnight at RT. The reaction was quenched with brine, then the mixture was washed with water (3 x 20 mL) and the combined aqueous phase was re-extracted with DCM (1 x 30 mL). The combined organic phase was dried over Na₂SO₄, filtrated, evaporated and dried in high vacuo to yield **17** (1.390 g, 7.38 mmol, 90%) as a colorless oil.

Analytical Data:

¹H NMR (300 MHz, CDCl₃): δ = 1.4 (s, 9 H, OC(CH₃)₃), 1.54–1.63 (m, 5 H, NH, NH₂, βCH₂NH₂), 2.6 (t, ³J_{H,H} = 6.9 Hz, 2 H, γCH₂NH₂), 2.72 (t, ³J_{H,H} = 6.8 Hz, 2 H, αCH₂NH₂), 3.23 (s, 2 H, CH₂COO).

¹³C NMR (125 MHz, CDCl₃): δ = 28.11 (C(CH₃)₃), 33.69 (βCH₂NH₂), 40.26 (αCH₂NH₂), 47.26 (γCH₂NH₂), 51.74 (CH₂CO), 81.03 (C(CH₃)₃), 171.63 (CO).

MS (ESI) *m/z*: 189.2 [M+H]⁺, 211.1 [M+Na]⁺, 377.3 [2M+H]²⁺.

HRMS (ESI): C₉H₂₀N₂O₂ [M+H]⁺ calcd. 189.1598, found 189.1608.

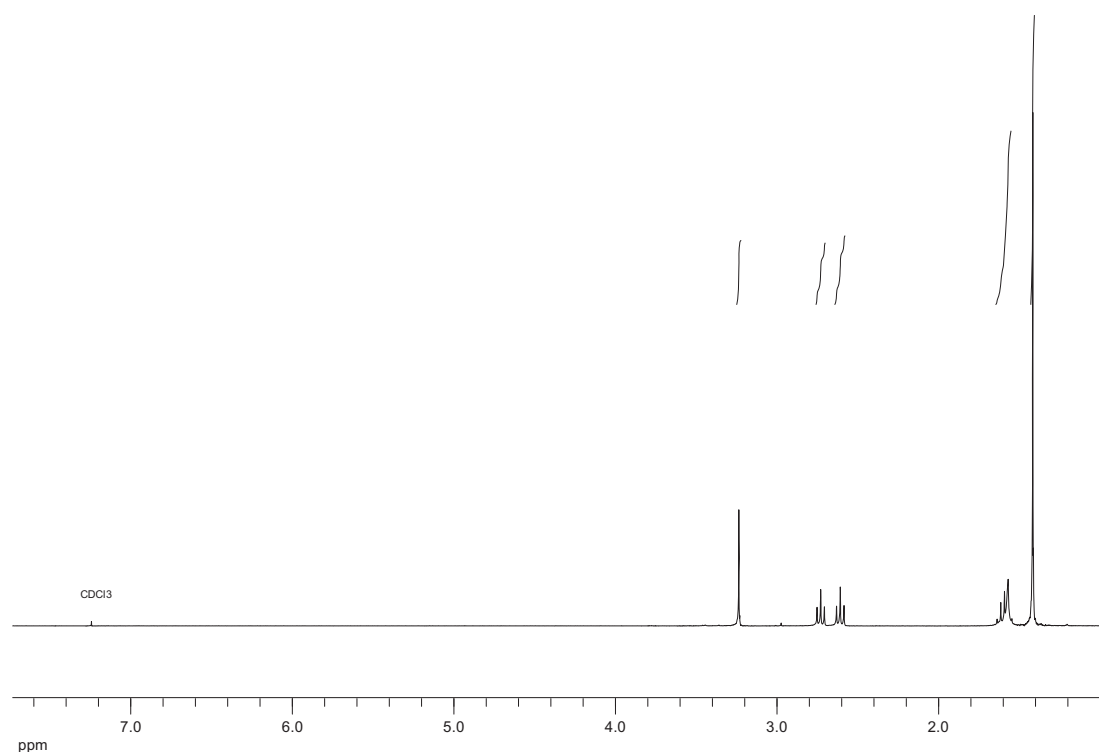
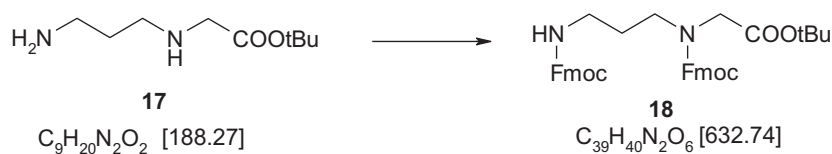


Figure 8.3 ^1H NMR Spectrum (300 MHz, CDCl_3) of compound **17**.

8.5.1.4 *tert*-Butyl *N*-Fmoc-(3-Fmoc-Aminopropyl)glycinate (**18**)



To a solution of *tert*-butyl *N*-(3-aminopropyl)glycinate **17** (1.37 g, 7.30 mmol, 1 eq.) in DCM (37 mL), DiPEA (3.75 mL, 21.91 mmol, 3 eq.) was added and the mixture was cooled to 0 °C. FmocCl (5.67 g, 21.91 mmol, 3 eq.) was added and the mixture was allowed to warm up to room temperature and stirred at RT for 2 days. The reaction was quenched with brine, the mixture was washed with water and the organic phase was dried over MgSO_4 . The residue was purified by column chromatography (pentane/ Et_2O 2:1, v/v \rightarrow pentane/ Et_2O 1:1, v/v) to yield product **18** (3.00 g, 47.41 mmol, 65%) as a white solid.

Analytical Data:

TLC (pentane/Et₂O 2:1, v/v): R_f = 0.06; (pentane/Et₂O 1:1, v/v): R_f = 0.21.

¹H NMR (300 MHz, C₂D₂Cl₄, 100 °C): δ = 1.49 (s, 9 H, OC(CH₃)₃), 1.58–1.74 (br s, 2 H, β CH₂NH), 3.08–3.21 (br s, 2 H, γ CH₂NH), 3.25–3.40 (br s, 2 H, α CH₂NH), 3.85 (s, 2 H, CH₂COO), 4.25 (m, 2 H, CH-Fmoc, CH-Fmoc'), 4.43 (d, ³J_{H,H} = 6.9 Hz, 2 H, CH₂-Fmoc), 4.52 (d, ³J_{H,H} = 6.2 Hz, 2 H, CH₂-Fmoc'), 7.33 (m, 4 H, H2-Fmoc, H2-Fmoc'), 7.41 (m, 4 H, H3-Fmoc, H3-Fmoc'), 7.61 (m, 4 H, H1-Fmoc, H1-Fmoc'), 7.77 (d, ³J_{H,H} = 7.48 Hz, 4 H, H4-Fmoc H4-Fmoc').

¹³C NMR (150 MHz, C₂D₂Cl₄, 100 °C): δ = 27.91 (CH₃), 28.16 (β CH₂NH), 38.32 (γ CH₂NH), 46.02 (α CH₂NH), 47.37 (CH-Fmoc), 47.39 (CH-Fmoc'), 49.89 (CH₂COO*t*Bu), 66.48 (CH₂-Fmoc), 67.90 (CH₂-Fmoc'), 81.67 (*Ct*Bu), 119.70 (C4-Fmoc, Fmoc'), 124.64 (C1-Fmoc), 124.77 (C1-Fmoc'), 126.83 (C2-Fmoc), 126.91 (C2-Fmoc'), 127.41 (C3-Fmoc), 127.49 (C3-Fmoc'), 141.11 (C6-Fmoc), 141.13 (C6-Fmoc'), 143.83 (C5-Fmoc), 143.95 (C5-Fmoc'), 156.05 (CO-Fmoc), 156.11 (CO-Fmoc'), 168.33 (COO*t*Bu).

MS (ESI) m/z : 655.3 [M+Na]⁺, 1287.6 [2M+Na]²⁺, 1920.8 [3M+Na]³⁺.

HRMS (ESI): C₃₉H₄₀N₂O₆ [M+Na]⁺ calcd. 655.2779, found 655.2774.

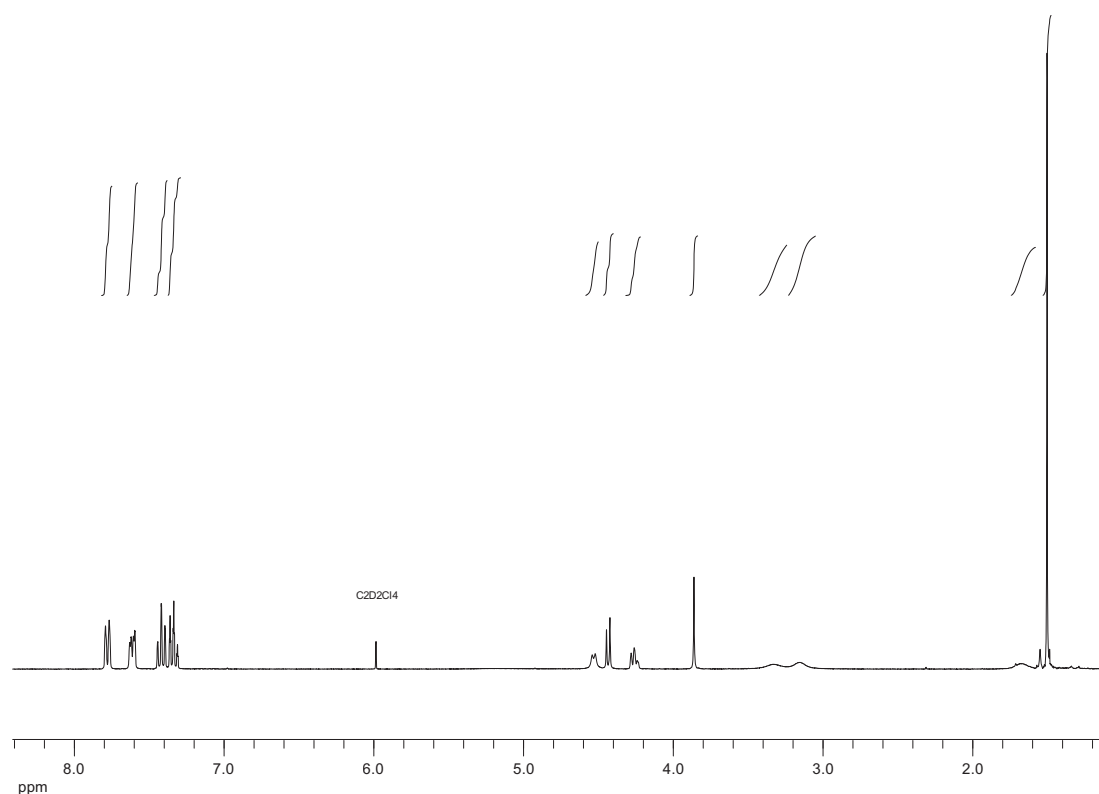


Figure 8.4 ^1H NMR Spectrum (300 MHz, $\text{C}_2\text{D}_2\text{Cl}_4$, 100 °C) of compound **18**.

8.5.1.5 *N*-Fmoc-(3-Fmoc-Aminopropyl)glycine (**19**)



tert-Butyl *N*-Fmoc-(3-Fmoc-aminopropyl)glycinate **18** (2.82 g, 4.46 mmol) was dissolved in DCM (2.8 mL) and the solution was cooled to 0 °C, followed by dropwise addition of TFA (16.75 mL). The mixture was stirred at room temperature for 2 h. The solution was concentrated in *vacuo* and coevaporated with toluene (5 x 100 mL). The residue was solubilized in minimum amount of DCM, precipitated with pentane and dried to give **19** as a white powder (2.20 g, 3.81 mmol, 85.5%).

Analytical Data:

^1H NMR (300 MHz, $\text{C}_2\text{D}_2\text{Cl}_4$, 100 °C): δ = 1.53–1.68 (br s, 2 H, $\beta\text{CH}_2\text{NH}$), 3.02–3.13 (br s, 2 H, $\gamma\text{CH}_2\text{NH}$), 3.19–3.32 (br s, 2 H, $\alpha\text{CH}_2\text{NH}$), 3.93 (s, 2 H, CH_2COO),

Experimental Part

4.24 (t, $^3J_{\text{H,H}} = 6.3$ Hz, CH-Fmoc, 2 H, CH-Fmoc'), 4.45 (d, $^3J_{\text{H,H}} = 6.7$ Hz, 2 H, CH₂-Fmoc), 4.58 (d, $^3J_{\text{H,H}} = 5.9$ Hz, 2 H, CH₂-Fmoc'), 4.85–5.25 (br s, 1 H, NH), 7.32 (m, 4 H, H2-Fmoc, H2-Fmoc'), 7.36–7.44 (m, 4 H, H3-Fmoc, H3-Fmoc'), 7.58 (t, $^3J_{\text{H,H}} = 7.9$ Hz, 4 H, H1-Fmoc, H1-Fmoc'), 7.76 (t, $^3J_{\text{H,H}} = 6.8$ Hz, 4 H, H4-Fmoc, H4-Fmoc').

¹³C NMR (150 MHz, C₂D₂Cl₄, 100 °C): $\delta = 28.09$ (β CH₂NH), 38.28 (γ CH₂NH), 46.12 (α CH₂NH), 47.29 (CH-Fmoc, CH-Fmoc'), 48.74 (CH₂COOH), 66.61 (CH₂-Fmoc), 67.35 (CH₂-Fmoc'), 119.70 (C4-Fmoc, C4-Fmoc'), 124.28 (C1-Fmoc), 124.69 (C1-Fmoc'), 126.83 (C2-Fmoc), 126.91 (C2-Fmoc'), 127.44 (C3-Fmoc), 127.48 (C3-Fmoc'), 141.10 (C6-Fmoc), 141.14 (C6-Fmoc'), 143.63 (C5-Fmoc), 143.81 (C5-Fmoc'), 156.14 (CO-Fmoc), 156.40 (CO-Fmoc'), 171.35 (COOH).

MS (ESI) m/z : 599.2 [M+Na]⁺, 615.2 [M+K]⁺, 1174.9 [2M+Na]²⁺, 575.1 [M-H]⁻.

HRMS (ESI): C₃₅H₃₂N₂O₆ [M+Na]⁺ calcd. 599.2153, found 599.2147, [M-H]⁻ calcd. 575.2188, found 575.2182.

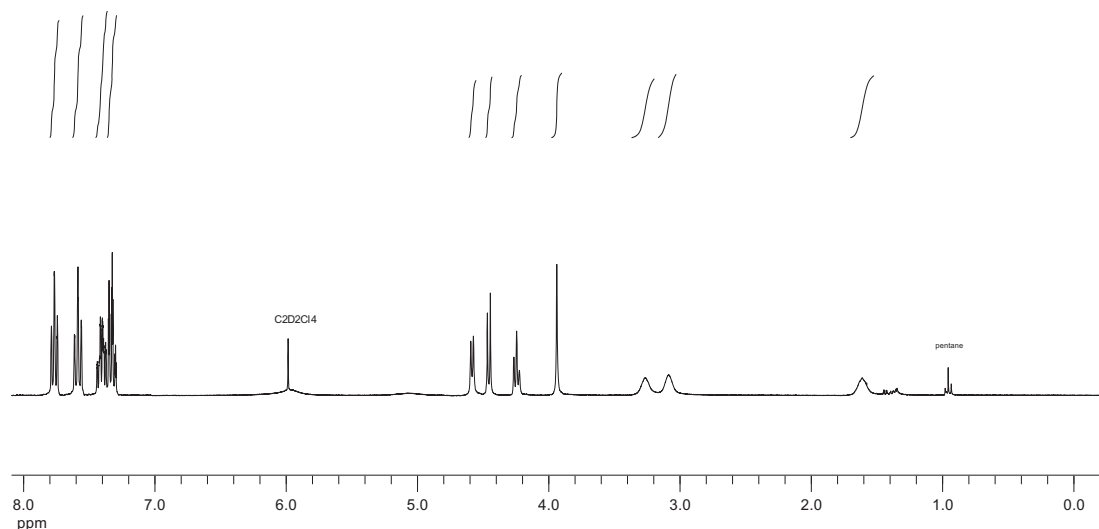


Figure 8.5 ¹H NMR Spectrum (300 MHz, C₂D₂Cl₄, 100 °C) of compound **19**.

8.5.1.6 *N*-(3-Aminopropyl)glycine (**20**)

tert-Butyl *N*-(3-aminopropyl)glycinate **17** (0.17 g, 0.87 mmol) was dissolved in DCM (0.6 mL) and the solution was cooled to 0 °C, followed by addition of TFA (3.2 mL). The mixture was stirred at room temperature for 2 h. The volatiles were evaporated in *vacuo* and co-evaporated with toluene (6 x 100 mL). The resulting residue was lyophilized to give the TFA salt of **20** as colorless solid in quantitative yield.

Analytical Data:

^1H NMR (300 MHz, $[\text{D}_6]\text{DMSO}$): δ = 1.87–1.97 (m, 2 H, $\beta\text{CH}_2\text{NH}_2$), 2.88 (t, $^3J_{\text{H,H}}$ = 7.60 Hz, 2 H, $\gamma\text{CH}_2\text{NH}_2$), 3.01 (t, $^3J_{\text{H,H}}$ = 7.63 Hz, 2 H, $\alpha\text{CH}_2\text{NH}_2$), 3.84 (s, 2 H, CH_2COO), 7.75–9.45 (br s, 4 H, COOH, NH, NH_2).

MS (ESI) m/z : 133.4 $[\text{M}+\text{H}]^+$, 131.1 $[\text{M}-\text{H}]^-$.

HRMS (ESI): $\text{C}_5\text{H}_{12}\text{N}_2\text{O}_2$ $[\text{M}+\text{H}]^+$ calcd. 133.0972, found 133.0972, $[\text{M}-\text{H}]^-$ calcd. 131.0826, found 131.0826.

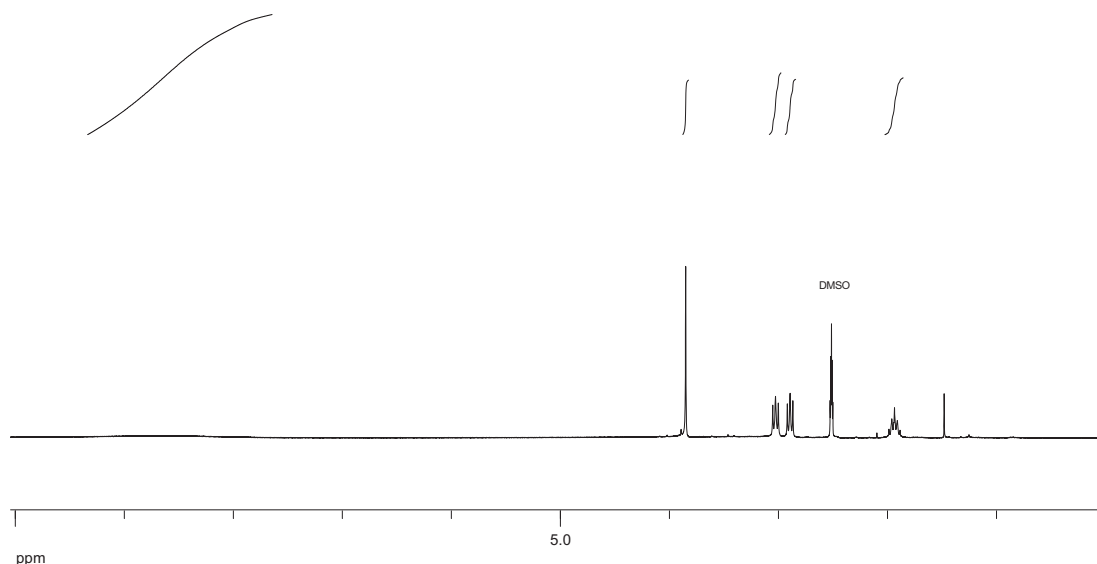
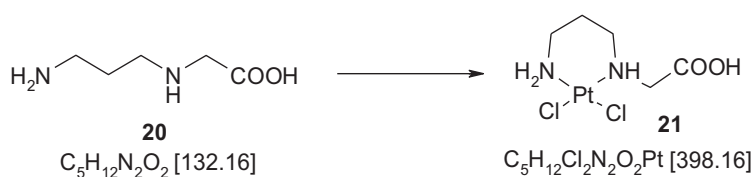


Figure 8.6 ^1H NMR Spectrum (300 MHz, $[\text{D}_6]\text{DMSO}$) of compound **20**.

8.5.1.7. [*N*-(3-Aminopropyl)glycine]dichloroplatinum(II) (**21**)



The TFA salt of **20** (0.87 mmol) was dissolved in water (20 mL), added to a solution of K_2PtCl_4 (0.36 g, 0.87 mmol) in water (20 mL) and refluxed for 40 h in the dark. The solution was concentrated at reduced pressure and the resulted precipitate was filtrated and recrystallized from water to give **21** as a yellowish solid (0.10 g, 0.26 mmol, 30.1%).

Analytical Data:

1H NMR (400 MHz, DMSO): δ = 1.83–1.98 (m, 1 H, H_A , β CH₂NH₂), 2.28–2.40 (m, 1 H, H_B , β CH₂NH₂), 2.57–2.74 (m, 2 H, γ CH₂NH₂), 2.81–2.93 (m, 2 H, α CH₂NH₂), 3.01 (dd, $^3J_{H,H}$ = 2.67, $^2J_{H,H}$ = 16.3 Hz, 1 H, H_A , CH₂COO), 3.40 (dd, $^3J_{H,H}$ = 7.0, $^2J_{H,H}$ = 16.3 Hz, 1 H, H_B , CH₂COO), 6.41 (s, 1 H, NH), 7.78 (s, 1 H, NH₂).

^{195}Pt NMR (64.5 MHz, DMSO): δ = –2995.63.

MS (ESI) m/z : 397.0 [$M-H$][–], 817.0 [$2M+Na-2H$][–], 1236.9 [$3M+2Na-3H$][–].

HRMS (ESI): $C_5H_{12}Cl_2N_2O_2Pt$ [$M-H$][–] calcd. 396.9847, found 396.9835.

Elemental analysis: calcd. C 15.08%, H 3.04%, N 7.04%, found C 14.89%, H 3.11%, N 6.59%.

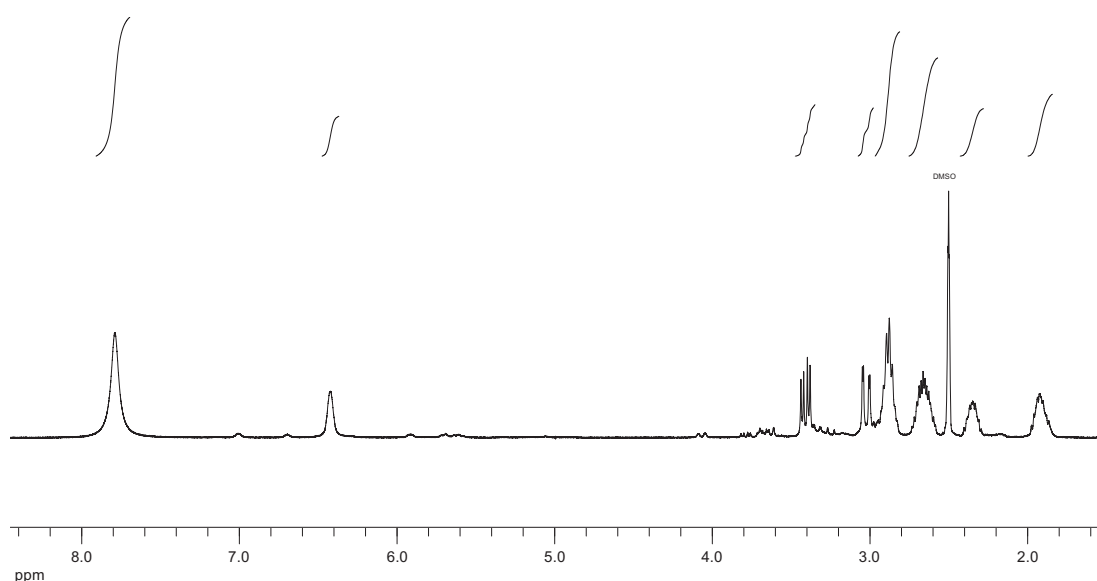


Figure 8.7 $^1\text{H-NMR}$ Spectrum (400 MHz, $[\text{D}_6]\text{DMSO}$ of compound **21**.

8.5.2 Synthesis of Peptide Oligomers and of the Platinum Complex/ Peptide Chimera

The peptides were synthesized by automated SPPS on a manual loaded *NovaSyn*[®] TGR resin according to standard Fmoc chemistry protocols (0.10 mmol scale) described in Section 8.3. Double coupling was performed for Fmoc-Lys(Boc)-OH and Fmoc-Ala-OH. After automated synthesis, the resin was placed in a syringe equipped with a PE-frit and dried over KOH in a desiccator. All further reactions were performed in the syringe.

For **C6**, **C7** and **C8**, the peptides were cleaved from the resin with a TFA/TES/H₂O (95:2.5:2.5, v/v/v) solution (100 mg resin/1.0–2.0 mL) at room temperature. All solvents were evaporated and the crude product was precipitated with cold diethyl ether (5 mL) and purified by reverse phase HPLC to give the desired products as white or colorless solids.

Further coupling for **C1–C5** with the desired building block (3,3-bis-(1-methylimidazol-2-yl)-propionic acid (**13**) for **C1**, **C3**, **C4** or *tert*-butyl *N*-Fmoc-(3-Fmoc-aminopropyl)-glycine (**19**) for **C2**, **C5** was carried out manually. The resin was swollen for 2 h in DMF, a mixture of the building block (5 eq.), HBTU (4.5 eq.),

HOBt (4.5 eq.), DiPEA (10 eq.) in DMF (2.0–3.0 mL) was added to the resin and shaken at room temperature for 40 min. The resin was thoroughly washed with DMF, DCM and dried over KOH in desiccator. A test cleavage was accomplished before further proceeding.

In the next step, platination was performed on the resin. A solution of K_2PtCl_4 (10 eq., 0.05 M) in DMF/H₂O (9:1, v/v) was added to the resin and shaken in the dark for 30 h. Cleavage from the resin was carried out with a TFA/H₂O (95:5, v/v) solution (100 mg resin/1.0–2.0 mL) for 2 h, followed by evaporation, precipitation of the crude products with cold diethyl ether. Purification by reverse phase HPLC resulted in complexes **C1–C5** as white solids.

8.5.2.1 H-GGGKKKKKK-NH₂ (C6)

C₄₂H₈₄N₁₆O₉ [957.21]

Yield: 38.0 mg (40%).

Analytical Data:

HPLC (0→50% B in 30 min), t_R : 10.41 min.

MS (ESI) m/z : 319.9 [M+3H]³⁺, 479.3 [M+2H]²⁺, 955.8 [M-H]⁻.

HRMS (ESI): [M+2H]²⁺ calcd. 479.3376, found 479.3379.

8.5.2.2 H-GGGGGGKKK-NH₂ (C7)

C₃₀H₅₇N₁₃O₉ [743.85]

Yield: 7.5 mg (10%)

Analytical Data:

HPLC (0→5% B' in 30 min), t_R : 11.10 min

MS (ESI) m/z : 372.7 [M+2H]²⁺, 744.5 [M+H]⁺, 742.4 [M-H]⁻.

HRMS (ESI): [M+H]⁺ calcd. 744.44750, found 744.44717, [M+Na]⁺ calcd. 766.4294, found 766.4294, [M-H]⁻ calcd. 742.4329, found 742.4328.

8.5.2.3 H-GGGAAAAAA-NH₂ (C8)

C₂₄H₄₂N₁₀O₉ [614.65]

Yield: 10 mg (20%, synthesis on 0.08 mmol resin).

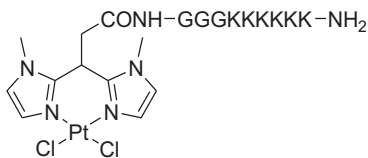
Analytical Data:

HPLC (0→50% B in 15 min), *t_R*: 10.64 min.

MS (ESI) *m/z*: 615.3 [M+H]⁺, 637.3 [M+Na]⁺, 613.4 [M-H]⁻.

HRMS (ESI): [M+H]⁺ calcd. 615.3209, found 615.3202.

8.5.2.4 [3,3-Bis(1-methylimidazol-2-yl)propionyl]-GGGKKKKKK-NH₂-dichloroplatinum(II) (C1)



C₅₃H₉₆Cl₂N₂₀O₁₀Pt [1439.44]

Yield: 22 mg (15%).

Analytical Data:

HPLC (5→45% B in 30 min) *t_R*: 17.35 min or (0→60% B' in 30 min) *t_R*: 18.58 min.

MS (ESI) *m/z*: 1438.6 [M+H]⁺, 719.8 [M+2H]²⁺, 480.2 [M+3H]³⁺.

HRMS (ESI): [M+2H]²⁺ calcd. 719.3384, found 719.3384.

8.5.2.5 N-(3-Aminopropyl)glycinyI-GGGKKKKKK-NH₂-dichloroplatinum(II) (C2)



C₄₇H₉₄Cl₂N₁₈O₁₀Pt [1337.34]

Yield: 10 mg (8%).

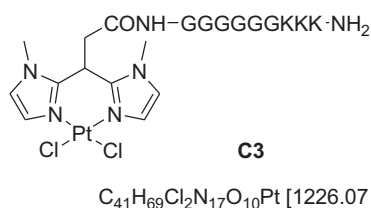
Analytical Data:

HPLC (5→30% B in 17 min) t_R : 10.52 min or (5→10% B' in 30 min) t_R : 10.37 min.

MS (ESI) m/z : 1336.6 $[M+H]^+$, 668.3 $[M+2H]^{2+}$, 446.2 $[M+3H]^{3+}$.

HRMS (ESI): $[M-Cl]^+$ calcd. 1299.6710, found 1299.6721.

8.5.2.6 [3,3-Bis(1-methylimidazol-2-yl)propionyl]-GGGGGGKKK-NH₂-dichloroplatinum(II) (C3)



Yield: 35.6 mg (29%).

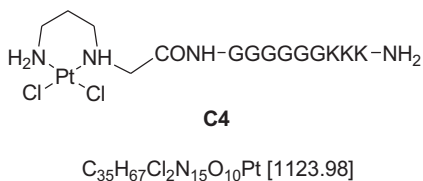
Analytical Data:

HPLC (0→50% B in 30 min) t_R : 21.14 min.

MS (ESI) m/z : 1226.5 $[M+H]^+$, 613.8 $[M+2H]^{2+}$.

HRMS (ESI): $[M+2H]^{2+}$ calcd. 612.7281, found 612.7281.

8.5.2.7 N-(3-Aminopropyl)glycinyl-GGGGGGKKK-NH₂-dichloroplatinum(II) (C4)



Yield: 16 mg (14%).

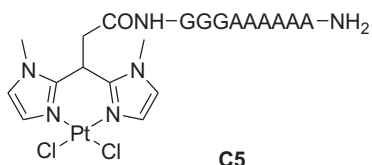
Analytical Data:

HPLC (0→40% B in 30 min) t_R : 12.43 min.

MS (ESI) m/z : 1123.4 $[M+H]^+$, 562.2 $[M+2H]^{2+}$.

HRMS (ESI): $[M+H]^+$ calcd. 1122.4271, found 1122.4261, $[M-Cl]^+$ calcd. 1086.4505, found 1086.4500.

8.5.2.8 [3,3-Bis(1-methylimidazol-2-yl)propionyl]-GGGAAAAAA-NH₂-dichloroplatinum(II) (C5)



$C_{35}H_{54}Cl_2N_{14}O_{10}Pt$ [1096.87]

Yield: 7 mg, 13% (scale 0.05 mmol resin).

Analytical Data:

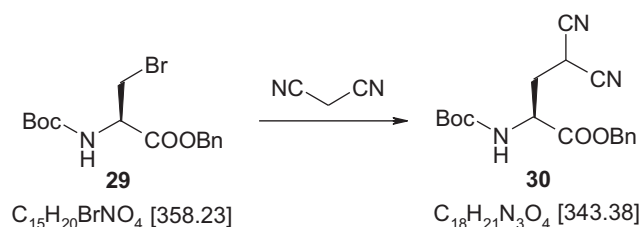
HPLC (15→75% B in 30 min) t_R : 13.58 min.

MS (ESI) m/z : 1096.4 $[M+H]^+$.

HRMS (ESI): $[M+H]^+$ calcd. 1095.3223, found 1095.3229.

8.6 Synthesis of Unnatural Amino Acids

8.6.1 (*S*)-2-(*tert*-butoxycarbonyl)-4,4-dicyano-butanoic acid benzyl ester (**30**)



To a solution of malononitrile (147 mg, 2.23 mmol, 1.2 eq.) in dry THF (8.5 mL), a solution of *t*BuOK 1M in THF (2.23 mL, 2.23 mmol, 1.2 eq.) was added dropwise at 0 °C. The mixture was stirred for 20 min at 0 °C, followed by dropwise addition of a solution of compound **29** (665 mg, 1.85 mmol) in THF (2.5 mL) at 0 °C. The reaction mixture was stirred for 20 min at 0 °C, then for 1 h at RT, followed by evaporation of the solvent under reduced pressure. Water (30 mL) was added and the crude compound was extracted with ethylacetate (4 x 60 mL). The combined organic phase was dried (Na₂SO₄) and the solvent was removed under reduced pressure. Purification by column chromatography (silica gel, *n*-pentane → EtOAc/*n*-pentane 1:9, v/v) afforded **30** as a colorless oil (130 mg, 0.38 mmol, 20.4%).

Analytical Data:

TLC (pentane/EtOAc 9:1, v/v): $R_f = 0.14$.

¹H NMR (600 MHz, CDCl₃): $\delta = 1.43$ (s, 9 H, *t*Bu), 2.36–2.43 (m, 1 H, $\beta_1\text{CH}_2$), 2.61–2.71 (m, 1 H, $\beta_2\text{CH}_2$), 3.98 (t, $^3J_{\text{H,H}} = 7.30$ Hz, 1 H, CNCHCN), 4.42–4.48 (m, 1 H, αCH), 5.21 (m, 2 H, CH₂Ph), 5.30 (s_{br}, 1 H, NH), 7.33–7.40 (m, 5 H, Ph).

¹³C NMR (125 MHz, CDCl₃): $\delta = 19.6$ (γCH), 28.2 (3 x CH₃, *t*Bu), 34.0 (βCH_2), 51.3 (αCH), 68.4 (CH₂Ph), 81.4 (*Ct*Bu), 112.1 (CN), 128.7, 128.8, 129.0 (Ph), 134.4 (Ph_{ipso}), 155.2 (COBoc), 169.5 (COBn).

MS (ESI) m/z : 344.3 [M+H]⁺, 366.5 [M+Na]⁺, 342.3 [M-H]⁻.

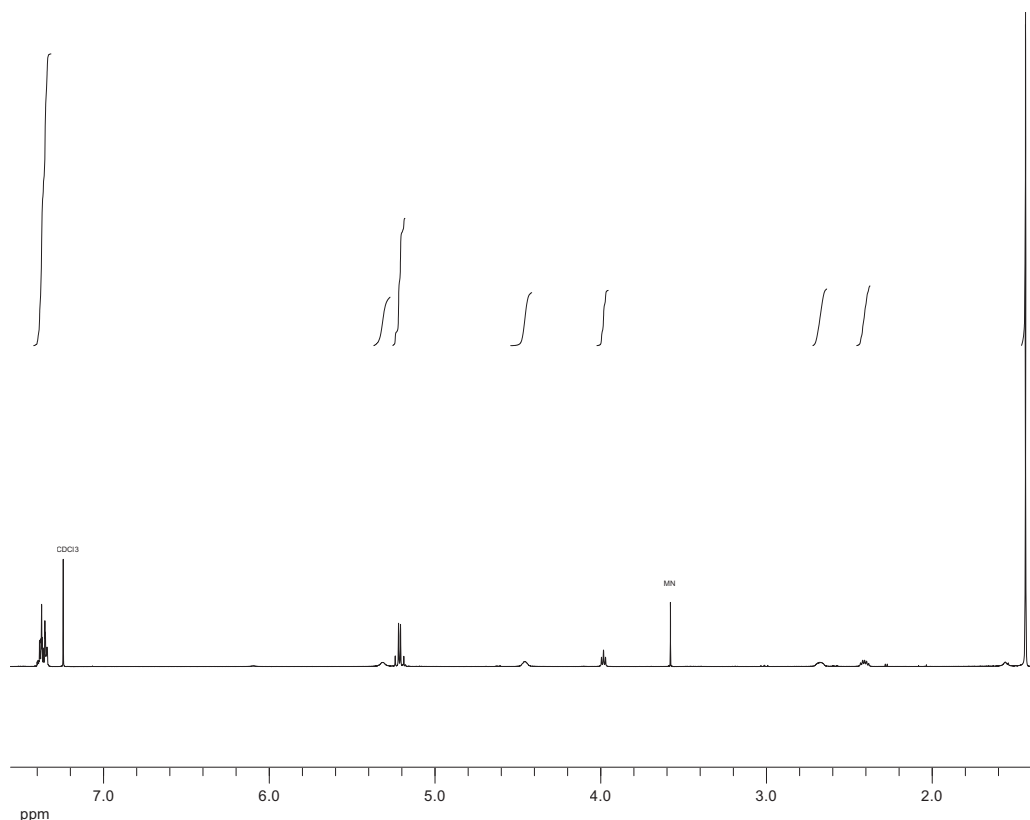
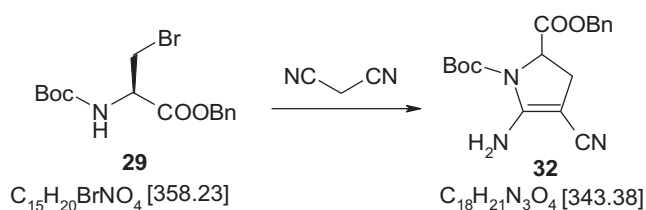


Figure 8.8 ^1H NMR Spectrum (600 MHz, CDCl_3) of compound **30**.

8.6.2 2-Benzyl-1-*tert*-butyl-5-amino-4-cyano-2,3-dihydropyrrole-1,2-dicarboxylate (**32**)



To a solution of NaH (20 mg, 0.84 mmol, 1.5 eq.) in dry THF (0.5 mL), malononitrile (56 mg, 0.84 mmol, 1.5 eq.) in THF (1.5 mL) was added at 0 °C. The mixture was stirred for 10 min at 0 °C, followed by dropwise addition of a solution of compound **29** (200 mg, 0.56 mmol) in THF (1 mL) at 0 °C. The reaction mixture was stirred for 20 min at 0 °C, then for 6 h at RT, followed by evaporation of the solvent under reduced pressure. Water (15 mL) was added and the crude compound was extracted with ethylacetate (3 x 30 mL). The combined organic phase was dried

Experimental Part

(Na₂SO₄) and the solvent was removed under reduced pressure. Purification by column chromatography (silica gel, EtOAc/*n*-pentane 1:9, v/v) afforded **32** as a colorless oil (95 mg, 0.28 mmol, 50%).

Analytical Data:

TLC (pentane/EtOAc 9:1, v/v): $R_f = 0.14$.

¹H NMR (300 MHz, CDCl₃): $\delta = 1.31$ (s, 9 H, *t*Bu), 2.57 (dd, ²J_{H,H} = 13.35 Hz, ³J_{H,H} = 4.06 Hz, 1 H, β_1 CH₂), 3.00 (dd, ²J_{H,H} = 13.34 Hz, ³J_{H,H} = 11.39 Hz, 1 H, β_2 CH₂), 4.61 (dd, ³J_{H,H} = 4.07, ³J_{H,H} = 11.36 Hz, 1 H, α CH), 5.21 (m, 2 H, CH₂Ph), 6.10 (s_{br}, 2 H, NH₂), 7.34 (s, 5 H, Ph).

¹³C NMR (125 MHz, CDCl₃): $\delta = 27.8$ (3 x CH₃, *t*Bu), 28.8 (β CH₂), 54.5 (γ C=), 59.2 (α CH), 67.4 (CH₂Ph), 83.9 (*Ct*Bu), 119.0 (CN), 128.6, 128.7 (Ph), 135.0 (Ph_{ipso}), 151.6 (δ C=), 156.9 (COBoc), 170.3 (COOBn).

MS (ESI) m/z : 344.3 [M+H]⁺, 366.5 [M+Na]⁺, 709.1 [2M+Na]⁺, 342.3 [M-H]⁻.

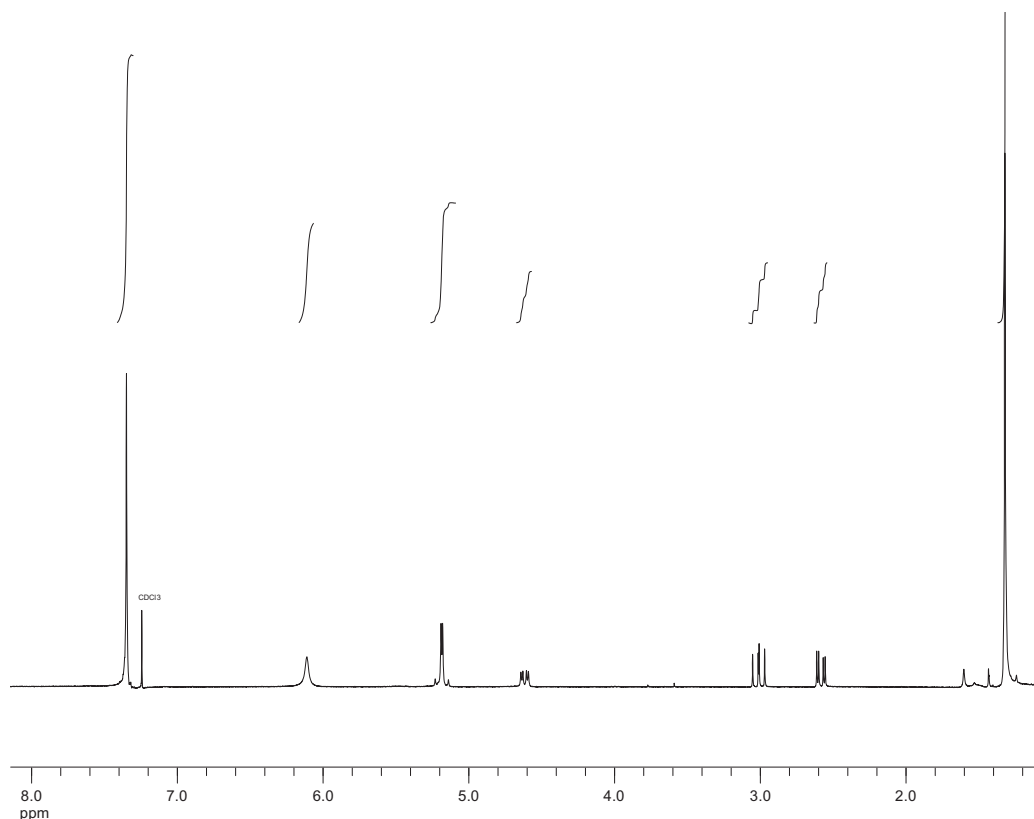
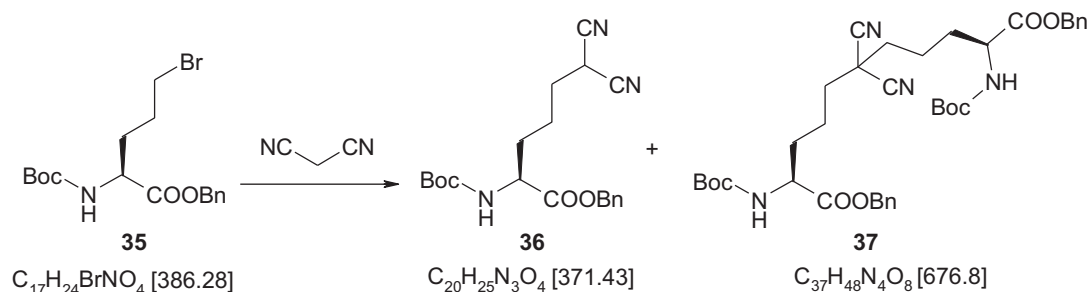


Figure 8.9 ¹H NMR Spectrum (300 MHz, CDCl₃) of compound **32**.

8.6.3 (S)-2-(tert-butoxycarbonyl)-6,6-dicyano-hexanoic acid benzyl ester (36)
and 8.6.4 (2S, 10S)-dibenzyl-2, 10-bis(tert-butoxycarbonyl)-6,6-
dicyanoundecandioate (37)



To a solution of malononitrile (273 mg, 4.13 mmol, 1.56 eq.) in dry THF (15.5 mL), a solution of *t*BuOK 1M in THF (4.13 mL, 4.13 mmol, 1.56 eq.) was added dropwise at 0 °C. The mixture was stirred for 20 min at 0 °C, followed by dropwise addition of a solution of (*R*)-3-bromo-2-(*tert*-butoxycarbonyl) pentanoic acid benzyl ester **35** (1.02 g, 2.64 mmol) in THF (3.5 mL). The reaction mixture was stirred for 20 min at RT, heated up to 50 °C, stirred for 6 h at 50 °C, then stirred overnight at RT. The solvent was evaporated under reduced pressure. Water (40 mL) was added and the crude compound was extracted with ethylacetate (4 x 70 mL). The combined organic phase was dried (Na_2SO_4) and the solvent was removed under reduced pressure. Purification by column chromatography (silica gel, EtOAc/*n*-pentane 1:9 → EtOAc/*n*-pentane 2:8, v/v) afforded **36** as a colorless oil (390 mg, 1.05 mmol, 39.82%) and its dimer **37** as a colorless oil (180 mg, 0.27 mmol, 10%).

Analytical Data:

TLC (pentane/EtOAc 8:2, v/v): R_f = 0.24.

^1H NMR (600 MHz, CDCl_3): δ = 1.41 (s, 9 H, *t*Bu), 1.52–1.75 (m, 4 H, $\gamma\beta\text{CH}_2$), 1.85–1.98 (m, 2 H, δCH_2), 3.64 (t, $^3J_{\text{H,H}}$ = 6.91 Hz, 1 H, ϵCH), 4.30–4.37 (m, 1 H, αCH), 5.10–5.23 (m, 3 H, NH, CH_2Ph), 7.30–7.37 (m, 5 H, Ph).

^{13}C NMR (125 MHz, CDCl_3): δ = 22.4 (ϵCH), 22.4 (γCH_2), 28.3 (3 x CH_3 , *t*Bu), 30.0 (δCH_2), 31.6 (βCH_2), 52.6 (αCH), 67.3 (CH_2Ph), 80.2 (*Ct*Bu), 112.2, 112.3 (2 x CN), 128.4, 128.5, 128.6 (Ph), 135.0 (Ph_{ipso}), 155.2 (COBoc), 171.7 (COOBn).

MS (ESI) m/z : 394.2 [$\text{M}+\text{Na}$] $^+$, 765.4 [$2\text{M}+\text{Na}$] $^+$, 370.2 [$\text{M}-\text{H}$] $^-$.

HRMS (ESI): C₂₀H₂₅N₃O₄ [M+Na]⁺ calcd. 394.1737, found 394.1736, [M-H]⁻ calcd. 370.1772, found 370.1771.

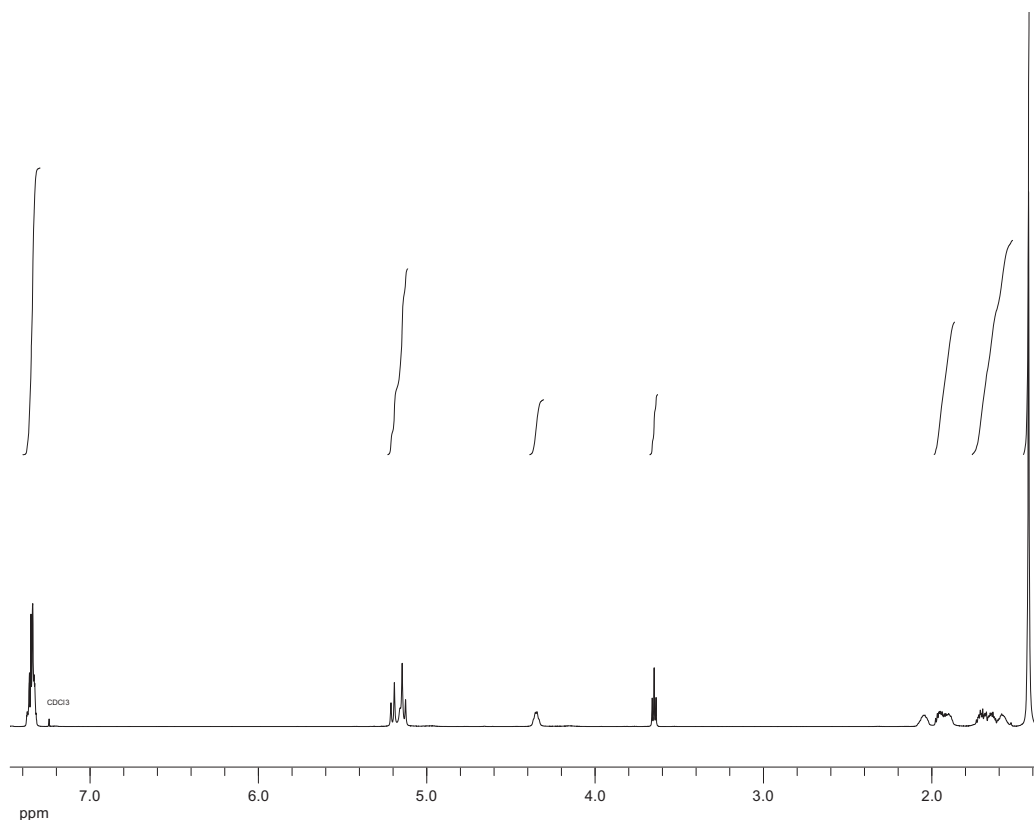


Figure 8.10 ¹H NMR Spectrum (600 MHz, CDCl₃) of compound **36**.

Dimer (37):

TLC (pentane:EtOAc 8:2, v/v): *R*_f = 0.14.

¹H NMR (300 MHz, CDCl₃): δ = 1.41 (s, 18 H, *t*Bu), 1.60–1.95 (m, 12 H, γ, β, δCH₂), 4.29–4.39 (m, 2 H, αCH), 5.04–5.22 (m, 6 H, NH, CH₂Ph), 7.34 (s, 10 H, Ph).

¹³C NMR (125 MHz, CDCl₃): δ = 21.4 (γCH), 28.3 (6 x CH₃, *t*Bu), 32.0 (δCH₂), 37.0 (βCH₂), 52.7 (αCH₂), 67.4 (CH₂Ph), 80.2 (*Ct*Bu), 115.1 (2 x CN), 128.4, 128.5, 128.6 (Ph), 135.0 (Ph_{ipso}), 155.2 (COBoc), 171.8 (COOBn).

MS (ESI) *m/z*: 699.3 [M+Na]⁺, 1375.7 [2M+Na]⁺, 675.3 [M-H]⁻.

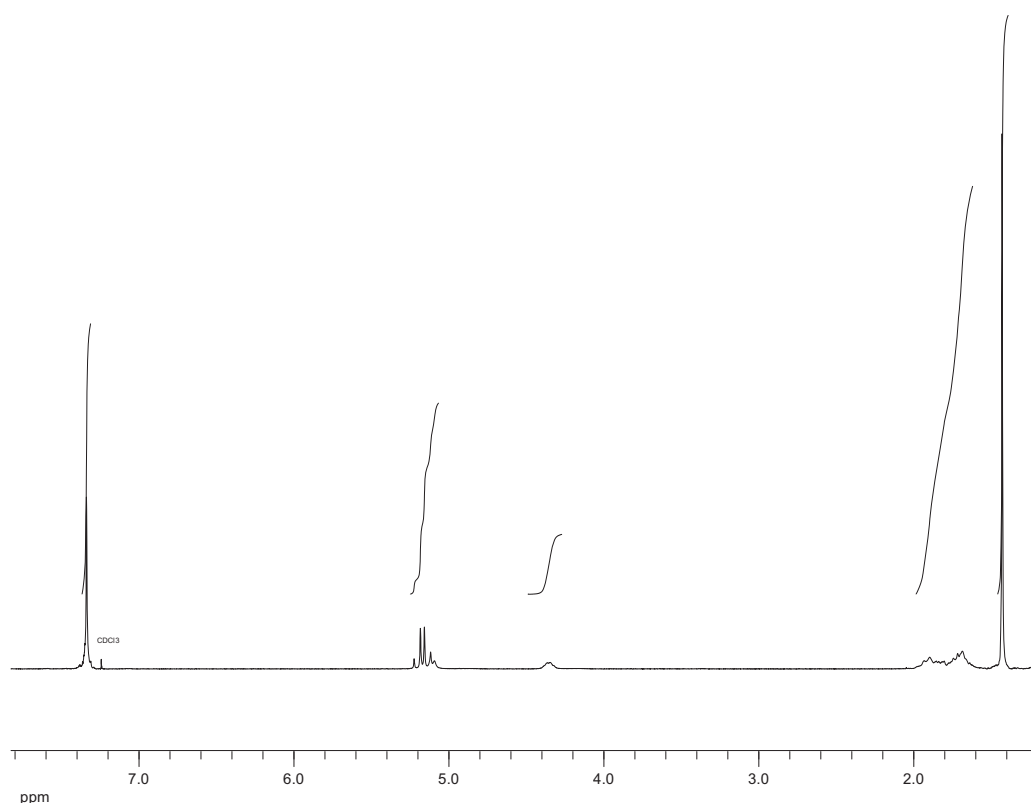
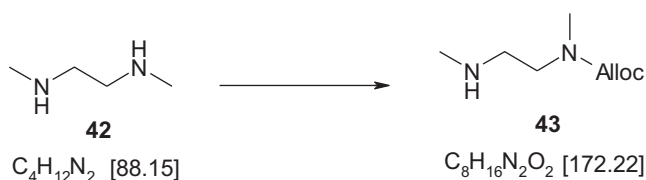


Figure 8.11 ^1H NMR Spectrum (300 MHz, CDCl_3) of compound **37**.

8.6.5 N-allyloxycarbonyl-N,N'-dimethylethylenediamine (**43**)



Allyl phenyl carbonate (0.755 mL, 4.64 mmol, 1 eq.) was added dropwise to a stirring solution of N, N'-dimethylethylenediamine **42** (0.5 mL, 4.64 mmol, 1 eq.) in ethanol p.a. (20 mL). The reaction mixture was stirred overnight at RT. The solvent was evaporated under reduced pressure. Water (30 mL) was added and the pH adjusted to 3 with HCl 1M, followed by extraction with DCM (3 x 50 mL). The aqueous phase was made strongly alkaline (*pH* 13) by addition of aq. NaOH 2M and extracted with DCM (4 x 100 mL). The combined organic phase was concentrated under reduced pressure, washed with NaOH 2M (3 x 50 mL), dried over Na_2SO_4 and evaporated in *vacuo* to afford **43** as colorless oil (0.6 g, 3.48 mmol, 75%).

Analytical data:

¹H NMR (300 MHz, CDCl₃): δ = 1.36 (s_{br}, 1 H, NH), 2.41 (s, 3 H, NHCH₃), 2.71 (t, ³J_{H,H} = 6.47 Hz, 2 H, NHCH₂), 2.91 (s, 3 H, NCH₃), 3.36 (t, ³J_{H,H} = 6.51 Hz, 2 H, NCH₂), 4.51–4.58 (m, 2 H, OCH₂), 5.12–5.30 (m, 2 H, CH=CH₂), 5.81–5.97 (m, 1 H, CH=CH₂).

¹³C NMR (125 MHz, CDCl₃): δ = 35.1 (NCH₃), 36.4 (NHCH₃), 48.4 (NCH₂), 49.5(NHCH₂), 65.9 (OCH₂), 117.1 (=CH₂), 133.0 (CH=), 156.1 (C=O).

MS (ESI) *m/z*: 173.1 [M+Ha]⁺, 195.1 [M+Na]⁺, 345.2 [2M+H]⁺, 367.2 [2M+Na]⁺

HRMS (ESI): C₈H₁₆N₂O₂ [M+H]⁺ calcd. 173.1285, found 173.1289, [M+Na]⁺ calcd. 195.1104, found 195.1109.

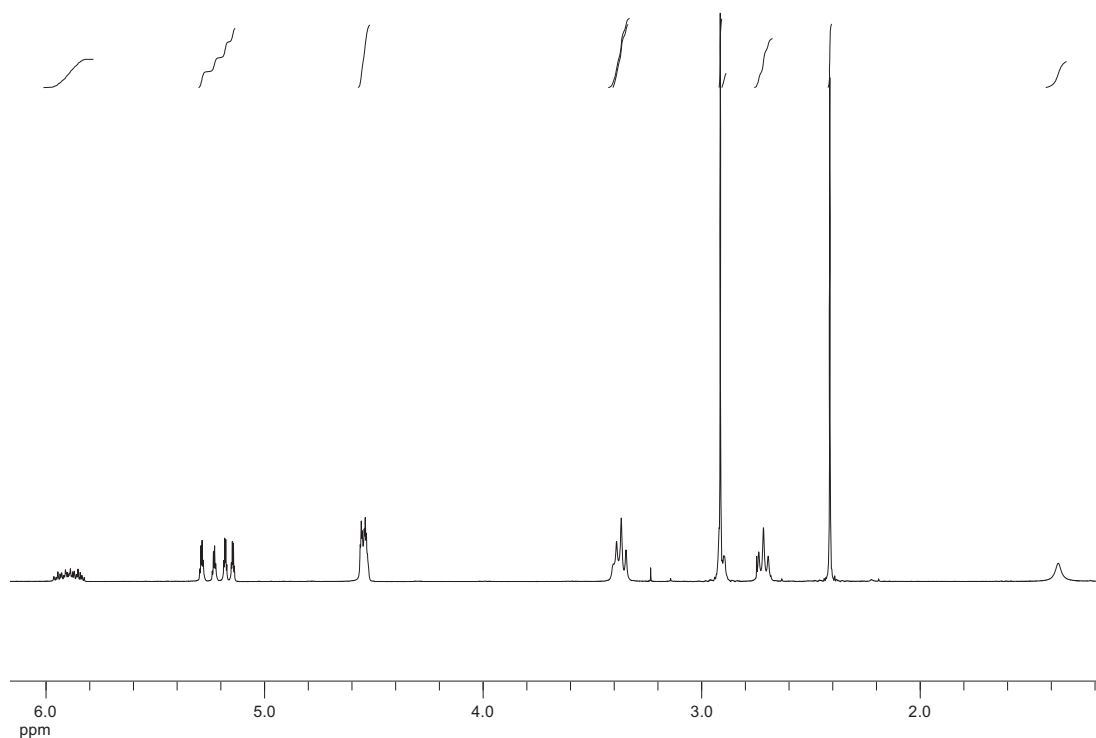
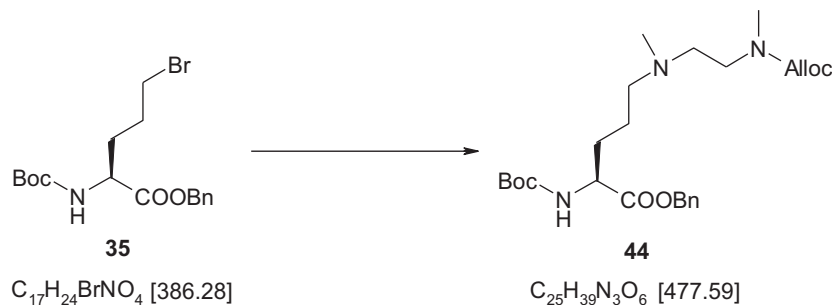


Figure 8.12 ¹H NMR Spectrum (300 MHz, CDCl₃) of compound **43**.

8.6.6 (*S*)-2-(*tert*-butoxycarbonylamino)-5-(2-(allyloxycarbonyl)-*N,N'* dimethyl ethylenediamino)pentanoic acid benzyl ester (**44**)



To a solution of compound **43** (2.75 g, 16 mmol, 3 eq.) in dry DMF (15 mL), DiPEA (2.39 mL, 16 mmol, 3 eq.) was added at RT under Ar, followed by dropwise addition of compound **35** (2.06 g, 5.33 mmol, 1 eq.) in DMF (12 mL). The solution was stirred at RT for 2 d. The solvent was evaporated under reduced pressure. The residue was dissolved in ethyl acetate and washed with water. The organic phase was dried (Na_2SO_4). The crude compound was purified by column chromatography (silicagel, pentane/ethyl acetate 1:1, v/v \rightarrow ethyl acetate 100%) to afford **44** as a colorless oil (2.05 g, 4.29 mmol, 80.5%).

Analytical data:

TLC (ethyl acetate): $R_f = 0.18$.

^1H NMR (300 MHz, $[\text{D}_6]\text{DMSO}$): $\delta = 1.31$ (s, 1 H, *t*Bu, rotamer), 1.39 (s, 8 H, *t*Bu), 1.42–1.50 (m, 2 H, γCH_2), 1.55–1.76 (m, 2 H, βCH_2), 2.12 (s, 3 H, NCH_3), 2.28 (t, $^3J_{\text{H,H}} = 6.92$ Hz, 2 H, δCH_2), 2.39 (t, $^3J_{\text{H,H}} = 6.73$ Hz, 2 H, NCH_2), 2.84 (s, 3 H, CONCH_3), 3.28 (t, $^3J_{\text{H,H}} = 6.72$ Hz, 2 H, CONCH_2), 3.98–4.09 (m, 1 H, αCH), 4.50 (dt, $^4J_{\text{H,H}} = 1.51$ Hz, $^3J_{\text{H,H}} = 5.20$ Hz, 2 H, CH_2Alloc), 5.05–5.30 (m, 4 H, CH_2Ph , $\text{CH}=\text{CH}_2$), 5.91 (ddt, $^3J_{\text{H,H}} = 5.21$ Hz, $^3J_{\text{H,H}} = 10.45$ Hz, $^3J_{\text{H,H}} = 17.18$ Hz, 1 H, $\text{CH}=\text{CH}_2$), 7.27 (d, $^3J_{\text{H,H}} = 7.77$ Hz, 1 H, NH), 7.30–7.40 (m, 5 H, Ph).

^{13}C NMR (125 MHz, $[\text{D}_6]\text{DMSO}$): $\delta = 23.1$ (γCH_2), 28.1 (3 x CH_3 , *t*Bu), 28.4 (βCH_2), 33.9 (CONCH_3), 41.6 (NCH_3), 46.1 (CONCH_2), 53.5 (αCH), 54.4 (NCH_2), 56.5 (δCH_2), 64.9 (CH_2Alloc), 65.6 (CH_2Ph), 78.2 (*Ct*Bu), 116.4 ($=\text{CH}_2\text{Alloc}$),

127.5, 127.7, 128.1 (Ph), 133.3 (CH=Alloc), 135.8 (Ph_{ipso}), 154.9 (COAlloc), 155.3 (COBoc), 172.2 (COOBn).

MS (ESI) *m/z*: 478.3 [M+H]⁺, 977.6 [2M+Na]⁺, 476.3 [M-H]⁻.

HRMS (ESI): C₂₅H₃₉N₃O₆ [M+H]⁺ calcd.478.2912, found 478.2913, [M+Na]⁺ calcd. 500.2731, found 500.2736.

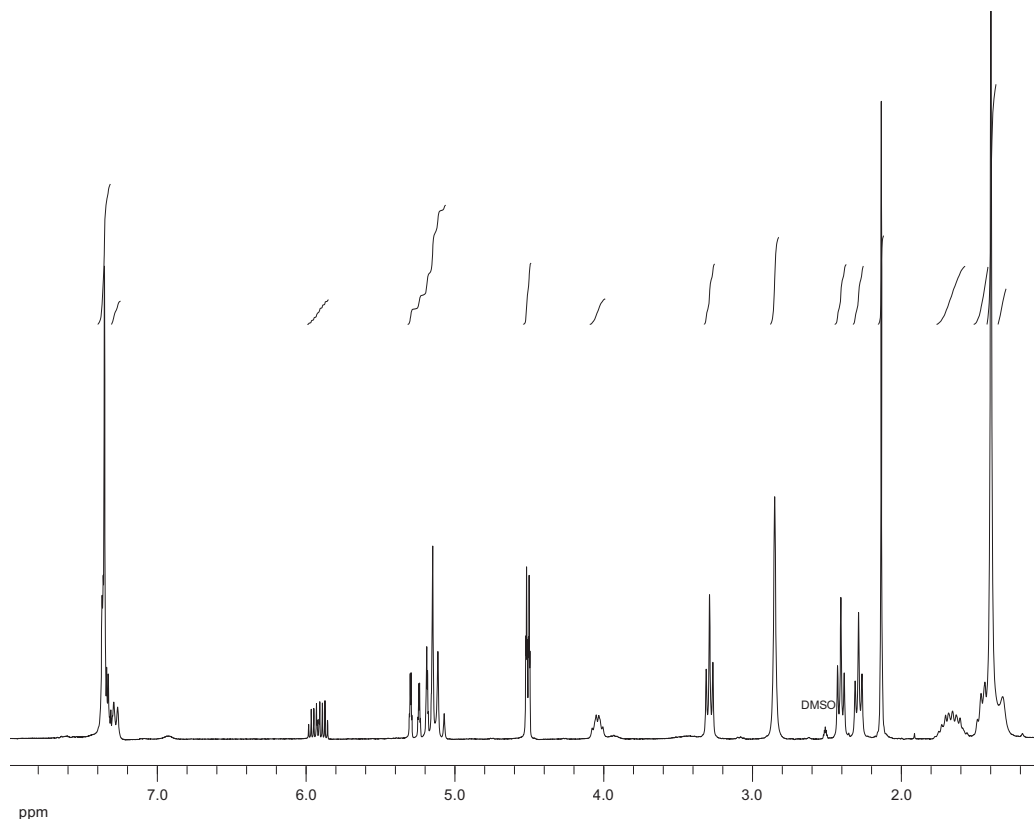
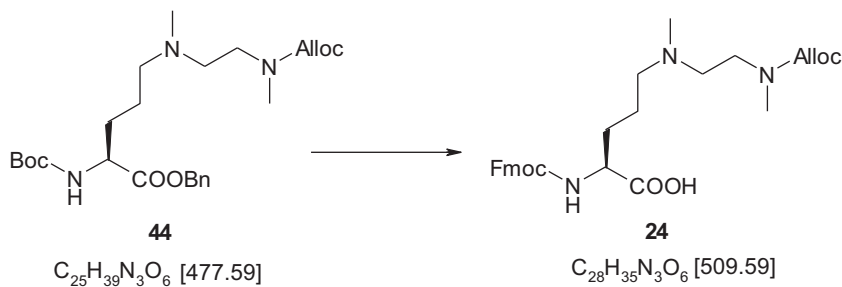


Figure 8.13 ¹H NMR Spectrum (300 MHz, [D₆]DMSO) of compound **44**.

8.6.7 (S)-2-(((9H-fluoren-9-yl)metoxy)carbonyl)-5-(2-(allyloxycarbonyl)-N,N'-dimethyl ethylenediamino)pentanoic acid (24**)**



To a solution of compound **44** (2 g, 4.19 mmol, 1 eq.) in dioxane (20 mL) and water (13.4 mL), NaOH 1M (6.7 mL) was added and the mixture was stirred at RT for 6 h. The solution was neutralized with HCl 1N (6.7 mL), concentrated under reduced pressure and lyophilized. The residue was solubilized in TFA/H₂O (95/5%, 40.2 mL) at 0 °C, stirred for 15 min at 0 °C and then for 6 h at RT. TFA is evaporated under low pressure, and the aqueous phase was co-evaporated with HCl 1N (3 x 20 mL), then lyophilized. The residue was solubilized in 10%Na₂CO₃ (30.5 mL), followed by dropwise addition of FmocOSu (1.85g, 5.48 mmol, 1.3 eq.) in dioxane (19.5 mL) at 0 °C. The mixture was further stirred for 15 min at 0 °C, then for 4 h at RT. The organic phase was evaporated under reduced pressure, the aqueous phase was diluted with water (40 mL), washed with Et₂O (3 x 80 mL) (was threw away afterwards), acidified with HCl 1N (*pH* 3) and extracted with ethyl acetate (4 x 80 mL). The combined organic phase was dried (MgSO₄), filtered and evaporated. The residue was subjected to chromatography (silica gel, DCM/MeOH 9:1, v/v →4:1) to result **24** as a white solid (1.92 g, 3.77 mmol, 90%).

Analytical Data:

TLC step1/2/3: CHCl₃/MeOH/H₂O/AcOH 70:30:3:0.35, v/v/v/v.

TLC (DCM/MeOH 4:1, v/v): *R_f* = 0.38.

¹H NMR (600 MHz, [D₆]DMSO): δ = 1.41–1.52 (m, 2 H, γ CH₂), 1.54–1.64 (m, 1 H, β_1 CH₂), 1.67–1.77 (m, 1 H, β_2 CH₂), 2.18 (s, 3 H, NCH₃), 2.35 (s_{br}, 2 H, δ CH₂), 2.47 (m, 2 H, NCH₂), 2.84 (s, 3 H, CONCH₃), 3.30 (t, ³J_{H,H} = 6.58 Hz, 2 H, CONCH₂), 3.89–4.95 (m, 1 H, α CH), 4.19–4.24 (m, 1 H, CH-Fmoc), 4.24–4.31 (m, 2 H, CH₂-Fmoc), 4.47–4.51 (m, 2 H, CH₂-Alloc), 5.51 (m, 1 H, =CH₂), 5.25 (d, ³J_{H,H} = 17.26 Hz, 1 H, =CH₂), 5.86–5.94 (m, 1 H, CH-Alloc), 7.29–7.34 (m, 2 H, C2-Fmoc), 7.41 (t, 2 H, ³J_{H,H} = 7.47 Hz, C3-Fmoc), 7.72 (m, 2 H, C1-Fmoc), 7.88 (d, 2 H, ³J_{H,H} = 7.53 Hz, C4-Fmoc).

¹³C NMR (125 MHz, [D₆]DMSO): δ = 22.9 (γ CH₂), 28.9 (β CH₂), 33.9 (CONCH₃), 40.0 (NCH₃), 45.8 (CONCH₂), 46.6 (CH-Fmoc), 54.0 (α CH), 54.6 (NCH₂), 56.5 (δ CH₂), 64.9 (CH₂Alloc), 64.7 (CH₂-Fmoc), 116.5 (=CH₂-Alloc), 119.9 (C4-Fmoc),

Experimental Part

125.0 (C1-Fmoc), 126.8 (C2-Fmoc), 127.4 (C3-Fmoc), 133.4 (CH=Alloc), 140.5 (C5-Fmoc), 143.7 (C6-Fmoc), 154.9 (CO-Alloc), 155.7 (CO-Fmoc), 173.9 (COOH).

$[\alpha]_D^{20} = +32.08$ ($c = 1.2$, CHCl_3).

MS (ESI) m/z : 510.2 $[\text{M}+\text{H}]^+$, 532.2 $[\text{M}+\text{Na}]^+$, 508.2 $[\text{M}-\text{H}]^-$, 1017.5 $[\text{2M}-\text{H}]^-$.

HRMS (ESI): $\text{C}_{28}\text{H}_{35}\text{N}_3\text{O}_6$ $[\text{M}+\text{H}]^+$ calcd. 510.2599, found 510.2609, $[\text{M}-\text{H}]^-$ calcd. 508.2453, found 508.2454.

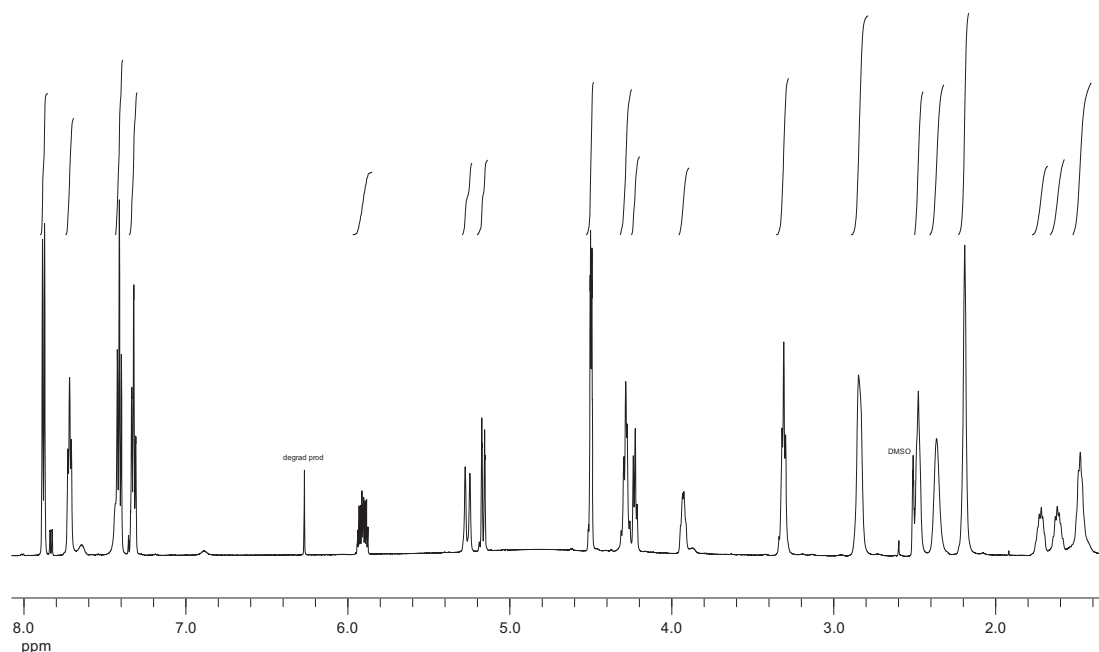
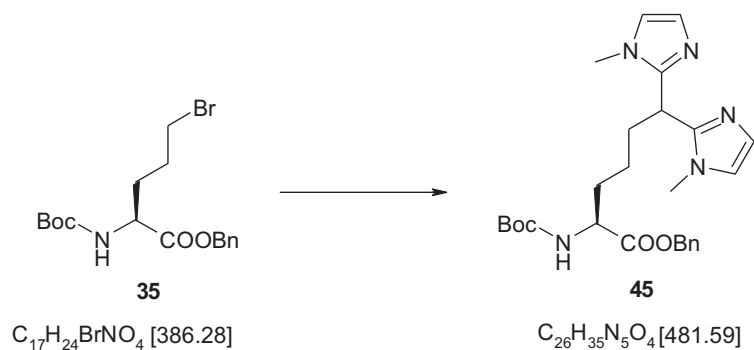


Figure 8.14 ^1H NMR Spectrum (600 MHz, $[\text{D}_6]\text{DMSO}$) of compound **24**.

8.6.8 (*S*)-2-(*tert*-butoxycarbonyl)-6,6-bis(1-methylimidazol-2-yl)hexanoic acid benzyl ester (**45**)



A solution of *n*-butyllithium in hexane (0.42 mL, 0.67 mmol, 1.6 M in hexane, 1.015 eq.) was added dropwise to a stirred solution of bis (1-methyl-imidazo-2-yl)methane (117 mg, 0.66 mmol, 1.0 eq.) in THF (3 mL) at $-78\text{ }^{\circ}\text{C}$. The solution was stirred at $-78\text{ }^{\circ}\text{C}$ for 1 h, followed by dropwise addition of compound **35** (261 mg, 0.67 mmol, 1.015 eq.) in THF (2 mL). The temperature was allowed to rise to RT overnight. The reaction mixture was quenched with water (5 mL) and all volatiles were evaporated *in vacuo*. The water layer was extracted with EtOAc (4 x 10 mL), the combined organic phase was dried (MgSO_4) and the solvent was evaporated to dryness. The residue was subjected to column chromatography (silicagel, EtOAc/pentane, 25% to 50% to 100% \rightarrow EtOAc/MeOH 9:1, v/v) to result **45** as a colorless solid (65 mg, 0.13 mmol, 20 %).

Analytical Data:

TLC (EtOAc/MeOH 9:1, v/v): $R_f = 0.06$.

$^1\text{H NMR}$ (300 MHz, CDCl_3): $\delta = .1.26\text{--}1.34$ (m, 2 H, γCH_2), 1.37 (s, 9 H, *t*Bu), 1.60–1.73 (m, 1 H, $\beta_1\text{CH}_2$), 1.75–1.87 (m, 1 H, $\beta_2\text{CH}_2$), 2.17–2.33 (m, 2 H, δCH_2), 3.35 (s, 5 H, 2 x Me), 3.38 (s, 1 H, 2 x Me), 4.18–4.29 (m, 1 H, αCH), 4.35 (t, $^3J_{\text{H,H}} = 7.91$ Hz, 1 H, ϵCH), 5.07 (m, 2 H, CH_2Ph), 5.32 (d, $^3J_{\text{H,H}} = 8.23$ Hz, 1 H, NH), 6.69 (m, 2 H, CH_{imid}), 6.87 (m, 2 H, CH_{imid}), 7.25–7.31 (m, 5 H, Ph).

$^{13}\text{C NMR}$ (75 MHz, CDCl_3): $\delta = 23.3$ (γCH_2), 28.2 (3 x CH_3 , *t*Bu), 30.3 (δCH_2), 31.7 (βCH_2), 32.7, (2 x Me), 38.3 (ϵCH), 53.2 (αCH), 66.8 (CH_2Ph), 79.5 (*Ct*Bu), 121.8, 121.9 (CH_{imid}), 126.7, 126.8 (CH_{imid}), 128.1, 128.2, 128.4 (Ph), 135.4 (Ph_{ipso}), 145.8, 145.9 (C_{imid}) 155.4 (COBoc), 172.6 (COOBn).

MS (ESI) m/z : 504.3 [$\text{M}+\text{Na}$] $^+$, 985.5 [$2\text{M}+\text{Na}$] $^+$, 480.3 [$\text{M}-\text{H}$] $^-$.

HRMS (ESI): $\text{C}_{26}\text{H}_{35}\text{N}_5\text{O}_4$ [$\text{M}+\text{Na}$] $^+$ calcd. 504.2581, found 504.2582, [$\text{M}-\text{H}$] $^-$ calcd. 480.2616, found 480.2620.

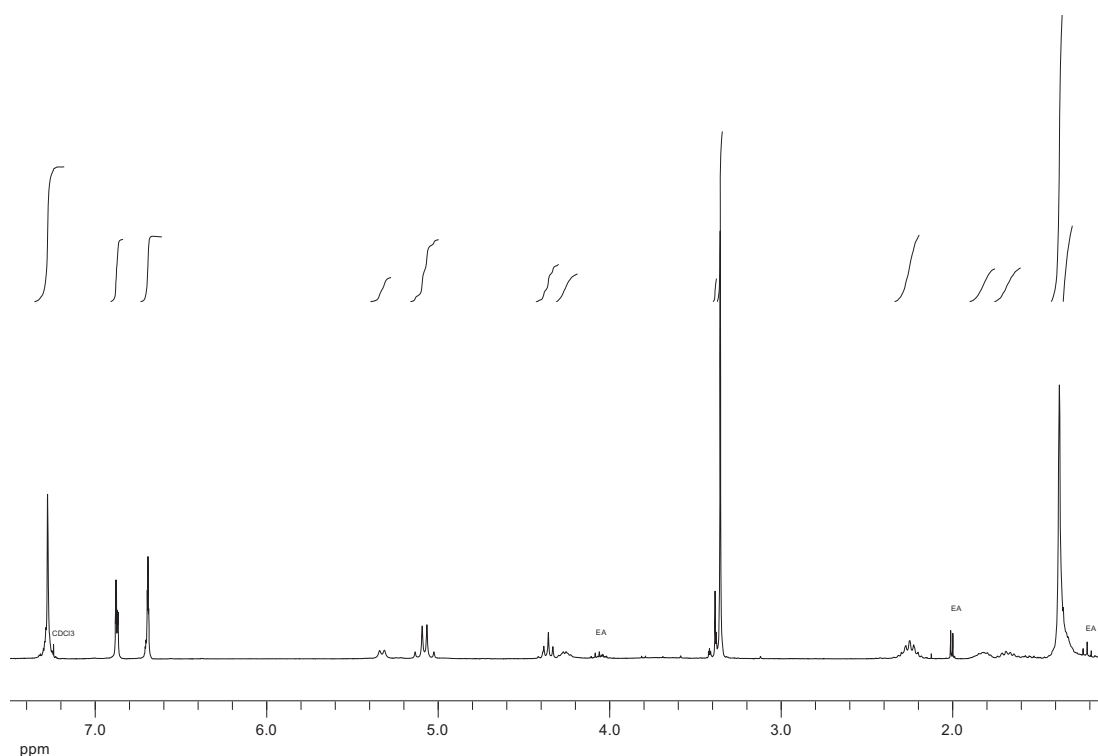
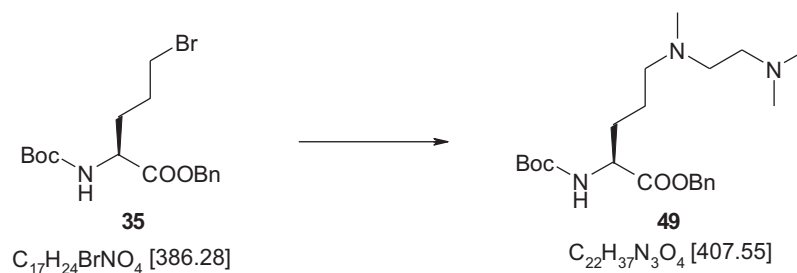


Figure 8.15 ^1H NMR Spectrum (300 MHz, CDCl_3) of compound **45**.

8.6.9 (*S*)-2-(*tert*-butoxycarbonylamino)-5-(*N,N,N'*-trimethylethylenediamino) pentanoic acid benzyl ester (**49**)



To a solution of *N,N,N'*-trimethylethylenediamine (1.09 mL, 8.40 mmol, 3 eq.) in dry DMF (8 mL), DiPEA (1.25 mL, 8.40 mmol, 3 eq.) was added at RT under Ar, followed by dropwise addition of compound **35** (1.08 g, 2.80 mmol, 1 eq.) in DMF (4 mL) at 0 °C. The solution was stirred for 30 min at 0 °C, then at RT for 1 d. The liquids were evaporated under reduced pressure and the residue was subjected to column chromatography (silica gel, acetone→acetone/water 3:2, v/v) to afford product **49** as a colorless oil, mixture of 2 conformers (1.1 g, 2.7 mmol, 96.4%).

Analytical Data:

TLC (CHCl₃/MeOH/H₂O/AcOH, 70:30:3:0.35, v/v/v/v): R_f = 0.36 (conformer 1); R_f = 0.30 (conformer 2).

¹H NMR conformer1 (300 MHz, [D₆]DMSO): δ = 1.28 (m, 2 H, *t*Bu, rotamer), 1.38 (s, 7 H, *t*Bu), 1.46–1.57 (m, 2 H, γ CH₂), 1.57–1.76 (m, 2 H, β CH₂), 2.31 (s, 3 H, NCH₃), 2.53 (m, 2 H, δ CH₂), 2.61 (s, 6 H, N(CH₃)₂), 2.75 (m, 2 H, MeNCH₂), 3.00 (m, 2 H, Me₂NCH₂), 3.97–4.09 (m, 1 H, α CH), 5.12 (m, 2 H, CH₂Ph), 7.32–7.39 (m, 5 H, Ph).

MS (ESI) m/z : 408.3 [M+H]⁺, 837.5 [2M+Na]⁺.

HRMS (ESI): C₂₂H₃₇N₃O₆ [M+H]⁺ calcd. 408.2857, found 408.2857, [M+Na]⁺ calcd. 430.2676, found 430.2676.

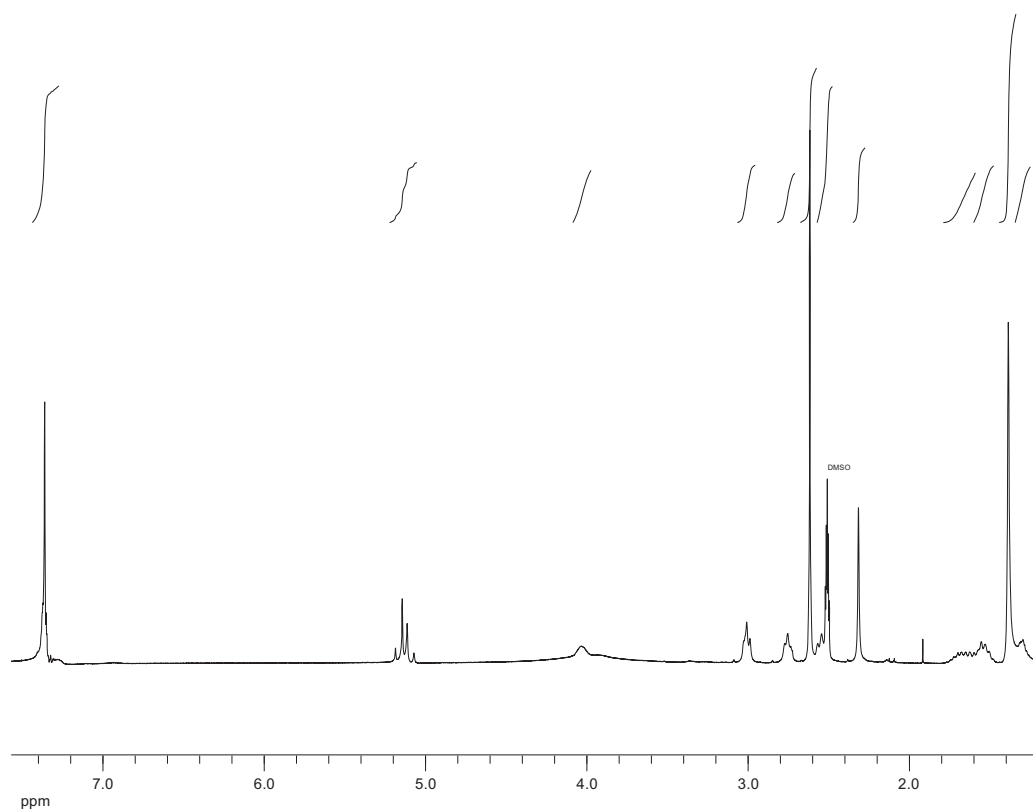


Figure 8.16 ¹H NMR Spectrum (300 MHz, [D₆]DMSO) of compound **49** (conformer 1).

Experimental Part

^1H NMR conformer 2 (300 MHz, $[\text{D}_6]$ DMSO): $\delta = 1.29$ (m, 1 H, *t*Bu, rotamer), 1.38 (s, 8 H, *t*Bu), 1.41–1.51 (m, 2 H, γCH_2), 1.53–1.72 (m, 2 H, βCH_2), 2.16 (s, 3 H, NCH₃), 2.28 (s, 6 H, N(CH₃)₂), 2.34 (t, $^3J_{\text{H,H}} = 7.08$ Hz, 2 H, δCH_2), 2.45–2.57 (m, 4 H, MeNCH₂, Me₂NCH₂), 3.96–4.05 (m, 1 H, αCH), 5.12 (m, 2 H, CH₂Ph), 7.29–7.37 (m, 5 H, Ph).

^{13}C NMR (125 MHz, $[\text{D}_6]$ DMSO): $\delta = 22.6$ (γCH_2), 28.2 (3 x CH₃, *t*Bu), 28.4 (βCH_2), 41.5 (NCH₃), 44.7 (N(CH₃)₂), 53.4 (αCH), 53.8 (MeNCH₂), 55.7 (Me₂NCH₂), 56.4 (δCH_2), 65.7 (CH₂Ph), 78.1 (C*t*Bu), 127.6, 127.8, 128.2 (Ph), 135.9 (Ph_{ipso}), 155.4 (COBoc), 172.2 (COOBn).

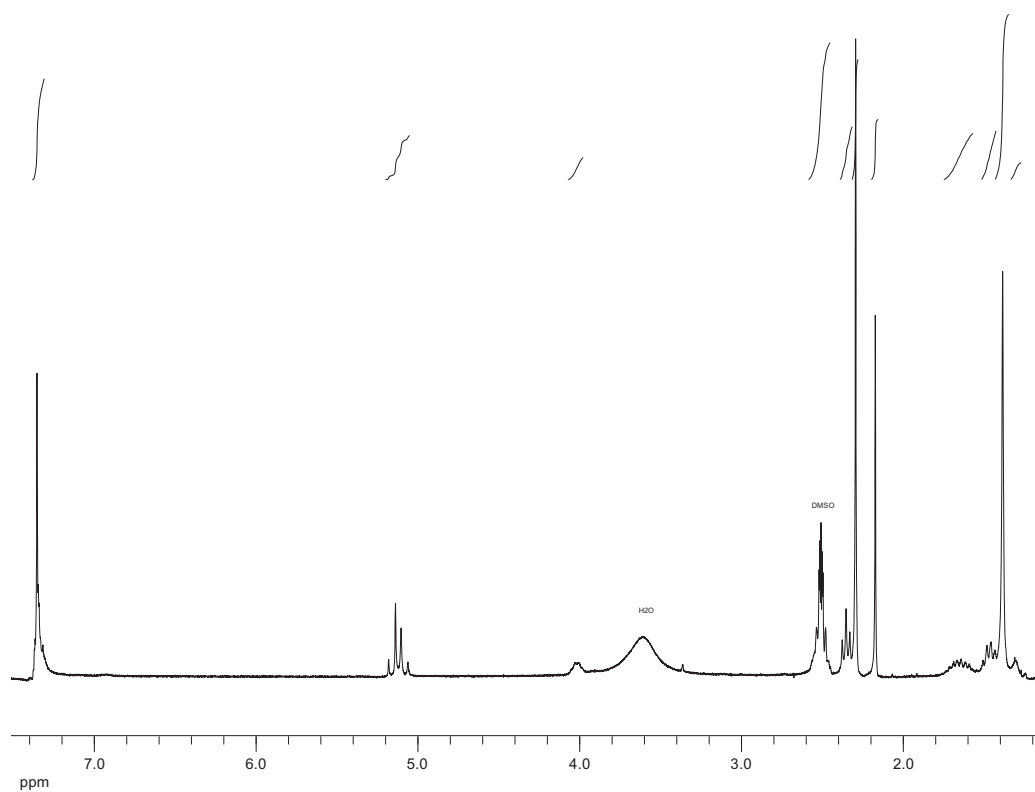
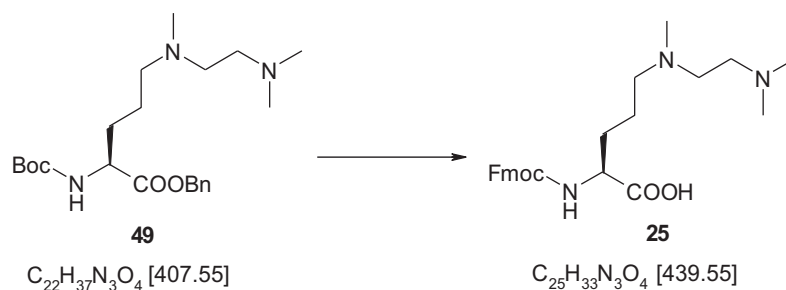


Figure 8.17 ^1H NMR Spectrum (300 MHz, $[\text{D}_6]$ DMSO) of compound **49** (conformer 2).

8.6.10 (S)-2-(((9H-fluoren-9-yl)metoxy)carbonyl)-5-(N,N,N'-trimethylethylene diamino)pentanoic acid (**25**)



To a solution of compound **49** (0.56 g, 1.37 mmol, 1 eq.) in dioxane (6.7 mL) and water (4.5 mL), NaOH 1M (2.3 mL) was added dropwise at 0 °C. The mixture was stirred at 0 °C for 30 min, then at RT for 5 h. The solution was neutralized with HCl 1N (2.3 mL), concentrated under reduced pressure and lyophilized. The residue was solubilized in TFA/H₂O (95/5, 14 mL) at 0 °C, stirred for 15 min at 0 °C and then for 6 h at RT. TFA was evaporated under low pressure, and the aqueous phase was coevaporated with HCl 1N (3 x 20 mL), then lyophilized. The residue was solubilized in 10%Na₂CO₃ (6.7 mL), followed by dropwise addition of FmocOSu (0.60g, 1.78 mmol, 1.3 eq.) in dioxane (6.7 mL) at 0 °C. The mixture was stirred for 15 min at 0 °C, then for 8 h at RT. The organic phase was evaporated under reduced pressure, the aqueous phase was diluted with water (20 mL), washed with Et₂O (2 x 30 mL) (was thrown away afterwards), acidified with HCl 1N (pH 2-3) concentrated and lyophilized. The residue was subjected to chromatography (silica gel, acetone→acetone/H₂O 3:2, v/v or RP-C18 silicagel, MeOH/H₂O, 25% to 100 % MeOH) to result **25** as a white solid (0.43 g, 0.98 mmol, 71.52%).

Analytical Data:

TLC step1/2/3: CHCl₃/MeOH/H₂O/AcOH 70:30:3:0.35, v/v/v/v.

TLC (acetone/H₂O 3:2, v/v): *R_f* = 0.26.

¹H NMR (600 MHz, [D₆]DMSO): δ = 1.47–1.54 (m, 2 H, γCH₂), 1.61–1.67 (m, 1 H, β₁CH₂), 1.69–1.75 (m, 1 H, β₂CH₂), 2.25 (s, 3 H, NCH₃), 2.39 (s, 6 H, N(CH₃)₂). 2.44–2.49 (m, 2 H, δCH₂), 2.58–2.62 (m, 2 H, Me₂NCH₂), 2.68–2.72 (m, 2 H, MeNCH₂), 3.90 (s_{br}, 1 H, αCH), 4.22 (t, ³J_{H,H} = 7.01 Hz, 1 H, CH-Fmoc), 4.28 (d,

Experimental Part

$^3J_{\text{H,H}} = 6.91$ Hz, 2 H, CH₂-Fmoc), 7.30–7.34 (m, 2 H, C2-Fmoc), 7.41 (t, $^3J_{\text{H,H}} = 7.44$ Hz, 2 H, C3-Fmoc), 7.70–7.73 (m, 2 H, C1-Fmoc), 7.88 (d, 2 H, $^3J_{\text{H,H}} = 7.52$ Hz, C4-Fmoc).

^{13}C NMR (125 MHz, [D₆]DMSO): $\delta = 22.2$ (γCH_2), 28.7 (βCH_2), 41.3 (NCH₃), 44.2 (N(CH₃)₂), 46.2 (CH-Fmoc), 53.1 (Me₂NCH₂), 53.6 (αCH), 54.8 (MeCH₂), 56.3 (δCH_2), 64.8 (CH₂-Fmoc), 119.8 (C4-Fmoc), 121.1 (C1-Fmoc), 127.1 (C2-Fmoc), 128.7 (C3-Fmoc), 137.2 (C5-Fmoc), 139.2 (C6-Fmoc), 142.4 (CO-Fmoc), 170.8 (COOH).

$[\alpha]_D^{20} = +13.94$ (c = 0.66, DMSO).

MS (ESI) m/z : 440.3 [M+H]⁺, 462.2 [M+Na]⁺, 879.5 [2M+Na]⁺, 438.3 [M-H]⁻, 877.5 [2M-H]⁻.

HRMS (ESI): C₂₅H₃₃N₃O₄ [M+H]⁺ calcd. 440.2544, found 440.2544, [M+Na]⁺ calcd. 462.2363, found 462.2370, [M-H]⁻ calcd. 438.2398, found 438.2393.

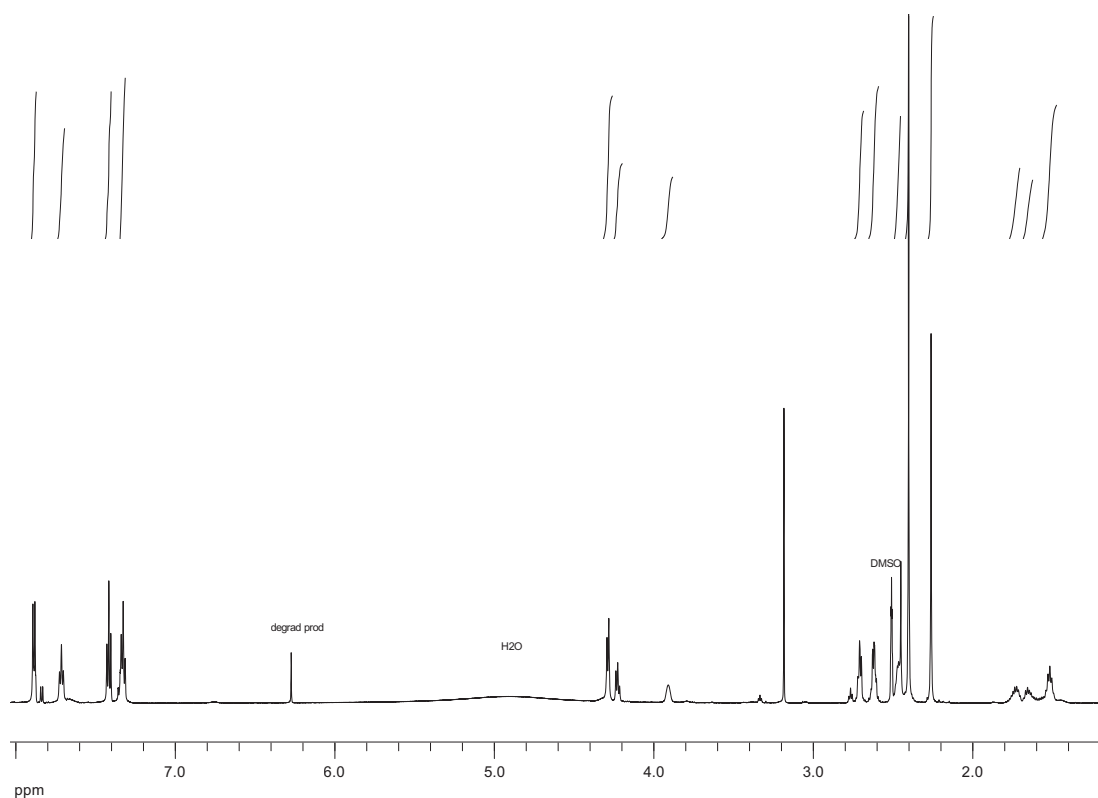


Figure 8.18 ^1H NMR Spectrum (600 MHz, [D₆]DMSO) of compound **25**.

8.6.11 N,N'-dimethylethylenediamine dichloroplatinum(II) (26)


To a solution of K_2PtCl_4 (0.207 g, 0.5 mmol, 1 eq.) in water (10 mL), a solution of N,N'-dimethylethylenediamine (**42**) (53.81 μL , 0.5 mmol, 1 eq.) in water (10 mL) was added dropwise at 30 °C and the resulting mixture was heated up to 40 °C and stirred overnight at 40 °C, then cooled to room temperature. The suspension was kept at 0 °C for 1 h with slow stirring and the resulting precipitate was filtrated and washed with water to give **26** as a green solid (105 mg, 0.296 mmol, 59.3%) (mixture of diastereoisomers: *RS/SR* (symmetry plan), *RR/SS* (C_2 symmetry axis))

Analytical data:

^1H NMR (400 MHz, $[\text{D}_6]\text{DMSO}$): δ = 2.15–2.28 (m, 2 H, H_a), 2.32–2.40 (m, 2 H, H_b), 2.46 (d, $^3J_{\text{H,H}} = 5.81$ Hz, 6 H, 2Me_a), 2.50 (d, $^3J_{\text{H,H}} = 5.83$ Hz, 6 H, 2Me_b), 2.51–2.60 (m, 2 H, H_b'), 2.71–2.76 (m, 2 H, H_a'), 6.14–6.24 (s_{br}, 4 H, NH).

^{13}C NMR (100 MHz, $[\text{D}_6]\text{DMSO}$): δ = 40.3 (CH_{3b}), 40.6 (CH_{3a}), 56.1 (CH_{2b}), 56.4 (CH_{2a}).

^{195}Pt NMR (85.84 MHz, $[\text{D}_6]\text{DMSO}$): δ = –2376.84, –2378.79.

MS (ESI) *m/z*: 377.0 $[\text{M}+\text{Na}]^+$, 731.0 $[2\text{M}+\text{Na}]^+$, 1085.0 $[3\text{M}+\text{Na}]^+$, 1438.1 $[4\text{M}+\text{Na}]^+$, 1793.1 $[5\text{M}+\text{Na}]^+$, 353.0 $[\text{M}-\text{H}]^-$, 707.0 $[2\text{M}-\text{H}]^-$.

HRMS (ESI): $\text{C}_4\text{H}_{12}\text{Cl}_2\text{N}_2\text{Pt}$ $[\text{M}+\text{Na}]^+$ calcd. 374.9896, found. 374.9895; $[\text{M}-\text{H}]^-$ calcd. 350.9931, found 350.9938.

Elemental analysis: calcd. C 13.57%, H 3.42%, N 7.91%, Cl 20.02% found C 13.44%, H 3.47%, N 7.81%. Cl 20.15%.

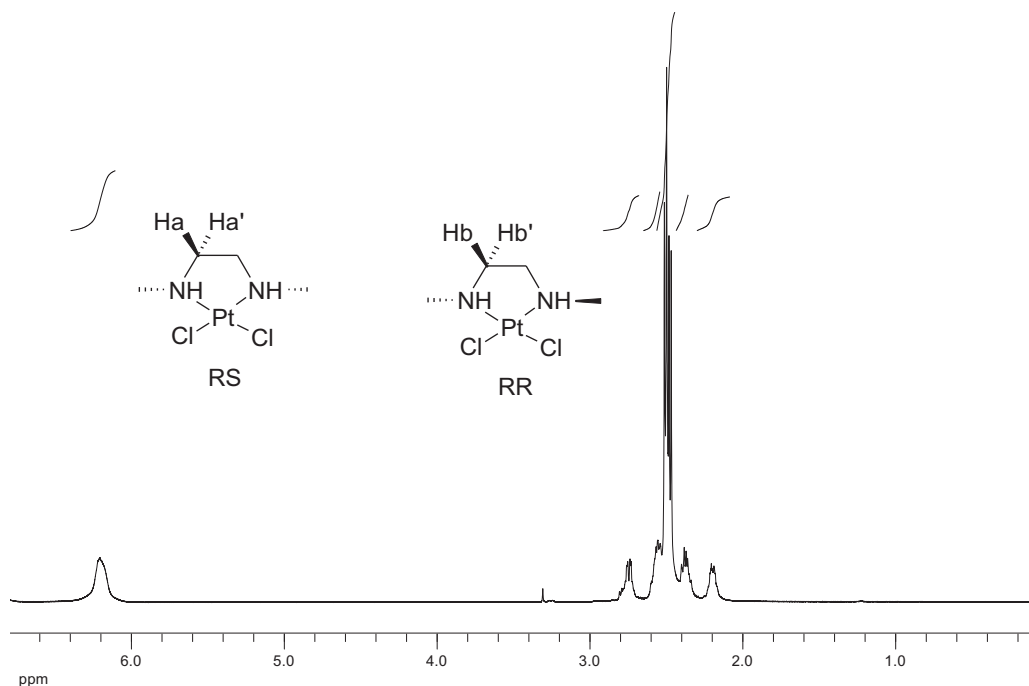
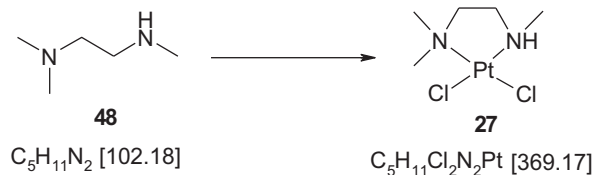


Figure 8.19 ^1H -NMR Spectrum (400 MHz, $[\text{D}_6]$ DMSO) of compound **26**.

8.6.12 N,N,N'-trimethylethylenediamine dichloroplatinum(II) (**27**)



To a solution of K_2PtCl_4 (0.207 g, 0.5 mmol, 1 eq.) in water (10 mL), a solution of N,N,N'-trimethylethylenediamine (**48**) (65.0 μL , 0.5 mmol, 1 eq.) in water (10 mL) was added dropwise at 30 $^\circ\text{C}$ and the resulting mixture was heated up to 40 $^\circ\text{C}$ and stirred overnight at 40 $^\circ\text{C}$, then cooled to room temperature. The suspension was kept at 0 $^\circ\text{C}$ for 1 h with slow stirring and the resulting precipitate was filtrated and washed with water to give compound **27** as an olive solid (137 mg, 0.371 mmol, 74.22%).

Analytical data:

^1H NMR (400 MHz, $[\text{D}_6]$ DMSO): δ = 2.35–2.42 (m, 1 H, $\alpha_1\text{CH}_2$), 2.45–2.48 (m, 1 H, $\beta_1\text{CH}_2$), 2.51 (d, $^3J_{\text{H,H}} = 5.82$ Hz, 3 H, MeNH), 2.70–2.74 (m, 1 H, $\beta_2\text{CH}_2$), 2.75 (s, 3 H, NCH₃), 2.79 (s, 3 H, NCH₃), 2.80–2.82 (m, 1 H, $\alpha_2\text{CH}_2$), 6.21 (s_{brs}, 1 H, NH).

Experimental Part

^{13}C NMR (100 MHz, $[\text{D}_6]\text{DMSO}$): $\delta = 40.3$ (NHCH_3), 51.5 ($\text{N}(\text{CH}_3)_2$), 54.9 ($\text{NH}\alpha\text{CH}_2$), 65.6 ($\text{NH}\beta\text{CH}_2$).

^{195}Pt NMR (85.84 MHz, $[\text{D}_6]\text{DMSO}$): $\delta = -2315.73$.

MS (ESI) m/z : 391.0 $[\text{M}+\text{Na}]^+$, 759.0 $[2\text{M}+\text{Na}]^+$, 1127.0 $[3\text{M}+\text{Na}]^+$, 1495.1 $[4\text{M}+\text{Na}]^+$, 1863.1 $[5\text{M}+\text{Na}]^+$, 367.0 $[\text{M}-\text{H}]^-$, 735.1 $[2\text{M}-\text{H}]^-$.

HRMS (ESI): $\text{C}_5\text{H}_{11}\text{Cl}_2\text{N}_2\text{Pt}$ $[\text{M}-\text{H}]^-$ calcd. 365.0088, found 365.0090.

Elemental analysis: calcd. C 16.27%, H 4.10%, N 7.59%, found C 16.08%, H 3.52%, N 7.49%.

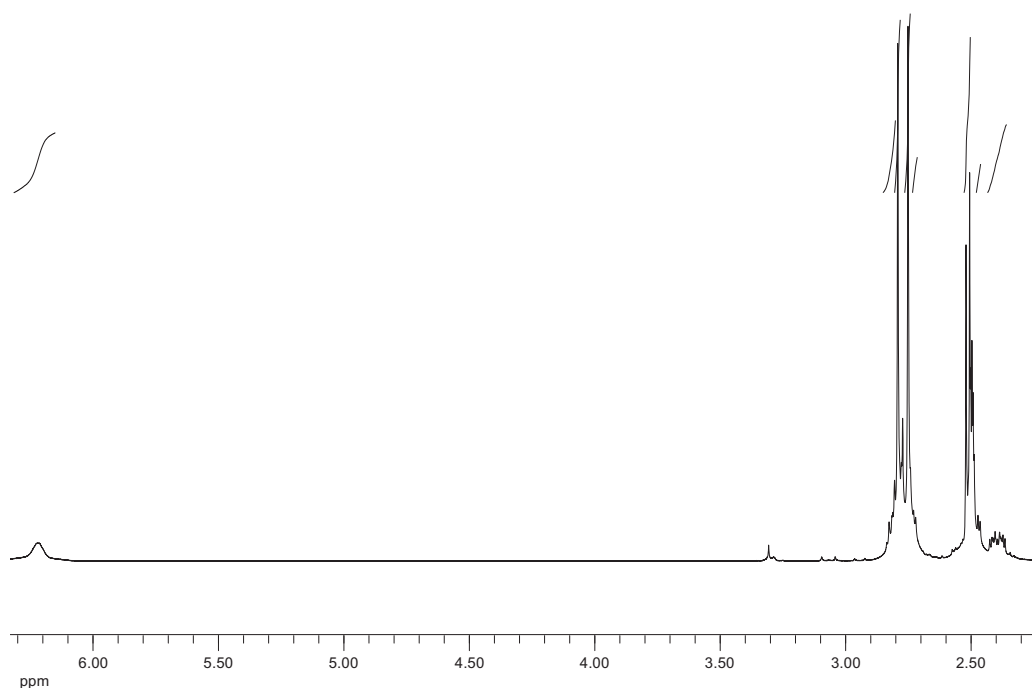
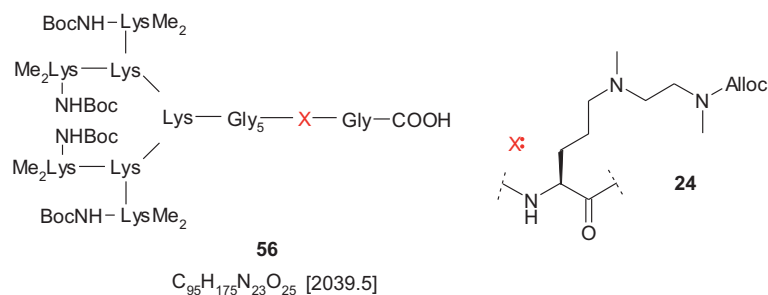


Figure 8.20 ^1H NMR Spectrum (400 MHz, $[\text{D}_6]\text{DMSO}$) of compound **27**.

8.7 Synthesis of Platinated-IHF Mimicking Peptides

8.7.1 [Boc-Lys(Me₂)]₄Lys₂LysGly₅-(S)-5-(2-(allyloxycarbonyl)-N,N'-dimethylethylene diamino)pentanoic acid-Gly-OH (**56**)



Peptide **56** was synthesized by manual Fmoc-SPPS protocol (0.10 mmol) on glycine preloaded 2-chlorotrityl resin (0.55 mmol) using the following amino acids: Fmoc-Gly-OH, Fmoc-Lys(Boc)-OH, Fmoc-Lys(Fmoc)-OH, Boc-Lys(Me₂)-OH and **24**. The synthesis protocol was modified by omitting the final deprotection step of the Boc group. The dendrimer was cleaved from the resin with 30% HFIP in DCM (5 mL) for 45 min at RT. The crude product was precipitated with cold ether (5 mL) and purified by RP-HPLC to give **56** as a white solid (43 mg, 0.02 mmol, 21%).

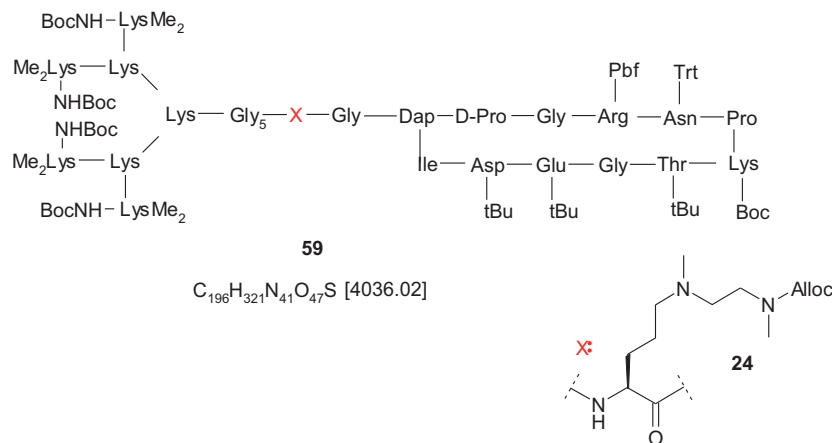
Analytical Data:

HPLC (10→60% B in 30 min), t_R : 24.35 min.

MS (ESI) m/z : 1020.16 [M+2H]²⁺, 680.45 [M+3H]³⁺, 510.59 [M+4H]⁴⁺.

HRMS (ESI): C₉₅H₁₇₅N₂₃O₂₅ [M+3H]³⁺ calcd. 680.44493, found 680.44483.

8.7.2 [Boc-Lys(Me₂)]₄Lys₂LysGly₅-(S)-5-(2-(allyloxycarbonyl)-N,N'-dimethylethylenediamino)pentanoic acid-Gly-cyclo[DapD-ProGlyArg(Pbf)Asn(Trt)Pro Lys(Boc)Thr(*t*Bu) GlyGlu(*t*Bu)Asp(*t*Bu)Ile] (59)



To a solution of dendrimer **56** (8 mg, 3.92 μmol, 2 eq.) and cyclopeptide **52** (4 mg, 1.98 μmol, 1 eq.) in dry DMF (500 μL), DIC (2.45 μL, 15.84 μmol, 8 eq.), HOAt 0.5 M in DMF (31.28 μL, 15.64 μmol, 7.9 eq.) and NMM (2.18 μL, 19.8 μmol, 10 eq.) were added under argon. The reaction mixture was stirred at RT for 3.5 days. The solvent was removed in *vacuo*, the residue was purified by RP-HPLC to give **59** as a white solid (5 mg, 1.24 μmol, 62.56%).

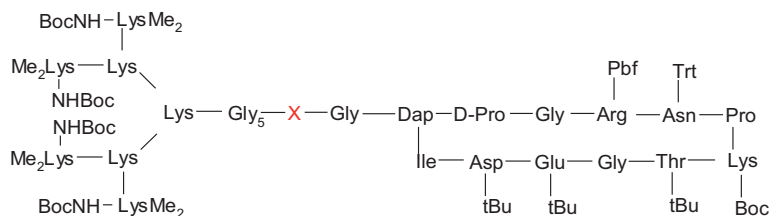
Analytical Data:

HPLC (65→100% B'' in 30 min), *t_R*: 11.24 min.

MS (ESI) *m/z*: 1345.81 [M+3H]³⁺, 1006.11 [M+4H]⁴⁺, 807.89 [M+5H]⁵⁺.

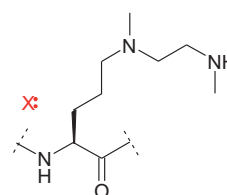
HRMS (ESI): C₁₉₆H₃₂₁N₄₁O₄₇S [M+4H]⁴⁺ calcd. 1009.35001, found 1009.35042. [M+5H]⁵⁺ calcd. 807.68146, found 807.68.142.

8.7.3 [Boc-Lys(Me₂)]₄Lys₂LysGly₅-(S)-5-N,N'-dimethylethylenediamino) pentanoic acid-Gly-cyclo[DapD-ProGlyArg(Pbf)Asn(Trt)ProLys(Boc)Thr(tBu)GlyGlu(tBu)Asp(tBu)Ile] (60)



60

C₁₉₂H₃₁₇N₄₁O₄₅S [3951.88]



Compound **59** (5 mg, 1.24 μmol, 1 eq.) was dissolved in dry DMF (500 μL) under inert atmosphere. Me₂NHBH₃ (3 mg, 49.6 μmol, 40 eq.) and Pd(PPh₃)₄ (0.15 mg, 0.12 μmol, 0.1 eq.) were added. The reaction mixture was stirred at RT for 6 h. The solvent was evaporated in *vacuo*, the residue was purified by RP-HPLC to give **60** as a white solid (3 mg, 0.76 μmol, 61.32%).

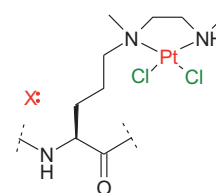
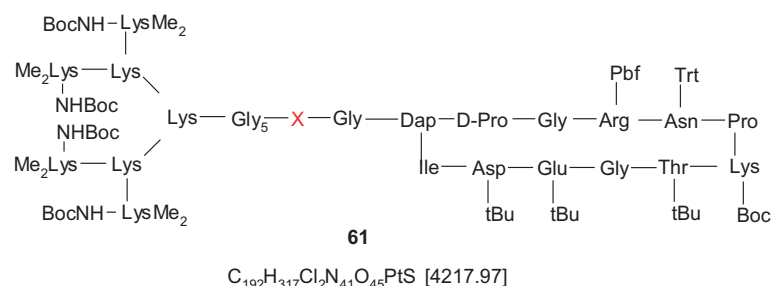
Analytical Data:

HPLC (60→100% B in 30 min), *t_R*: 16.85 min.

MS (ESI) *m/z*: 1317.80 [M+3H]³⁺, 988.60 [M+4H]⁴⁺.

HRMS (ESI): C₁₉₂H₃₁₇N₄₁O₄₅S [M+4H]⁴⁺ calcd. 988.3447, found 988.3448.

8.7.4 [Boc-Lys(Me₂)]₄Lys₂LysGly₅-(S)-5-N,N'-dimethylethylenediamino) pentanoic acid-Gly-cyclo[DapD-ProGlyArg(Pbf)Asn(Trt)ProLys(Boc)Thr(tBu)GlyGlu(tBu)Asp(tBu)Ile]-dichloroplatinum(II)(61)



A solution of K₂PtCl₄ (9.45 mg, 22.77 μmol, 30 eq., 0.05 M) in DMF/H₂O (455 μL, 9:1, v/v) was added to compound **60** (3 mg, 0.76 μmol, 1 eq.) and stirred at RT in the dark for 2 days. The solvent was removed in *vacuo*. Analytical RP-HPLC showed formation of **61** as a white solid.

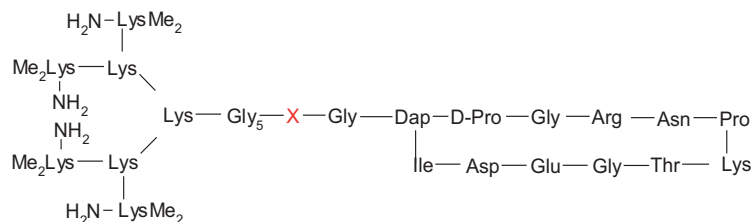
Analytical Data:

HPLC (5→60% B in 30 min), *t_R*: 36.58 min.

MS (ESI) *m/z*: 1406.10 [M+3H]³⁺, 1054.82 [M+4H]⁴⁺, 845.08 [M+5H]⁵⁺.

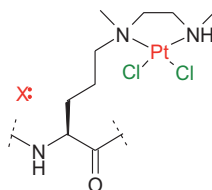
HRMS (ESI): C₁₉₂H₃₁₇Cl₂N₄₁O₄₅PtS [M+4H]⁴⁺ calcd. 1054.3199, found 1054.3196, [M+5H]⁵⁺ calcd. 843.6573, found 843.6568.

8.7.5 [Lys(Me₂)₄Lys₂LysGly₅-(S)-5-N,N'-dimethylethylenediamino)pentanoic acid-Gly-cyclo[DapD-ProGlyArgAsnProLysThrGlyGluAspIle]-dichloro platinum(II) (22)



22

C₁₂₃H₂₂₃Cl₂N₄₁O₃₂Pt [3054.40]



Compound **61** was dissolved in TFA/H₂O (500 μL, 95:5) and stirred for 45 min at RT. in the dark. The solvent was evaporated in *vacuo*, the residue was purified by RP-HPLC to give **22** as a white solid (0.3 mg, 0.096 μmol, 12.92%).

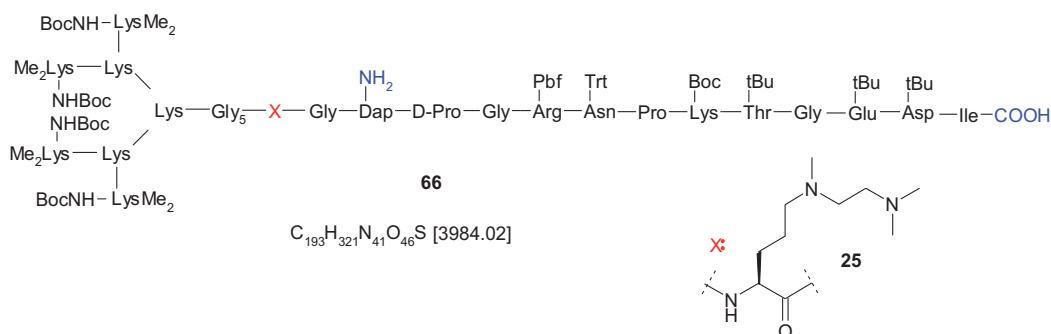
Analytical Data:

HPLC (5→60% B in 30 min), *t_R*: 11.73 min.

MS (ESI) *m/z*: 1018.54 [M+3H]³⁺, 763.9 [M+4H]⁴⁺.

HRMS (ESI): C₁₂₃H₂₂₃Cl₂N₄₁O₃₂Pt [M+4H]⁴⁺ calcd. 764.4104, found 764.4105.

8.7.6 [Boc-Lys(Me₂)]₄Lys₂LysGly₅-(S)-5-N,N,N'-trimethylethylenediamino) pentanoic acid-Gly-DapD-ProGlyArg(Pbf)Asn(Trt)ProLys(Boc)Thr(*t*Bu)GlyGlu(*t*Bu)Asp(*t*Bu)Ile-OH (66**)**



Peptide **66** was synthesized by automated (until X coupling) and manual microwave Fmoc-SPPS protocol (0.05 mmol) on isoleucine preloaded 2-chlorotrityl resin using the following amino acids: Fmoc-Asp(*O**t*Bu)-OH, Fmoc-Glu(*O**t*Bu)-OH, Fmoc-Gly-OH, Fmoc-Thr(*t*Bu)-OH, Fmoc-Lys(Boc)-OH, Fmoc-Pro-OH, Fmoc-Asn(Trt)-OH, Fmoc-Arg(Pbf)-OH, Fmoc-D-Pro-OH, Alloc-Dap(Fmoc)-OH, **25**, Fmoc-Lys(Boc)-OH, Fmoc-Lys(Fmoc)-OH, Boc-Lys(Me₂)-OH. For **25** double coupling was performed in DMF, respectively in DMSO, for 30 min each, at 50 °C, 25 W. After synthesis, the resin was placed in a syringe equipped with a PE-frit and washed with DCM and dried over KOH in a desiccator. All further reactions were performed in the syringe. A mixture of Me₂NHBH₃ (120 mg, 2.0 mmol, 40 eq.) and Pd(PPh₃)₄ (6 mg, 5 μmol, 0.1 eq.) in 2 mL DMF was added and the reaction mixture was agitated at RT for 6 h. The resin was washed with DCM until it became colorless. Cleavage was carried out with 30% HFIP in DCM (2 mL) for 45 min. The solvent was evaporated in *vacuo*, the residue was purified by RP-HPLC to give **66** as a white solid (5 mg, 1.26 μmol, 2.51%).

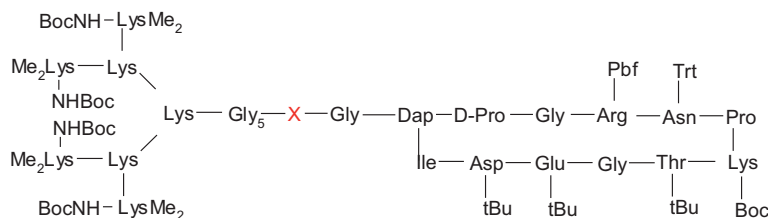
Analytical Data:

HPLC (60→100% B'' in 30 min), *t_R*: 22.16 min.

MS (ESI) *m/z*: 1328.13 [M+3H]³⁺, 996.60 [M+4H]⁴⁺, 797.49 [M+5H]⁵⁺.

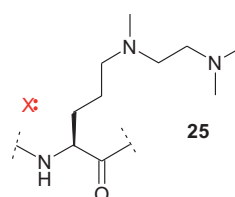
HRMS (ESI): C₁₉₃H₃₂₁N₄₁O₄₆S [M+4H]⁴⁺ calcd. 797.2825, found 797.2821.

8.7.7 [Boc-Lys(Me₂)]₄Lys₂LysGly₅-(S)-5-N,N,N'-trimethylethylenediamino) pentanoic acid-Gly-cyclo[DapD-ProGlyArg(Pbf)Asn(Trt)ProLys(Boc)Thr(tBu)GlyGlu(tBu)Asp(tBu)Ile] (67)



67

C₁₉₃H₃₁₉N₄₁O₄₅S [3966.01]



To a solution of peptide **66** (5 mg, 1.25 μmol, 1 eq.) in dry DCM/DMF (9/1, 1 mM, 1.3 mL), DIC (1.94 μL, 12.55 μmol, 10 eq.), HOAt 0.5 M in DMF (2.51 μL, 1.26 μmol, 1 eq.) and NMM (0.42 μL, 3.76 μmol, 3 eq.) were added under argon. The reaction mixture was stirred at RT for 2.5 days. The solvent was removed in *vacuo*, the residue was purified by RP-HPLC to give **67** as a white solid (3.5 mg, 0.88 μmol, 70%).

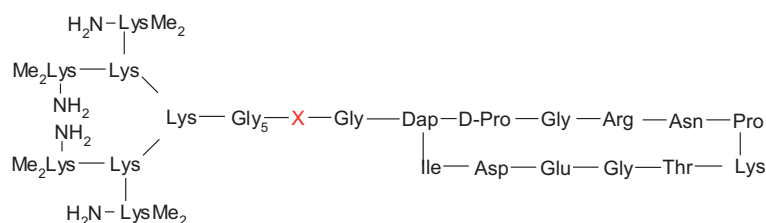
Analytical Data:

HPLC (40→100% B in 30 min), *t_R*: 22.16 min.

MS (ESI) *m/z*: 793.88 [M+3H]³⁺, 992.11 [M+4H]⁴⁺, 1322.47 [M+5H]⁵⁺.

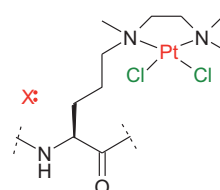
HRMS (ESI): C₁₉₃H₃₁₉N₄₁O₄₅S [M+5H]⁵⁺ calcd. 793.6804, found 793.6801.

8.7.8 [Lys(Me₂)]₄Lys₂LysGly₅-(S)-5-N,N,N'-trimethylethylenediamino) pentanoic acid-Gly-cyclo[DapD-ProGlyArgAsnProLysThrGlyGluAspIle]-dichloroplatinum (II)



23

C₁₂₄H₂₂₅Cl₂N₄₁O₃₂Pt [3068.35]



A solution of K₂PtCl₄ (11 mg, 26.5 μmol, 30 eq., 0.05 M) in DMF/H₂O (530 μL, 9:1) was added to compound **67** (3 mg, 0.76 μmol, 1 eq.) and stirred at RT in the dark for 2 days. The solvent was removed in *vacuo*. Final cleavage was performed with TFA/H₂O (500 μL, 95:5) and stirred for 45 min at RT in the dark. The solvent was evaporated in *vacuo*, the residue was purified by RP-HPLC to give **23** as a white solid (0.3 mg, 0.097 μmol, 12.86%).

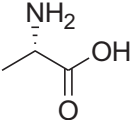
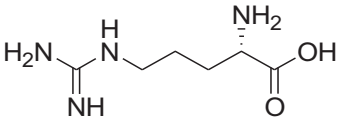
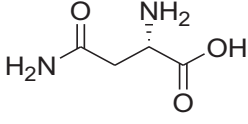
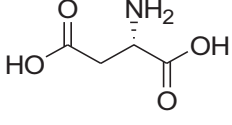
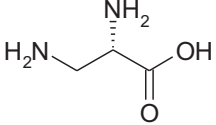
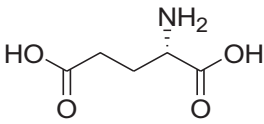
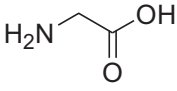
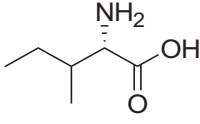
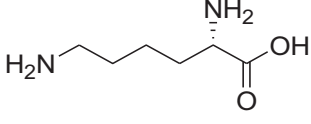
HPLC (5→30% C in 30 min), *t_R*: 8.52 min.

MS (ESI) *m/z*: 614.34 [M+5H]⁵⁺, 512.12 [M+6H]⁶⁺.

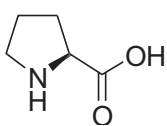
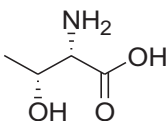
HRMS (ESI): C₁₂₄H₂₂₅Cl₂N₄₁O₃₂Pt [M+5H]⁵⁺ calcd. 614.5330, found 614.5328.

Experimental Part

Table 8.1 Structures and codes of amino acids used in this work

Trivial name	Structure	Three-letter code	One-letter code
Alanine		Ala	A
Arginine		Arg	R
Asparagine		Asn	N
Aspartic acid		Asp	D
Diaminopropanoic acid		Dap	-
Glutamic acid		Glu	E
Glycine		Gly	G
Isoleucine		Ile	I
Lysine		Lys	K

Experimental Part

Proline		Pro	P
Threonine		Thr	T

9. Abbreviations

A	adenine
Ado	adenosine
Å	angstrom (10^{-8} cm)
ACN	acetonitrile
Alloc	allyloxycarbonyl
Ar	argon
aq.	aqueous
Boc	<i>tert</i> -butyloxycarbonyl
Boc ₂ O	di- <i>tert</i> -butyldicarbonate
Bn	benzyl
bp	base pairs
br	broad
C	cytosine
C	Carboxy terminus of a peptide
<i>c</i>	concentration
°C	degree Celsius
CDCl ₃	deuteriochloroform
C ₂ D ₂ Cl ₄	deuterotetrachlorethane
cDDP	cisplatin
COSY	correlation spectroscopy
calcd.	Calculated
2-Cl-Trt	2-chloro-trityl resin
δ	chemical shift

Abbreviations

d	dublet
d	days
DCM	dichloromethane
Degrad. Prod.	degradation product
DIC	<i>N,N'</i> -diisopropylcarbodiimid
DiPEA	(ethyl)diisopropylamine
DMAP	4-(dimethylamino)pyridine
DMF	dimethyl formamide
DMSO	dimethyl sulfoxide
[D ₆]DMSO	hexadeuterodimethyl sulfoxide
DNA	deoxyribonucleic acid
ds	double stranded
ε	absorption coefficient
EtBr	ethidium bromide
EA	ethyl acetate
eq.	equivalent
ESI	electrosprayionisation
Et	ethyl
EtOAc	ethyl acetate
EtOH	ethanol
Fmoc	9-fluorenylmethyloxycarbonyl
G	guanine
Guo	guanosine
h	hours
HATU	O-(7-azabenzotriazol-1-yl)- <i>N,N,N',N'</i> -tetramethyluronium hexafluorophosphate (IUPAC: <i>N</i> -(dimethylamino)(1 <i>H</i> -1,2,3-triazolo[4,5- <i>b</i>]pyridin-1-iumhexafluorophosphate- <i>N</i> -oxide)

Abbreviations

HBTU	<i>O</i> -(1 <i>H</i> -benzotriazol-1-yl)-1,1,3,3-tetramethyluroniumhexafluorophosphat (IUPAC: 1-[Bis(dimethylamino)methylen]-1 <i>H</i> -benzotriazolium-hexafluorophosphat-3-oxid)
HCl	hydrochloric acid
HMBC	heteronuclear multiple bond correlation
HMQC	heteronuclear multiple quantum coherence
HMG	High Mobility Group
HOAt	7-aza-1-hydroxybenzotriazol
HOBt	1-hydroxybenzotriazol
HPLC	high performance liquid chromatography
HR	high resolution
Hz	hertz
IHF	Integration Host Factor
<i>J</i>	coupling constant
K	Kelvin
KHCO ₃	potassium bicarbonate
λ	wavelength
<i>l</i>	length
M	molar
m	multiplet
M	molecular weight
Me	methyl
MeOH	methanol
MHz	megahertz
min	minutes
MS	mass spectrometry
<i>m/z</i>	ratio of mass to charge

Abbreviations

<i>N</i>	amino terminus of a peptide
N	normal
NaOH	sodium hydroxide
NaH	sodium hydride
NMM	<i>N</i> -methylnmorpholine
NMP	<i>N</i> -methylpyrrolidin-2-one
NMR	nuclear magnetic resonance
NOESY	nuclear overhauser enhancement spectroscopy
o.n.	overnight
<i>p</i>	para
PCR	polymerase chain reaction
PDB	protein data base
PE	polyethylene
PFPOH	pentafluorophenol
Ph	phenyl
pH	the negative logarithm hydrogen-ion activity ($-\log_{10} [\text{H}_3\text{O}^+]$)
PI	propidium iodide
ppm	parts per million
q	quartet
quant.	quantitative
rel.	relative
R_f	retention factor
RP	reverse phase
RT	room temperature
s	singlet
s	second

Abbreviations

SPPS	solid phase synthesis
T	thymine
t	triplet
<i>t</i> Bu	<i>tert.</i> -butyl
<i>tert.</i>	Tertiary
Trt	trityl
TFA	trifluoroacetic acid
THF	tetrahydrofuran
TLC	thin-layer chromatography
T_m	melting temperature
TMS	tetramethylsilane
t_R	retention time
UV	ultraviolet spectroscopy

10. References

- [1] *Metal Ions in Biological Systems: Interactions of Metal Ions with Nucleotides, Nucleic Acids and Their Constituents, Vol. 32*, Ed. A. Siegel and H. Siegel, Marcel Dekker, **1996**.
- [2] J. Reedijk, *PNAS* **2003**, *100*, 3611–3616.
- [3] J. Reedijk, *Platinum Metal Rev.* **2008**, *52*, 2–11.
- [4] I. Ott, R. Gust, *Arch. Pharm. Chem. Life Sci.* **2007**, *340*, 117–126.
- [5] C. Sanchez-Cano, M. J. Hannon, *Dalton Trans.* **2009**, *48*, 10702–10711.
- [6] B. Rosenberg, I. Van Camp, T. Krigas, *Nature* **1965**, *205*, 698–699.
- [7] B. Rosenberg, L. Van Camp, J. E. Trosko, V. H. Mansour, *Nature* **1969**, *222*, 385–386.
- [8] T. Boulikas, M. Vougiouka, *Oncol. Rep.* **2004**, *11*, 559–595.
- [9] A. M. Fichtinger-Schepman, J. L. van-derVeer, J. H. J. denHartog, P. H. M. Lohman, J. J. Reedijk, *Biochemistry* **1985**, *3*, 707–713.
- [10] A. Eastman, *Biochemistry* **1986**, *13*, 3912–3915.
- [11] P. M. Takahara, A. C. Rosenzweig, C. A. Frederick, S. J. Lippard, *Nature* **1995**, *377*, 649–652.
- [12] D. Wang, S. J. Lippard, *Nature Rev. Drug Disc.* **2005**, *4*, 307–320.
- [13] Y. Jung, S. J. Lippard, *Chemical Reviews* **2007**, *107*, 1387–1407.
- [14] S. F. Bellon, S. J. Lippard, *Biophys. Chem.* **1990**, *35*, 179–188.
- [15] S. F. Bellon, J. H. Coleman, S. J. Lippard, *Biochemistry* **1991**, *30*, 8026–8035.
- [16] R. C. Todd, S. J. Lippard, *Metallomics* **2009**, *1*, 280–291.
- [17] D. Yang, S. S. G. E. van Boom, J. Reedijk, J. H. van Boom, A. H. J. Wang, *Biochemistry* **1995**, *34*, 12912–12920.
- [18] P. M. Takahara, C. A. Frederick, S. J. Lippard, *J. Am. Chem. Soc.* **1996**, *118*, 12309–11232.
- [19] J. C. Huang, D. B. Zamble, J. T. Reardon, S. J. Lippard, A. Sancar, *Proc. Nat. Acad. Sci. USA* **1994**, *22*, 10394–10398.
- [20] U. M. Ohndorf, M. A. Rould, Q. He, C. O. Pabo, S. J. Lippard, *Nature* **1999**, *399*, 708–712.
- [21] P. J. Sadler, *ChemBioChem* **2009**, *10*, 73–74.
- [22] T. W. Hambley, *Coord. Chem. Rev.* **1997**, *166*, 181–223.
- [23] F. R. Keene, J. A. Smith, J. G. Collins, *Coord. Chem. Rev.* **2009**, *253*, 2021–2035.
- [24] D. Lebwohl, R. Canetta, *European Journal of Cancer* **1998**, *10*, 1522–1534.
- [25] K. S. Lovejoy, S. J. Lippard, *Dalton Tans.* **2009**, *48*, 10651–10659.
- [26] S. K. C. Elmroth, S. J. Lippard, *JACS* **1994**, *116*, 3633–3634. .
- [27] S. K. C. Elmroth, S. J. Lippard, *Inorg. Chem.* **1995**, *34*, 5234–5243.
- [28] J. Kjellstrom, S. K. C. Elmroth, *Chem. Comm.* **1997**, 1701–1702.

References

- [29] A. S. Snygg, M. Brindell, G. Stochel, S. K. C. Elmroth, *Dalton Trans.* **2005**, 1221–1227.
- [30] A. Sykfont, A. Ericson, S. K. C. Elmroth, *Chem. Comm.* **2001**, 1190–1191.
- [31] M. S. Davies, S. J. Berners Price, T. W. Hambley, *Inorg. Chem* **2000**, *39*, 5603–5613.
- [32] S. Hanlon, L. Wong, G. R. Pack, *Biophys. J* **1997**, *72*, 291–300.
- [33] G. Dirscherl, B. König, *Eur. J. Org. Chem.* **2008**, 597–634.
- [34] G. Dirscherl, R. R. Knape, P. Hanson, B. König, *Tetrahedron* **2007**, *63*, 4918–4928.
- [35] S. I. Kirin, P. Dübon, T. Weyhermüller, E. Bill, N. Metzler Nolte, *Inorg. Chem.* **2005**, *44*, 5405–5415.
- [36] F. Noor, R. Kinscherf, G. A. Bonaterra, S. Walczak, S. S. Wölfl, N. Metzler Nolte, *ChemBioChem* **2009**, *10*, 493–502.
- [37] F. Noor, A. Wüstholtz, R. Kinscherf, N. A. Metzler Nolte, *Angew. Chem. Int. Ed.* **2005**, *44*, 2429–2432.
- [38] S. Khrapunov, M. Brenowitz, P. A. Rice, C. E. Catalano, *PNAS* **2006**, *103*, 19217–19218.
- [39] R. J. McDonald, A. I. Dragan, W. R. Kirk, K. L. Neff, P. L. Privalov, L. J. Maher, *Biochemistry* **2007**, *46*, 2306–2316.
- [40] M. S. Damian, H. K. Hedman, S. K. C. Elmroth, U. Diederichsen, *Eur. J. Org. Chem.* **2010**, 6161–6170.
- [41] E. K. Liebler, U. Diederichsen, *Org. Lett.* **2004**, *6*, 2893–2896.
- [42] G. M. Dhavan, D. M. Crothers, M. R. Chance, M. Brenowitz, *J. Mol. Biol.* **2002**, *315*, 1027–1037.
- [43] P. A. Rice, *Curr. Opin. Struct. Biol* **1997**, *7*, 86–93.
- [44] P. A. Rice, S. Yang, K. Mizuuchi, H. A. Nash, *Cell* **1996**, *87*, 1295–1306.
- [45] K. K. Swinger, P. A. Rice, *Curr. Opin. Struct. Biol* **2004**, *14*, 28–35.
- [46] J. D. Watson, F. H. Crick, *Nature* **1953**, *171*, 737–738.
- [47] O. Kennard, *Pure & Appl. Chem.* **1993**, *65*, 1213–1222.
- [48] J. D. Watson, T. A. Backer, S. P. Bell, A. Gann, M. Levine, R. Losick, *Molecular Biology of the Gene 5th Edition*, Cold Spring Harbor Laboratory Press, **2004**.
- [49] P. Yakovchuk, E. Protozanova, M. D. Frank Kamenetskii, *Nucleic Acids Research* **2006**, *34*, 564–574.
- [50] W. Saenger, *Principles of Nucleic Acids Structure*, Springer Verlag, New York, **1984**.
- [51] A. Ghosh, M. Bansal, *Acta Cryst.* **2003**, *D59*, 620–626.
- [52] R. Wing, H. Drew, T. Takano, C. Broka, S. Tanaka, K. Itakura, R. Dickerson, *Nature* **1980**, *5784*, 755–758.
- [53] <http://www.mun.ca/biochem/courses/3107/images/VVP/Ch23/23-2a.jpg>.
- [54] C. J. Benham, S. P. Mielke, *Annu. Rev. Biomed. Eng.* **2005**, *7*, 21–53.
- [55] P. E. Nielson, *Chem. Eur. J.* **1997**, *3*, 505–508.
- [56] C. Pabo, R. Sauer, *Annu. Rev. Biochem* **1984**, *53*, 293–321.
- [57] P. B. Dervan, *Bioorg. Med. Chem* **2001**, *9*, 2215–2235.
- [58] A. D. Richards, A. Rodger, *Chem. Soc. Rev.* **2007**, *36*, 471–483.

References

- [59] E. F. Gale, E. Cundliffe, P. E. Reynolds, M. H. Richmond, M. J. Waring, *The Molecular Basis of Antibiotic Action*, John Wiley&Sons Ltd. 2nd Ed, **1981**.
- [60] S. Neidle, *DNA Structure and Recognition*, OUP, Oxford, **1994**.
- [61] S. Neidle, *Nat. Prod. Rep* **2001**, *18*, 291–309.
- [62] C. L. Warren, N. C. S. Kratochvil, K. E. Hauschild, S. Foister, M. L. Brezinsky, P. B. Dervan, G. N. Phillips Jr., A. Z. Ansari, *PNAS* **2006**, *103*, 867–872.
- [63] *Metal Complex-DNA Interactions*, N. Hadjiliadis, E. Sletten ed., Wiley-Blackwell, UK., **2009**.
- [64] G. S. Manning, *Quat. Rev Biophys. II* **1978**, *2*, 179–246.
- [65] M. Prabhakaran, S. C. Harvey, *Biopolym.* **1988**, *27*, 1239–1248.
- [66] C. F. Anderson, M. T. Record Jr., *Annu. Rev. Biophys. Biophys. Chem.* **1990**, *19*, 423–465.
- [67] C. F. Anderson, M. T. Record Jr., *Annu. Rev. Phys. Chem.* **1995**, *46*, 657–700.
- [68] A. P. Lyubartsev, *Dekker Encyclopedia of Nanoscience and Nanotechnology: Molecular Simulations of DNA Counterion Distributions* **2004**, *1*, 2131–2143.
- [69] *J. Biol. Inorg. Chem.* **2009**, *14*, S175–S184.
- [70] L. Kelland, *Nature Reviews Cancer* **2007**, *7*, 573–584.
- [71] J. B. Chaires, *Biopolym.* **1996**, *44*, 201–215.
- [72] M. A. Schwaller, J. Aubard, C. Auclair, C. Paoletti, G. Dodin, *Eur. J. Biochem.* **1989**, *181*, 129–134.
- [73] W. I. P. Mainwaring, J. H. Parish, J. D. Pickering, N. H. Mann, *Nucleic Acid Biochemistry and Molecular Biology*, Blackwell Scientific Publications, Oxford., **1982**.
- [74] M. Blackburn, J. M. Gait, D. Loakes, D. M. Williams, *Nucleic acids in chemistry and biology*, RSC publishing 3rd edition, **2006**.
- [75] L. S. Lerman, *J. Mol. Biol.* **1961**, *3*, 18–30.
- [76] L. S. Lerman, H. L. Frisch, *Biopolym.* **1982**, *21*, 995–997.
- [77] N. J. Wheate, C. R. Brodie, J. G. Collins, S. Kemp, J. R. Aldrich Wright, *Mini Rev. Med. Chem.* **2007**, *7*, 627–648.
- [78] A. Petitjean, J. K. Barton, *JACS* **2004**, *126*, 14728–14729.
- [79] J. R. Choudhury, R. Guddneppanvar, G. Saluta, G. L. Kucera, U. Bierbach, *J. Med. Chem.* **2008**, *51*, 3069–3072.
- [80] A. M. Krause-Heuer, R. Grünert, S. Kühne, M. Buczkowska, N. J. Wheate, D. D. LePevelen, L. R. Boag, D. M. Fisher, J. Kasparkova, J. Malina, P. J. Bednarski, V. Brabec, J. R. Aldrich-Wright, *J. Med. Chem.* **2009**, *52*, 5474–5484.
- [81] P. Marques-Gallego, H. denDulk, J. Brouwer, H. Kooijman, A. L. Spek, O. Roubeau, S. J. Teat, J. Reedijk, *Inorg. Chem.* **2008**, *47*, 11171–11179.
- [82] M. A. Jakupec, M. Galanski, V. B. Arion, C. G. Hartinger, B. K. Keppler, *Dalton Transactions* **2008**, *2*, 183–194.
- [83] T. Boulikas, A. Pantos, E. Bellis, P. Christofis, *Cancer Therapy* **2007**, *5*, 537–583.

References

- [84] M. A. Fuertes, C. Alonso, J. M. Perez, *Chem. Rev.* **2003**, *103*, 645–662.
- [85] S. J. Berners-Price, T. A. Frenkiel, U. Frey, J. D. Ranford, P. J. Sadler, *J. Chem. Soc., Chem. Commun.* **1992**, *10*, 789–791.
- [86] B. Lippert(Ed.), *Cisplatin: Chemistry and Biochemistry of a Leading Anticancer Drug*, Wiley-VCH, **1999**.
- [87] Y. Kasherman, S. Sturup, D. Gibson, *J. Med. Chem.* **2009**, *52*, 4319–4328.
- [88] J. Reedijk, *Chem. Rev.* **1999**, *99*, 2499–2510.
- [89] E. R. Jamieson, S. J. Lippard, *Chem. Rev.* **1999**, *99*, 2467–2498.
- [90] A. V. Klein, T. W. Hambley, *Chem. Rev.* **2009**, *109*, 4911–4920.
- [91] M. S. Davies, S. J. Berners Price, T. W. Hambley, *JACS* **1998**, *120*, 11380–11390.
- [92] J. Raber, C. Zhu, L. A. Eriksson, *J. Phys. Chem. B* **2005**, *109*, 11006–11015.
- [93] Y. Mantri, S. J. Lippard, M. H. Baik, *JACS* **2007**, *129*, 5023–5030.
- [94] A. Gelasco, A. J. Lippard, *Biochemistry* **1998**, *37*, 9230–9239.
- [95] H. Huang, L. Zhu, B. R. Reid, G. P. Drobný, P. B. Hopkins, *Science* **1995**, *270*, 1842–1845.
- [96] K. Wozniak, J. Blasiak, *Acta Biochim. Pol.* **2002**, *49*, 583–596.
- [97] M. Bustin, *Molecular and Cellular Biology* **1999**, *19*, 5237–5246.
- [98] S. J. Brown, P. J. Kellett, S. J. Lippard, *Science* **1993**, *261*, 603–605.
- [99] S. L. Bruhn, P. M. Pil, J. M. Essigmann, D. E. Housman, *PNAS* **1992**, *89*, 2307–2311.
- [100] E. R. Jamieson, M. P. Jacobson, C. M. Barnes, C. S. Chow, S. J. Lippard, *J. Biol. Chem.* **1999**, *274*, 12346–12354.
- [101] M. Oren, *Cell Death Differ.* **2003**, *10*, 431–442.
- [102] S. Benchimol, *Cell Death Differ.* **2001**, *8*, 1049–1051.
- [103] D. J. Stewart, *Critical Reviews in Oncology/Hematology* **2007**, *63*, 12–31.
- [104] L. P. Martin, T. C. Hamilton, R. J. Schilder, *Clin. Cancer Res.* **2008**, *14*, 1291–1295.
- [105] T. Torigoe, H. Izumi, H. Ishiguchi, Y. Yoshida, M. Tanabe, T. Yoshida, T. Igarashi, I. Niina, T. Wakasugi, T. Imaizumi, Y. Momii, M. Kuwano, K. Kohno, *Curr. Med. Chem.-Anti-Cancer Agents* **2005**, *5*, 15–27.
- [106] C. A. Rabik, M. E. Dolan, *Cancer Treat. Rev.* **2007**, *33*, 9–23.
- [107] M. J. Cleare, J. D. Hoeschele, *Bioinorg. Chem.* **1973**, *2*, 187–210.
- [108] J. Reedijk, *Chem. Comm.* **1996**, 801–806.
- [109] Y. P. Ho, S. C. F. Au Yeung, K. K. W. To, *Med. Res. Rev.* **2003**, *23*, 633–655.
- [110] A. M. Montana, C. Batalla, *Curr. Med. Chem.* **2009**, *16*, 2235–2260.
- [111] I. Kostova, *Recent Patents on Anti-Cancer Drug Discovery* **2006**, *1*, 1–22.
- [112] F. S. Mackay, J. A. Woods, P. Heringova, J. Kasparkova, A. M. Pizzaro, S. A. Moggach, S. Parsons, V. Brabec, P. J. Sadler, *PNAS* **2007**, *104*, 20743–20748.
- [113] S. Dhar, S. J. Lippard, *PNAS* **2009**, *106*, 21199–22204.
- [114] S. vanZutphen, J. Reedijk, *Coord. Chem. Rev.* **2005**, *249*, 2845–2853.
- [115] C. Xu, B. Wang, S. Sun, *JACS* **2009**, *131*, 4216–4217.

References

- [116] S. Dhar, W. L. Daniel, D. A. Giljohann, C. A. Mirkin, S. J. Lippard, *JACS* **2009**, *131*, 14652–14653.
- [117] K. J. Haxton, H. M. Burt, *J. Pharm. Sciences* **2009**, *98*, 2299–2316.
- [118] M. A. Campbell, P. S. Miller, *Biochemistry* **2008**, *47*, 12931–12938.
- [119] S. Komeda, T. Moulaei, K. K. Woods, M. Chikuma, N. P. Farrell, L. D. Williams, *JACS* **2006**, *128*, 16092–16103.
- [120] J. D. Roberts, J. Peroutka, G. Beggiolin, C. Manzotti, L. Piazzoni, N. Farrell, *J. Inorg. Biochem.* **1999**, *77*, 47–50.
- [121] N. J. Wheate, R. I. Taleb, A. M. Krause Heuer, R. L. Cook, S. Wang, V. J. Higgins, J. R. Aldrich Wright, *Dalton Trans.* **2007**, 5055–5064.
- [122] R. I. Taleb, D. Jaramillo, N. J. Wheate, J. R. Aldrich-Wright, *Chem. Eur. J.* **2007**, *13*, 3177–3186.
- [123] P. J. Sanz-Miguel, M. Roitzsch, L. Yin, P. M. Lax, L. Holland, O. Krizanovic, M. Lutterbeck, M. Schürmann, E. C. Fusch, B. Lippert, *Dalton Trans.* **2009**, 10774–10786.
- [124] J. O. Thomas, *Molec. Comm.* **2001**, 395–401.
- [125] P. R. Hardwidge, J. D. Kahn, L. J. Maher, *Biochemistry* **2002**, *41*, 8277–8288.
- [126] M. J. Bloemink, H. Engelking, S. Karentzopoulos, B. Krebs, J. Reedijk, *Inorg. Chem.* **1996**, *35*, 619–627.
- [127] M. Grehl, B. Krebs, *Inorg. Chem.* **1994**, *33*, 3877–3885.
- [128] M. Joseph, T. Leigh, M. L. Swain, *Synthesis* **1977**, *7*, 459–461.
- [129] C. J. Campbell, W. L. Driessen, J. Reedijk, W. Smeets, A. L. Spek, *J. Chem. Soc., Dalton Trans.* **1998**, 2703–2706.
- [130] A. M. Brückner, H. W. Schmitt, U. Diederichsen, *Helvetica Chimica Acta* **2002**, *85*, 3855–3866.
- [131] M. S. Reddy, M. Narender, Y. V. D. Nageswar, K. R. Rao, *Synlett* **2006**, *7*, 1110–1112.
- [132] Z. Liko, H. S. Vargha, *Tetrahedron Lett.* **1993**, *34*, 1673–1676.
- [133] M. H. Cynamon, S. P. Klemens, *J. Med. Chem.* **1992**, *35*, 1212–1215.
- [134] M. H. Jakobsen, O. Buchardt, T. Engdahl, A. Holm, *Tetrahedron Lett.* **1991**, *32*, 6199–6202.
- [135] L. Kisfaludy, I. Schön, *Synthesis* **1983**, 325–327.
- [136] K. B. Lorenz, U. Diederichsen, *J. Org. Chem.* **2004**, *69*, 3917–3927.
- [137] N. Braussaud, T. Rüther, K. J. Cavell, B. W. Skelton, A. H. White, *Synthesis* **2001**, 626–632.
- [138] P. C. A. Bruijninx, M. Lutz, A. L. Spek, E. E. van Faassen, B. M. Weckhuysen, G. van Koten, R. J. M. Klein Gebbink, *Eur. J. Inorg. Chem.* **2005**, 779–787.
- [139] M. S. Robillard, A. R. P. M. Valentijn, N. J. Meeuwenoord, G. A. van der Marel, J. H. van Boom, J. Reedijk, *Angew. Chem.* **2000**, *112*, 3226–3229.
- [140] R. B. Merrifield, *JACS* **1963**, *85*, 2149–2154.
- [141] R. B. Merrifield, *Science* **1986**, *232*, 341–347.
- [142] G. L. Cohen, W. R. Bauer, J. K. Barton, S. J. Lippard, *Science* **1979**, *203*, 1014–1016.

References

- [143] M. Leng, *Biophys. Chem.* **1990**, *35*, 155–163.
- [144] M. J. Waring, *J. Mol. Biol.* **1965**, *13*, 269–282.
- [145] T. Suzuki, K. Fujikura, T. Higashiyama, K. Takata, *J. Histochem. Cytochem.* **1997**, *45*, 49–53.
- [146] M. C. Olmsted, J. P. Bond, C. F. Anderson, M. T. Record, *Biophysical Journal* **1995**, *68*, 634–647.
- [147] N. Poklar, D. S. Pitch, S. J. Lippard, E. A. Redding, S. U. Dunham, K. J. Breslauer, *PNAS* **1996**, *93*, 7606–7611.
- [148] C. A. Bewley, A. M. Gronenborn, G. M. Clore, *Annu. Rev. Biophys. Biomol. Struct.* **1998**, *27*, 105–131.
- [149] N. Goosen, P. van de Pute, *Molec. Microbiol.* **1995**, *16*, 1–7.
- [150] T. Ellenberger, A. Landy, *Structure* **1997**, *5*, 153–157.
- [151] E. K. Liebler, *Peptidische Proteinmimetika zum sequenzspezifischen Knicken von DNA*, Dissertation, Georg-August Universität Göttingen, **2005**.
- [152] P. C. Champe, R. A. Harvey, D. R. Ferrier, *Biochemistry*, Lippincott Williams & Wilkins, **2008**.
- [153] K. Fejfar, *Synthese von peptidischen IHF-/HU-Proteinmimetika zum Binden und Knicken von DNA*, Dissertation, Georg-August Universität Göttingen, **2009**.
- [154] S. Scholz, E. K. Liebler, B. Eickmann, H. J. Fritz, U. Diederichsen, *Eur. J. Org. Chem.* **2010**, *in preparation*.
- [155] R. S. Narayan, M. S. Van Nieuwenhze, *Org. Lett.* **2005**, *7*, 2655–2658.
- [156] X. Zhu, R. R. Schmidt, *Eur. J. Org. Chem.* **2003**, 4069–4072.
- [157] U. Diederichsen, D. Weicherding, N. Diezmann, *Org. Biomol. Chem* **2005**, *3*, 1058–1066.
- [158] M. Pittelkow, R. Lewinsky, J. B. Christensen, *Synthesis* **2002**, *15*, 2195–2202.
- [159] M. Milanesio, E. Monti, M. B. Gariboldi, E. Gabano, M. Ravera, D. Ossela, *Inorg. Ch. Acta* **2008**, *361*, 2803–2814.
- [160] B. Dittrich, T. Koritsanszky, M. Grosche, W. Scherer, R. Flaig, A. Wagner, H. G. Krane, H. Kessler, C. Riemer, A. M. M. Schreurs, P. Luger, *Acta Crystallgr., Sect. B* **2002**, *58*, 721–727.
- [161] R. M. Hughes, M. L. Benschoff, M. L. Waters, *Chem. Eur. J.* **2007**, *13*, 5753–5764.
- [162] S. Ahmed, R. Beleid, T. Sprules, K. Kaur, *Org. Lett.* **2007**, *9*, 25–28.
- [163] H.-M. Wu, D. M. Crothers, *Nature* **1984**, *308*, 509–513.
- [164] T. J. Appleton, R. D. Berry, C. A. Davies, J. R. Hall, H. A. Kimlin, *Inorg. Chem.* **1984**, *23*, 3514–3521.
- [165] A. S. Snygg, M. Hung, S. K. C. Elmroth, *J. Inorg. Biochem.* **2007**, *101*, 1153–1164.
- [166] M. Gude, J. Ryf, P. D. White, *Lett. Pept. Science* **2002**, *9*, 203–206.

Acknowledgements

I thank Professor Dr. Ulf Diederichsen for the chance to do PhD in Göttingen, for the confidence and support, for the freedom of research and, nevertheless, for the very interesting topic!

This work wouldn't have been possible without the contribution of several people to whom I bring my sincere gratitude.

Firstly, I would like to thank my colleagues in **lab 102**, the best lab in AKD☺, Dr. Ratika Srivastava, Brigitte Worbs, Karsten Meyenberg and Cornelia Panse for their support and cooperation during my PhD. They have provided a friendly and professional environment to study, work, but also to improve my German language knowledge☺. I express my special gratitude to Dr. Ratika Srivastava and Dr. Anmol Kumar Ray for their invaluable friendship, collegiality, help and all the nice moments spend together! I am grateful to Brigitte Worbs for her help within the last part of my PhD, to Karsten Meyenberg for his helpful, organizing and friendly nature.

I am grateful to Antonina Lygina for her friendship, advices, her encouragements and support in the last two years; I will always remember the *ceai* breaks! *Большое спасибо!* A very special *Danke* goes to Dr. Philipp Schneggenburger, to whom I am grateful for his friendship and all the help given during the PhD period, especially in the last step of the thesis! I have really improved my MicrosoftWord knowledge! Also, *Vielen Dank* is addressed to Juliane Gräfe for her support with all the administrative issues, which have facilitated things here in Germany. I guess she is part of AKD ...which can never be forgotten☺.

I would like to thank all the people that have been helping me in the writing process (corrections, formatting, summary translation): Dr. Philipp Schneggenburger, Dr. André Nadler, Juliane Gräfe, Karsten Meyenberg, Eike Sachs, Antonina Lygina, Stefanie Scholz. To the “new generation”: Tanja, Oleg, Diana, Selda, Ursula,

Acknowledgements

Daniela - it was nice having you around in the last part of my PhD. I am thankful to all the members of the *Abteilung Diederichsen*. To a certain extent, I have learned from you all!

I would like to mention my gratitude to all the people I have collaborated with in Sweden at Lund Kemikum: *Professor Dr. Sofi Elmroth, Hanna Hedman, Dr. Åse Snygg*. There, I have really improved my biochemistry knowledge. This project was possible due to the *Graduiertenkolleg International Research Training Group (IRTG 1422)*. Therefore, I would like to thank IRTG for the financial support, to *Professor Dr. Franc Meyer* for being the speaker of IRTG and the coreviewer of my thesis, but also to all the members within IRTG for collaboration, for the workshops and conferences we have attended together; hereby, I thank to: André Nadler, Friederike Fehr, Christina Hain. To Stefanie Scholz I am grateful for collaboration within the IHF project.

I thank Dr. Holm Frauendorf and Mrs. G. Udvarnoki for the mass spectrometric measurements. I express my sincere thanks to Mr. Reinhard Machinek and co-workers for the NMR measurements. A special thank you goes to Dr. Michael John in the Inorganic Chemistry Institut for the NMR measurements of the platinum compounds.

A sincere thank you is addressed to Professor Dr. Helmut Ritter and Mrs. Margot Hannerth, my first contact to Germany☺ and one of the causes for my coming to Göttingen.

I am especially grateful to my husband, Ciprian Damian for his love, endless support and encouragement. A special thank you is addressed to my sister, Iulia, my friends, Elena and Roxana in Iasi, but also to the Romanian community and all the friends (especially Dieter and Karin) in Göttingen.

Finally, my deepest gratitude is addressed to my parents for their love, education, encouragement and unconditional support!

I thank God for the existence of this thesis!

Acknowledgements

Mulumirile cele mai profunde se adreseaza parintilor mei, *Valerica* si *Vasile Balan*! Ei sunt esenta a ceea ce reprezint eu astazi. Lor le multumesc pentru dragostea oferita, pentru echilibrul sufletesc, pentru educatia, pentru sprijinul neconditionat si ambianta familiala. Alaturi de sora mea, *Iulia* am avut o copilarie perfecta, un sprijin in drumul meu spiritual si profesional. Iuliei ii multumesc pentru frumoasele momente petrecute impreuna in casa parintilor, pentru dragostea, increderea si incurajarile ei (qlaa☺).

Prietenelor mele din Iasi, *Elena Bedreag* si *Roxana Tucaliuc*. Sunt privilegiata sa ma pot numi prietena voastra. Va multumesc pentru increderea si sprijinul acordat!! Sunteti cu adevarat ca doua surori pentru mine!

Mulumesc prietenilor romani din Göttingen. Mi-a facut placere sa va intalnesc. Imi voi aminti cu placere de voi, de intalnirile si discutiile noastre, mai ales cele in spirit crestin filozofic☺. Amintesc mai ales pe: familia Petritan Any-Mary, Catalin si Ioan, Octavian Mihoc, Valentin Hodarnau, Maria Moloci; deasemenea mi-a facut placere sa ii cunosc pe: Dana si Ovidiu Ioan, Svetlana si Bogdan, Marian Pitulescu, Mihaela si George. Sincere multumiri sunt adresate Cornелиei König pentru prietenia ei.

Totusi, multumirile cele mai actuale se indreapta catre sotul meu, Ciprian. El reprezinta prezentul si viitorul meu, este o mare parte a cauzei venirii si sustinerii mele la doctorat in Germania. Ii multumesc pentru enorma sa dragostea, pentru sprijinul neconditionat, pentru increderea si sustinera continua.

Iubirea ta o impartasesc si multumesc Lui Dumnezeu pentru NOI!

Aceasta teza nu ar fi existat fara vointa si sustinerea *Lui Dumnezeu*!

CV

Name	Damian (born Balan)
Surname	Mariana Simona
Date and place of birth	06.09.1980, Iasi, Romania
Nationality	Romanian
Marital status	Married
E-mail	mbalan@gwdg.de ; almabrad@yahoo.com

Education

06.07.2010	Doctoral exam for the award of the degree “ <i>doctor rerum naturalium</i> ”; predicate: magna cum laude
11/2006–07/2010	PhD thesis Theme: “ <i>DNA Bending Molecules for Improvement of Cisplatin Binding</i> ” Institut für Organische und Biomolekulare Chemie Georg-August-Universität, Göttingen, Germany Group of Prof. Dr. Ulf Diederichsen Member (scholarship holder) in the INTERNATIONAL RESEARCH TRAINING GROUP (IRTG 1422): “ <i>Metal Sites in Biomolecules: Structures, Regulation and Mechanisms</i> ”, Göttingen, Germany
02/2006–07/2006	Research fellowship Institut für Organische und Makromolekulare Chemie Heinrich-Heine-Universität, Düsseldorf, Germany Group of Prof. Dr. Helmut Ritter
10/2003–06/2005	Master of Science

Curriculum Vitae

Specialization “*Chemistry and Biochemistry of Heterocyclic Compounds*”

Al. I. Cuza University, Iasi, Romania

Group of Prof. Dr. Ioan Druta

10/1999–06/2003

Faculty of Chemistry

Specialization “*Technological Biochemistry*”

Al. I. Cuza University, Iasi, Romania

09/1995–07/1999

Dimitrie Cantemir Theoretical Highschool

Iasi, Romania

Experience

01/2008–07/2009

Teaching assistant in the practical course: “Chemistry for Medicine Students”

04–07/2008

Teaching assistant for the lecture “Basic of Organic Chemistry”, weekly seminars

02/2004–12/2005

Control-laboratory assistant

S.C. TEBA INDUSTRY Iasi, Romania

